ATTACHMENTS

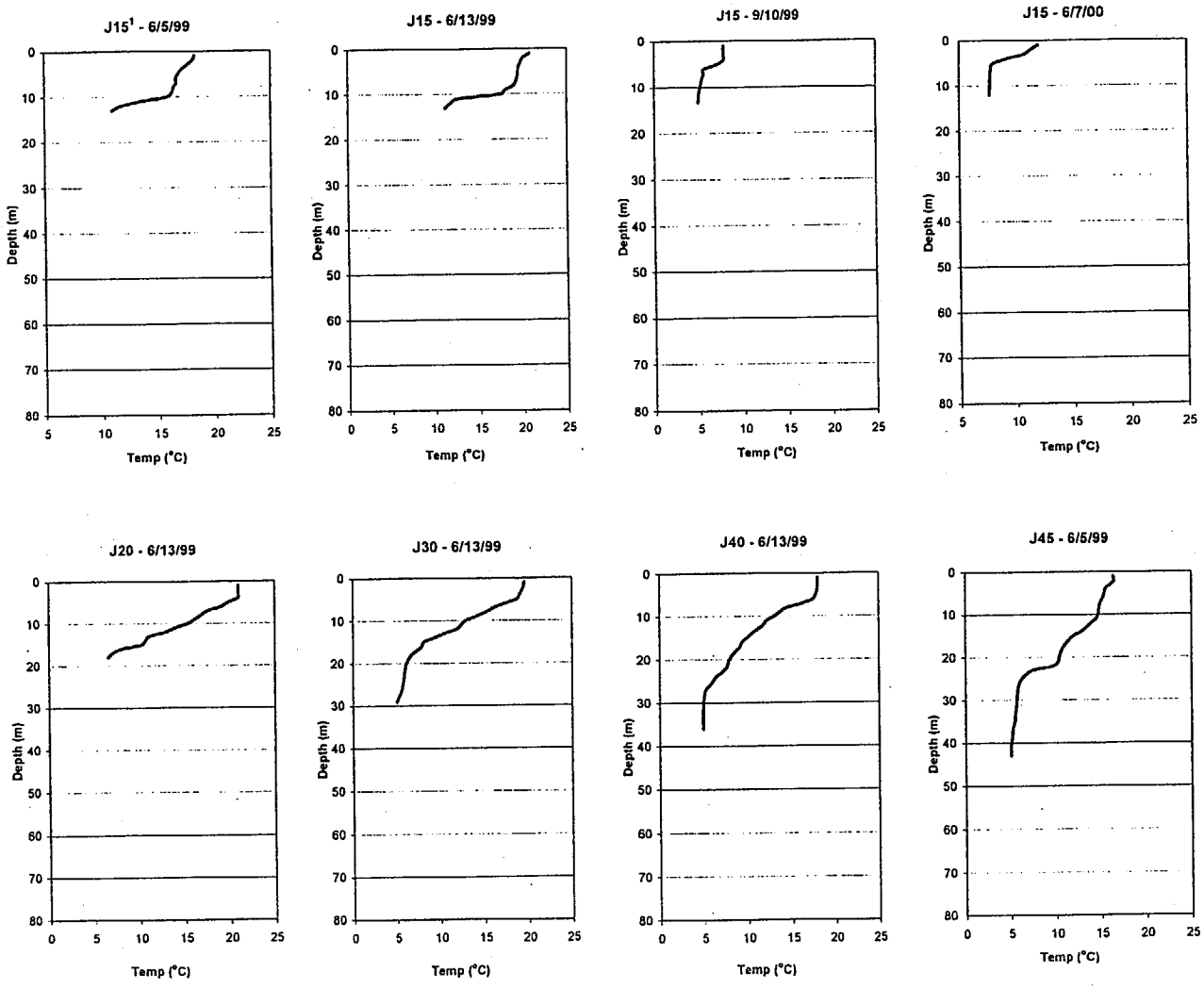

[1] Naming Convention: The letter corresponds to CTD location (J - St. Joseph, NB - New Buffalo)
The number corresponds to the water depth at the CTD

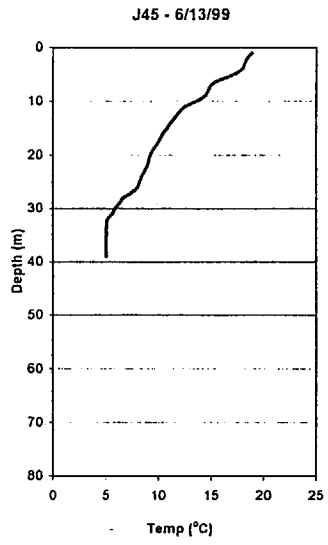
J45 - 6/13/99
Depth (m)
Temp (°C)

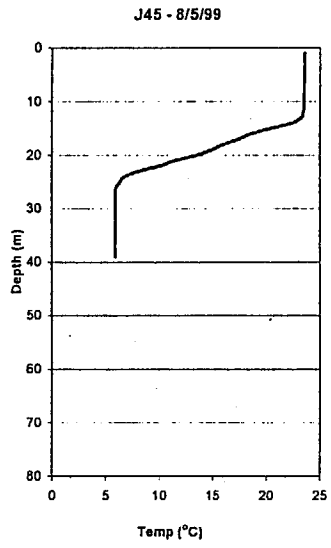
J45 - 8/5/99
Depth (m)
Temp (°C)

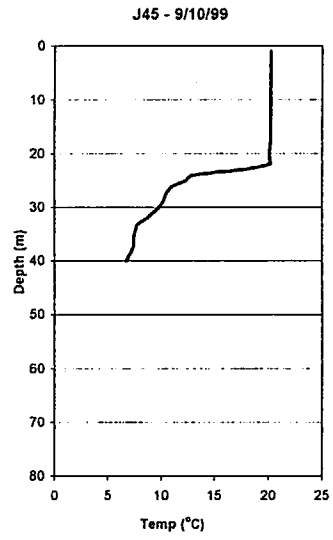
J45 - 9/10/99
Depth (m)
Temp (°C)

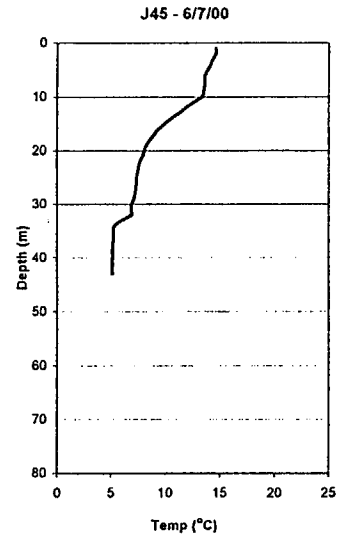
J45 - 6/7/00
Depth (m)
Temp (°C)

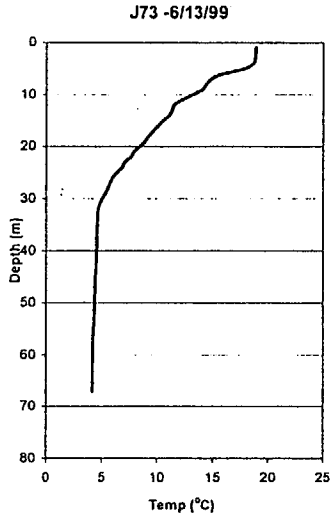
J73 -6/13/99
Depth (m)
Temp (°C)

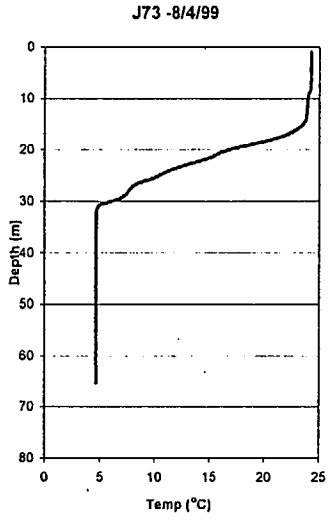
J73 -8/4/99
Depth (m)
Temp (°C)

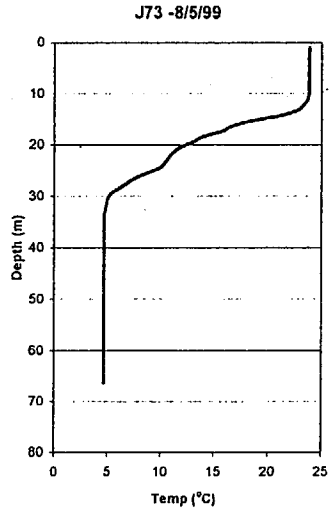
J73 -8/5/99
Depth (m)
Temp (°C)

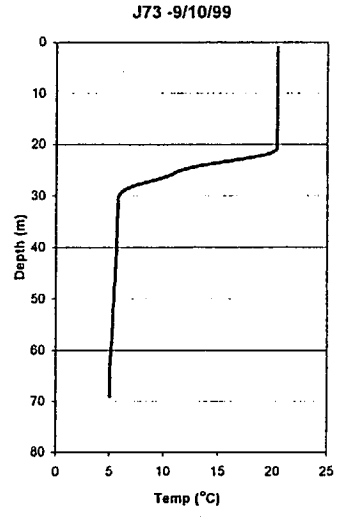
J73 -9/10/99
Depth (m)
Temp (°C)

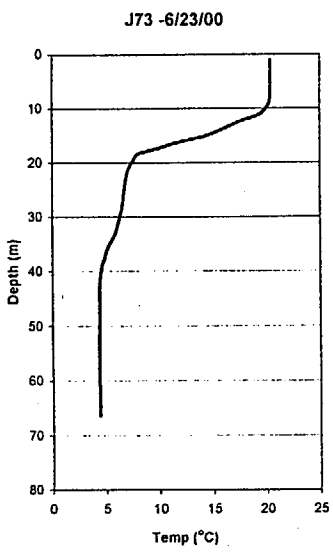
J73 -6/23/00
Depth (m)
Temp (°C)

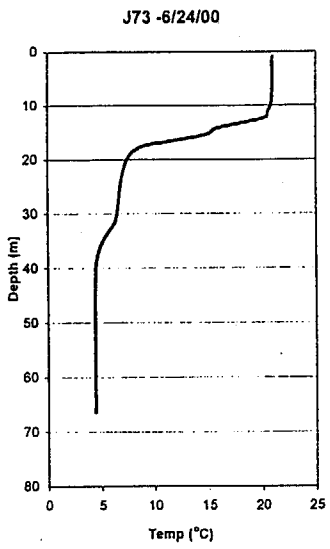
J73 -6/24/00
Depth (m)
Temp (°C)

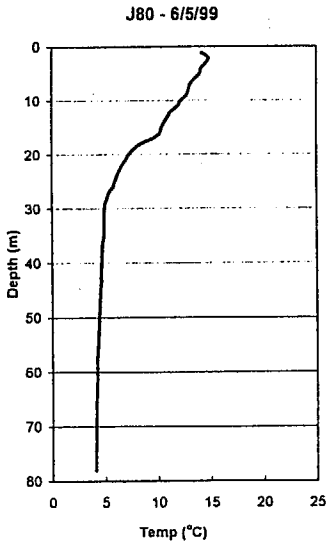
J80 - 6/5/99
Depth (m)
Temp (°C)

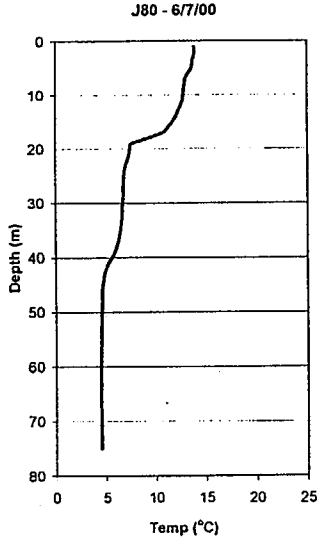
J80 - 6/7/00
Depth (m)
Temp (°C)

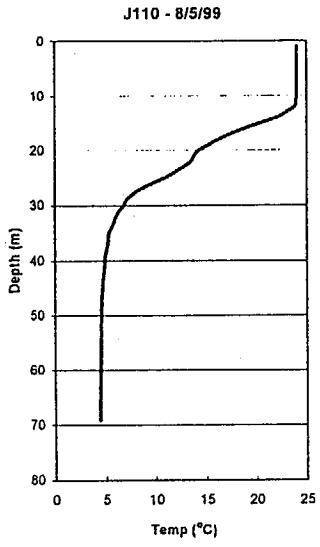
J110 - 8/5/99
Depth (m)
Temp (°C)

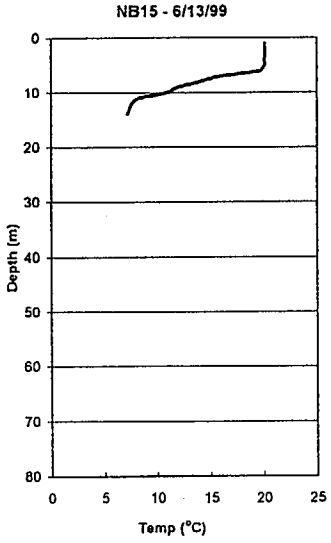
NB15 - 6/13/99
Depth (m)
Temp (°C)

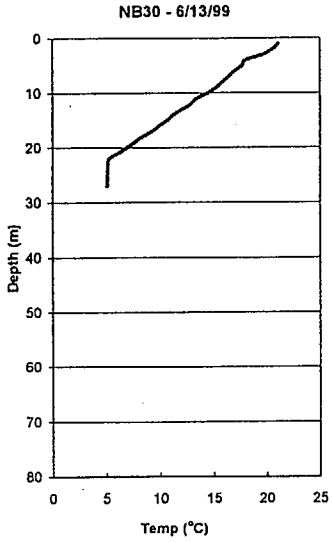
NB30 - 6/13/99
Depth (m)
Temp (°C)

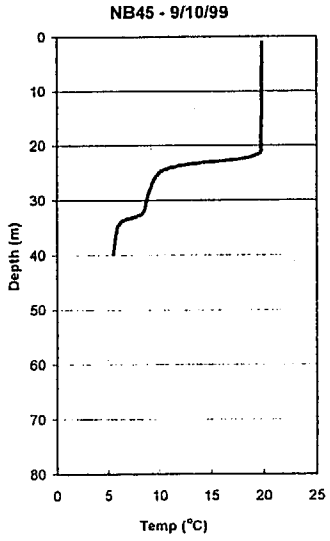
NB45 - 9/10/99
Depth (m)
Temp (°C)

Cook Plant Thermal Plume Study

Prepared for:

The Indiana Michigan Power Company
Bridgman, Michigan

May 16, 2000

Limno-Tech, Inc.

Excellence in Environmental Solutions Since 1975

Ann Arbor, Michigan

TABLE OF CONTENTS

LIST OF FIGURES III

LIST OF TABLES VI

LIST OF ATTACHMENTS VII

EXECUTIVE SUMMARY VIII

1.0 INTRODUCTION 1

1.1 PURPOSE OF REPORT 1
1.2 STUDY GOALS AND OBJECTIVES 1
1.3 AVAILABLE DATA 2
1.4 MODELING APPROACH 3
1.5 REPORT ORGANIZATION 4

2.0 BACKGROUND AND STUDY APPROACH 5

2.1 PLANT DESCRIPTION 5
2.2 PERMIT SPECIAL CONDITION 5
2.3 1978 – 1979 PLUME INVESTIGATION 6
2.4 DATA USED FOR MODEL ASSESSMENT, BOUNDARY CONDITIONS AND BATHYMETRY 7
2.4.1 1978-1979 Plume Investigation Data 7
2.4.2 LMMBS Data 8
2.4.3 Cook Plant Meteorological Data 8
2.4.4 Lake Michigan Bathymetry Data 9

3.0 THREE-DIMENSIONAL NEARSHORE CIRCULATION MODEL 10

3.1 MODEL ROUTINES FOR NEARSHORE APPLICATION 10
3.1.1 Cook Plant Effluent Heat Flux 10
3.1.2 Atmospheric Heat Flux 11
3.1.2.1 Short Wave Radiation 12
3.1.2.2 Penetration of Incoming Short Wave Radiation into the Water Column . 13
3.1.2.3 Long Wave Radiation 14
3.1.2.4 Sensible Heat Flux 15
3.1.2.5 Latent Heat Flux 15
3.1.2.6 Calculation of the C_D and C_H Coefficients 16
3.1.3 Boundary Conditions for Momentum 17
3.1.3.1 Plume Momentum 17
3.1.3.2 Momentum from Lake Michigan 17
3.1.4 Lake Michigan Boundary Condition for Heat 17
3.1.5 Turbulent Mixing 18
3.1.5.1 Background 18
3.1.5.2 Nearshore model application 19
3.1.6 Shoreline Drag 20

3.2 NEARSHORE GRID CONSTRUCTION 20
3.3 NEARSHORE BATHYMETRY 21
3.4 WATER VELOCITY OPEN BOUNDARY CONDITIONS 21
3.5 WATER TEMPERATURE BOUNDARY CONDITIONS 22
3.6 CONVERTING WATER TEMPERATURE INTO PLUME SIZE 22

4.0 MODEL PERFORMANCE ASSESSMENT 24

4.1 ADJUSTING VERTICAL MIXING 25
4.2 SEASONAL ASSESSMENT 26
4.3 SHORT TERM ASSESSMENT: DAILY RUNS 27
4.3.1 Plume Area 28
4.3.2 Plume Shape 29
4.4 CONCLUSIONS OF THE MODEL PERFORMANCE ANALYSIS 30

5.0 NEARSHORE MODEL RESULTS 31

5.1 FREQUENCY ANALYSIS OF PLUME SIZE 31
5.2 AVERAGE MONTHLY PLUMES 32
5.1 MAXIMUM PLUMES 33
5.3 CONCLUSIONS 34

6.0 SENSITIVITY ANALYSIS 35

6.1 WIND SPEED 35
6.2 WIND DIRECTION, CLOUD COVER, AIR TEMPERATURE, AND RELATIVE HUMIDITY 35
6.3 SENSITIVITY FINDINGS 36

7.0 CONCLUSIONS 37

8.0 REFERENCES 38

LIST OF FIGURES

Figure 1-1. Study Approach.

Figure 1-2. Model Approach.

Figure 2-1. Southern Lake Michigan with a 5 Kilometer Grid and the Nearshore Model Grid Centered on the Cook Plant.

Figure 2-2. Cook Plant Nearshore Map.

Figure 2-3. Nearshore Model Grid in Vicinity of Cook Plant, Showing Local Features.

Figure 2-4. LMMBS Model Grids Near the Cook Plant Model Domain.

Figure 3-1. Flow Chart for the 3-Dimensional Nearshore Circulation Model.

Figure 3-2. Nearshore Model Information Flow Chart.

Figure 3-3. Principal Mechanisms of Light Extinction.

Figure 3-4. Solar Radiation Versus Depth for Various Water Bodies.

Figure 3-5. Momentum Boundary Conditions for the Performance Assessment.

Figure 3-6. Vertical Mixing as a Function of **Ri**.

Figure 4-1. Plume Areas at the Surface, 1m, 2m, and 4m for a 72 Hour Test Run With $\nu = 10^{-2}$.

Figure 4-2. Plume Areas at the Surface, 1m, 2m, and 4m for a 72 Hour Test Run With $\nu = 10^{-3}$.

Figure 4-3. Plume Areas at the Surface, 1m, 2m, and 4m for a 72 Hour Test Run With $\nu = 10^{-4}$.

Figure 4-4. Nearshore Model Surface Temperature Compared to CORMIX Steady State Prediction.

Figure 4-5. Plume Comparison for July 1995 Modeled Plumes and July 1979 Measured Plumes.

Figure 4-6. Plume Comparison for September 1995 Modeled Plumes and September 1978 Measured Plumes.

Figure 4-7. Plume Comparison for November 1995 Modeled Plumes and November 1978 Measured Plumes.

Figure 4-8. Map of Study Domain and the Benton Harbor Airport.

Figure 4-9. Short Term Performance Assessment.

Figure 4-10. Plume Area and Wind Speed.

Figure 4-11. Computed Plume for November 1, 1978 am

Figure 4-12. Computed Plume for November 1, 1978 pm

Figure 4-13. Computed Plume for November 2, 1978 am

Figure 4-14. Computed Plume for November 2, 1978 pm

Figure 4-15. Computed Plume for November 3, 1978 am

Figure 4-16. Computed Plume for November 3, 1978 pm

Figure 5-1. Frequency Distribution for all of the Computed Plumes.

Figure 5-2. April Average Plume with High Plant Output.

Figure 5-3. May Average Plume with High Plant Output.

Figure 5-4. June Average Plume with High Plant Output.

Figure 5-5. July Average Plume with High Plant Output.

Figure 5-6. August Average Plume with High Plant Output.

Figure 5-7. September Average Plume with High Plant Output.

Figure 5-8. October Average Plume with High Plant Output.

Figure 5-9. November Average Plume with High Plant Output.

Figure 6-1. Plume Area Sensitivity to Wind Speed.

Figure 6-2. Plume Area Sensitivity to Wind Direction.

Figure 6-3. Plume Area Sensitivity to Cloud Cover.

Figure 6-4. Plume Area Sensitivity to Air Temperature.

Figure 6-5. Plume Area Sensitivity to Relative Humidity.

LIST OF TABLES

Table 1-1. Forcing Data and Field Data Used for the Model Runs.

Table 2-1. Summary of 1978 – 1979 Thermal Plume Mapping Event Characteristics and Results.

Table 2-2. Summary of Ambient Lake Temperature Data Available on Plume Mapping Days.

Table 2-3. Summary of Lake Current Data Available on Plume Mapping Days.

Table 3-1. Example of Light Extinction Coefficients.

Table 3-2. Momentum Boundary Conditions for Performance Assessment.

Table 3-3. Momentum Boundary Conditions for the 1995 Simulation.

Table 3-4. Naming Convention for Turbulence Models.

Table 4-1. Survey Plumes by Month and Wind Speeds During the Measurement Period.

Table 4-2. Measured Plume Area and Computed Area for 2 °C, 1.67 °C, and 1 °C.

Table 5-1. Operating Conditions for the Model Runs.

Table 5-2. Average Plume Area (hectares) at 1 meter Depth.

Table 5-3. Representative Maximum Plume Area (hectares) at 1 meter Depth.

LIST OF ATTACHMENTS

Attachment A CORMIX Application to the Cook Plant Discharge Structure.

EXECUTIVE SUMMARY

The Indiana Michigan Power Company (IMPC) owns and operates the Donald C. Cook Nuclear Power Plant in Bridgman, Michigan. The Cook Nuclear Plant's original NPDES permit contained an effluent limit for "heat addition" of 15,500 Million BTU/Hour. In the March 31, 1994 NPDES permit renewal application, Cook Plant requested an increase in the thermal effluent limit to 16,800 Million BTU/Hour. This effluent limit allowed the Cook Plant to operate at full power during the summer and also allowed for a planned uprating of Unit 1. The NPDES permit issued June 26, 1995 included the 16,800 Million BTU/Hour thermal effluent limit. The Michigan Department of Environmental Quality (MDEQ) maintains regulatory authority over the thermal effluent of the power plant and requires a demonstration that operating at the higher power levels will produce no adverse impacts on aquatic life. Therefore, the permit also included a special condition requiring Cook Plant to conduct a thermal plume study for outfalls 001 and 002 when the uprating project was completed. The thermal uprate project has not yet been initiated due to NRC related matters. However, there are plans to also uprate the generation of Unit 2. Cook Plant is not certain whether both uprating projects will take place during the term of the next NPDES renewal, but would like the thermal effluent limit to be increased to 17,300 Million BTU/Hour now to avoid modifying the permit later. Cook Nuclear Plant initiated a contract with Limno-Tech, Inc. (LTI), to develop a computer model to simulate the effects of both unit upgrades.

A numerical modeling system was created that computed the size of thermal plumes associated with the thermal discharge from the Cook Plant. The model computed plumes that compared well to 1978-79 field data both on the seasonal and daily time scales. For the daily test period, the modeling system accurately represented plume areas within a temperature variation of $\pm 0.5\ ^{o}C$. The numerical model was run to simulate April through November of 1995, using forcing conditions from a Lake Michigan circulation model, atmospheric data, and thermal input from the Cook Plant at the energy levels listed above. The results were analyzed to determine the effect of the uprate on plume size.

The model results showed that there is not a significant difference between the plumes generated by the Cook Plant operating at the current level and the plumes generated by operating at the uprated levels. A frequency analysis showed that the when the plant was running at high output there were 7% fewer small plumes, plumes in the 0-49 hectare range. In the next largest plume sizes classes, 50-99, 100-149, and 150-199 hectares, all three power levels had roughly the same number of plumes. The frequency analysis also showed that the plant operation at all of the power levels converge asymptotically. This means that all of the simulations produced a similar number of large plumes.

1.0 INTRODUCTION

1.1 PURPOSE OF REPORT

This report was prepared by Limno-Tech, Inc. (LTI) on behalf of the Indiana Michigan Power Company to summarize the results of a thermal plume study that was conducted for the Donald C. Cook Nuclear Plant (Cook Plant), located near Bridgman, Michigan.

The Cook Nuclear Plant's original NPDES permit contained an effluent limit for "heat addition" of 15,500 Million BTU/Hour. In the March 31, 1994 NPDES permit renewal application, Cook Plant requested an increase in the thermal effluent limit to 16,800 Million BTU/Hour. This effluent limit allowed the Cook Plant to operate at full power during the summer and also allowed for a planned uprating of Unit 1. The NPDES permit issued June 26, 1995 included the 16,800 Million BTU/Hour thermal effluent limit. The Michigan Department of Environmental Quality (MDEQ) maintains regulatory authority over the thermal effluent of the power plant and requires a demonstration that operating at the higher power levels will produce no adverse impacts on aquatic life. Therefore, the permit also included a special condition requiring Cook Plant to conduct a thermal plume study for outfalls 001 and 002 when the uprating project was completed. The thermal uprate project has not yet been initiated due to NRC related matters. However, there are plans to also uprate the generation of Unit 2. Cook Plant is not certain whether both uprating projects will take place during the term of the next NPDES renewal, but would like the thermal effluent limit to be increased to 17,300 Million BTU/Hour now to avoid modifying the permit later. Cook Nuclear Plant initiated a contract with LTI to develop a computer model to simulate the effects of both unit upgrades. The findings are presented in this report.

1.2 STUDY GOALS AND OBJECTIVES

The principal goal of this project was to conduct an investigation that would satisfy the technical requirements of the NPDES permit for the Cook Plant to operate at the proposed uprated capacities. The technical goal of the project was to quantify the relationship between thermal discharges from the Cook Plant and characteristics of the resulting thermal plumes in Lake Michigan.

The study approach is illustrated in Figure 1-1. Forcing data was used as input to a three-dimensional numerical model which simulated lake temperatures in the vicinity of the thermal discharge. Plume areas were then computed by:

- using the regulatory criterion that all discharge water which is 3 °F (1.67 °C), or more, above the ambient temperature be defined as a thermal plume, and by
- computing the ambient temperature.

Combining the numerical model with the routines to convert water temperature into plume area, lead to a modeling system that computed the spatial and temporal distributions of thermal plumes in Lake Michigan for different discharge temperatures from the Cook Plant.

The procedure used to implement the thermal plume modeling system was the following:

1. Construct and test a three-dimensional numerical model for simulating thermal plumes in Lake Michigan due to the Cook Plant discharge;
2. Conduct simulations with the tested model for the three proposed energy conditions, and an ambient case;
3. Conduct a sensitivity analysis with the thermal plume model to investigate the influence of environmental variability on the plume characteristics.

The attainment of these objectives will provide the technical information required for the NPDES permit process.

1.3 AVAILABLE DATA

Information about Lake Michigan currents and temperatures near the Cook Plant was available, as was data from a plume mapping studying. Although the information is not concurrent, we were able to make reasonable assumptions about the data so that it could be used to test the model. The assumptions were then tested and determined to be appropriate.

A study of the thermal effluent from the Cook Plant was conducted in 1978 and 1979. Twenty nine plumes were mapped. Water temperature and currents near the discharge were recorded. Atmospheric conditions were noted when the plumes were gathered, and weather conditions for 1978-79 were recorded at the Benton Harbor Airport, approximately 18 kilometers from the Cook Plant.

In 1998 researchers (Schwab and Beletsky, 1998), at the Great Lakes Environmental Research Laboratory (GLERL) conducted a numerical modeling study of Lake Michigan simulating the whole of 1995 for the Lake Michigan Mass Balance Study - Hydrodynamic Modeling Project (LMMBS-HMP). The study synthesized atmospheric data from around Lake Michigan which was used to drive a three-dimensional circulation model. The model used 5 km by 5 km grid boxes. This grid is too coarse to address the Cook Plant thermal plume, but provided boundary conditions that were necessary to run long term simulations of the Cook Plant thermal plume.

In 1978 thermal plumes were measured, but there is not enough available boundary data to run a circulation model for long periods of time. The LMMBS study of 1995 has sufficient data to support long term circulation models, but no plumes were measured in 1995. The mismatch of measured plumes and availability of boundary circulation data

means that model performance must be measured in ways other than a traditional calibration/verification.

1.4 MODELING APPROACH

Four numerical models were used to achieve the study objectives.

1. The nearshore circulation model (DGA)
2. The Lake Michigan circulation model (LMMBS-HMP)
3. The atmospheric heat exchange model
4. The high velocity discharge model (CORMIX)

The primary model used was the nearshore circulation model, the Dynamic Grid Adaptation (DGA) model (Podber 1997). This model computed water movement and heat transport in the area of the Cook Plant discharge. The Lake Michigan ci rculation model from the LMMBS was used to provide boundary information required by the nearshore model. A standard atmosphere-lake heat exchange model, created by the GLERL and described by Kelley (1995) was updated and applied by LTI. The heat flux model provided surface boundary conditions for the temperature module in the DGA model. Finally, the dynamics near the high velocity diffuser were modeled using the U.S. E.P.A. CORMIX (Jirka et. al. 1996) model. The results from CORMIX were used to adjust the vertical mixing for the DGA model near the diffuser. Figure 1-2 shows a schematic of the models and the information that was passed between them.

The modeling study was conducted by completing the following tasks;

<u>Performance Testing:</u>

- Create model runs to simulate the 1978-79 plume data.
- Adjust internal model parameters to best simulate the 1978-79 plume data.

<u>April – November 1995 Simulation:</u>

- Use the adjusted model and the LMMBS boundary conditions to simulate April – November 1995 with the nearshore model.
  - Simulate three Cook Plant power levels.
    - low (permitted operation) 15.8 x 10^9 BTU/hr,
    - medium 16.8 x 10^9 BTU/hr, and
    - high 17.3 x 10^9 BTU/hr.
  - Simulate the region with no heat flux from the power plant to create an ambient condition.
  - Convert temperatures computed by the model to plume area.

Sensitivity Analysis:

- Examine model sensitivity to variation in the forcing functions.

The atmospheric and boundary forcing data that was required to complete these tasks, and the field data used for the comparison are listed in Table 1-1.

The 1995 period was chosen for simulation of the different power levels because it was the period with the best available information on lake circulation. LTI made a thorough investigation of the precipitation and atmospheric data from 1995 and determined that 1995 was a normal (average) year.

1.5 REPORT ORGANIZATION

This report is organized in terms of the following chapters:

- Chapter 2 presents background information on the Plant site and NPDES permit special conditions, and available databases;
- Chapter 3 presents a description of the site specific modifications added to the three-dimensional nearshore circulation model, the model grid, the atmospheric heat flux model, the procedure used to incorporate the LMMBS data into the nearfield model, and a discussion of the conversion from water temperature to plume size;
- Chapter 4 presents results of performance testing of the thermal plume model;
- Chapter 5 presents results of the 1995 simulation of the thermal plume for the three energy levels;
- Chapter 6 presents results from the sensitivity analysis of the nearshore model; and
- Attachment A details the application of the CORMIX model to the Cook Plant discharge diffusers.

2.0 BACKGROUND AND STUDY APPROACH

This chapter is divided into four subsections that present background information about the Cook Plant thermal plume study. These subsections are;

- a description of the plant and its location,
- a description of the special condition of the plant operating permit,
- a description of a previous plume investigation conducted in 1978 and 1979,
- an overview of the data from the 1978/1979 plume investigation, Lake Michigan Mass Balance Study (LMMBS) and Cook Plant meteorological data.

To assist with the background summary, Figure 2-1 displays a map of southern Lake Michigan with a 5 km grid superimposed and the nearshore region around the Cook Plant shaded. Figure 2-2 shows the nearshore model grid with bathymetry. Figure 2-3 illustrates a site map, including the positions of water intake and discharge pipes and offshore current and temperature monitoring stations.

2.1 PLANT DESCRIPTION

The Cook Plant is located on the southeastern shore of Lake Michigan near Bridgman, Michigan, approximately 18 kilometers (11 miles) south of Benton Harbor, Michigan. The plant consists of two pressurized water reactors (Units 1 and 2), which have a Maximum Generator Nameplate Rating of 1152 Mwe and 1333 Mwe, respectively. Condenser cooling water for the plant is withdrawn from and returned to Lake Michigan via a once-through cooling system. Cooling water is drawn through three intake cribs located approximately 686 meters (2,250 feet) offshore in approximately 7.3 meters (24 feet) of water. The condenser cooling water is discharged into Lake Michigan via two discharge pipes connected to slot-type discharge structures. These structures are situated 91 meters (300 feet) apart, and are located approximately 366 meters (1,200 feet) offshore in approximately 5.5 meters (18 feet) of water. The Unit 1 structure consists of two discharge slots, each 9.1 meters (30 feet) wide by 0.61 meters (2 feet high) and 0.46 meters (1.5 feet) above the lake bottom. The Unit 2 structure has three discharge slots, each 9.1 meters (30 feet) wide by 0.84 meters (2.75 feet) high and 0.53 meters (1.75 feet) above the lake bottom. The average exit water velocity is calculated to be approximately 4 m/s (13 ft/s) for both units.

2.2 PERMIT SPECIAL CONDITION

The Michigan Department of Environmental Quality (MDEQ) maintains regulatory authority over the thermal discharge from the Cook Plant. MDEQ placed a special condition on the discharge permit for the Cook Plant to assure that the thermal discharge from the plant would not create any adverse impacts on the Lake. The special condition

specifies a thermal plume study for permitted outfalls 001 and 002, to be conducted seasonally during spring, summer and fall, according to the following conditions:

- Each seasonal study shall include determination of the current velocity and volume which serves to dilute the discharge in Lake Michigan;
- Each seasonal study shall include a determination of the stratification of the effluent, if any, in Lake Michigan; and
- Each seasonal study shall include a determination of the predominant wind direction and velocity at the time of the study, and detailed mapping of the plume for each study.

2.3 1978 – 1979 PLUME INVESTIGATION

Shortly after the Cook Plant became fully operational in 1978, IMPC conducted a field study to map the thermal plumes emanating from the plant to comply with the special permit condition described in Section 2.2. This investigation was conducted in accordance with 1978 modifications to the terms of the NPDES permit, originally issued by the State of Michigan in December 1974. The modification required monitoring of the characteristics of the thermal plume emanating from the combined discharges of Units 1 and 2. In addition, the study was designed to provide sufficient data to evaluate any effect of the cooling water discharges on Lake Michigan aquatic life. The scope of the study included measurements of the thermal discharge during three study periods: June 15 through September 15, 1978, November 1 through December 1, 1978, and April 15 through May 15, 1979. Each study period consisted of a minimum of five sampling days during which a minimum of two plume resolutions were made. During the summer 1978 mapping period, eleven plumes were mapped on six different days. During the winter 1978 mapping period, eight plumes were mapped on four days. During the summer of 1979, ten plumes were mapped on five days. The data obtained during the three thermal surveys were analyzed for the following information:

- the location of the centerline of the plumes;
- the rate of excess temperature decrease along the plume centerlines;
- plume widths;
- plume thickness; and
- the volume of water which served to dilute the discharge.

Other variables monitored during the survey periods included ambient lake temperatures, ambient lake currents, wind speed and direction, condenser intake and discharge temperatures, condenser flow rate, reactor power and the spatial distribution of temperatures within the thermal plume.

2.4 DATA USED FOR MODEL ASSESSMENT, BOUNDARY CONDITIONS AND BATHYMETRY

The 1978-1979 plume mapping field data were used to assess the performance of the nearshore model. Ambient lake current and temperature open water boundary conditions for the model simulations were derived from the output of the Lake Michigan Mass Balance Study Hydrodynamic Modeling Project (LMMBS-HMP). The LMMBS-HMP is a general circulation model of Lake Michigan for the year 1995 based on the Princeton Ocean Model (POM) (Blumberg and Mellor 1987). Current and temperatures computed by the LMMBS-HMP for April through November 1995 were used as input to the nearshore model. Meteorological data for the year 1995 were obtained from the LMMBS-HMP database and from a weather station located at the Cook Plant. These meteorological data were used as input to the heat flux model which computes heat exchange between Lake Michigan and the atmosphere. Lake Michigan bathymetry data also were used for the development of the nearshore model. Each of these four databases is described more fully below.

2.4.1 1978-1979 PLUME INVESTIGATION DATA

Prior to selecting a data set for model assessment, all of the 1978 – 1979 plume mapping field data were synthesized into a manageable format so that the data could be reviewed and analyzed more easily. In addition, the data were categorized according to the degree of lake calmness described for the various plume mapping days. Although this criterion is somewhat subjective, it serves as a broad screening tool for choosing model assessment data. The daily logs from the January 1980 thermal discharge report were referenced for information regarding the weather and lake conditions for each mapping event. The height of swells or relative calmness of Lake Michigan was documented in each daily log, and this information provided guidance on how to classify the plumes. Three broad categories were selected for the classification scheme, as presented in Table 2-1, plumes that were mapped on relatively calm lake days; plumes that were mapped when lake swells were less than or equal to approximately two feet in height (i.e. days with light lake chop); and plumes that were mapped when lake swells were greater than two feet in height (i.e. fairly choppy lake days).

For each plume mapping event in each category, the information provided in Table 2-1 includes: the date and time of the event; meteorological conditions (wind speed, wind direction and air temperature); percent reactor power and cooling water intake and discharge temperature for each of the two reactor Units; plume area at five depth horizons (surface, 1 meter, 2 meters, 3 meters and 4 meters); the maximum width of the plume at a depth of one meter; plume volume; the average, minimum and maximum lake water ambient temperatures at the five depth horizons; and surface current speed and direction at 500 meters (1,640 feet) offshore and 1000 meters (3,280 feet) offshore.

Additional ambient lake temperature and lake current information were recorded on the plume mapping days at various offshore stations. The Figure 2-3 site map depicts the locations of the three temperature recording stations (north inshore, south inshore and west offshore) and the four current recording stations (north inshore, north offshore,

south inshore and south offshore). Tables 2-2 and 2-3 summarize the ambient lake temperature and lake current data, respectively, for each plume mapping event. In addition, these data are categorized consistent with the classification system used in Table 2-1.

A set of model assessment data were selected from the 1978 – 1979 plume mapping data using the following selection criteria:

- reactor power for each of the two reactor units was above 75 percent;
- plume outlines were clear and distinct relative to ambient lake conditions;

A set of six plumes was selected for model assessment that satisfied the criteria listed above. They were mapped from November 1, 1978 through November 3, 1978. These data are available as plume maps, from which volume estimates and other plume statistics were derived for various depth horizons. Boundary temperatures and velocities were derived from the ambient lake current and temperature data associated with these event s.

2.4.2 LMMBS DATA

Figure 2-1 illustrates the 5 km computational grid used in the LMMBS-HMP for the southern part of Lake Michigan. The LMMBP-HMP grid blocks that overlap the Cook Plant nearshore model grid are depicted in Figure 2-4 which shows the nearshore model grid as the fine 100 x 100 meter mesh centered on the Cook Plant. The 5000 x 5000 meter grid blocks labeled 23-9,24-9,23-10, and 24-10 are the LMMBS grids closest to the Cook Plant. Water temperature and current vector information from LMMBS-HMP blocks 23-9, 24-9, 23-10 and 24-10 were used to derive open water boundary conditions and forcing functions for the nearshore model simulation runs. The current data are presented as the northern and eastern components of the resultant current vector in mete rs per second (m/s), and are referenced from the midpoints of the southern and western edges of the blocks, respectively. For each of the northern and eastern components, the data are presented by depth at 3 hour increments; therefore, eight curves are de picted for each day of the month (i.e. hours 0, 3, 6, 9, 12, 15, 18, 21). Water temperature data are presented by depth at 6 hour increments for each day (i.e. hours 0, 6, 12 and 18), and are referenced to the midpoints (centers) of the four LMMBS-HMP blocks.

Meteorological information for 1995 also were obtained from the LMMBS-HMP database, including cloud cover observations. Chapter 3 describes more fully how the LMMBS-HMP data were used to develop water column temperature and current forcing functions for use as open water boundary conditions in the predictive simulations.

2.4.3 COOK PLANT METEOROLOGICAL DATA

Additional input information was obtained from a weather station, at the Cook Plant which included hourly wind speed and direction, air temperature and rainfall. The Cook Plant weather station is located on the northwest corner of the Cook Plant, approximately 100 meters from the shore. Hourly dew point temperatures for Cook Plant were calculated from the Cook plant and LMMBS-HMP meteorological databases.

2.4.4 Lake Michigan Bathymetry Data

Water depth data were obtained from a compact disk of Lake Michigan bathymetric by NOAA (GLERL, 1998).

3.0 THREE-DIMENSIONAL NEARSHORE CIRCULATION MODEL

This chapter describes how the existing lake wide circulation model was modified for nearshore application through the addition of model routines and the development of the nearshore model grid and bathymetry, application of a heat flux model, and generation of open boundary conditions for velocity and temperature. Also discussed is the procedure used to convert the computed lake temperatures into plume sizes.

3.1 MODEL ROUTINES FOR NEARSHORE APPLICATION

The nearshore model application required the modification of an existing circulation model to be used in the nearshore region. The existing model, the Dynamic Grid Adaptation (DGA) model (Podber 1997, Podber and Bedford 1998) solves the Reynold's averaged Navier-Stokes equations with the hydrostatic approximation and the Boussinesq approximation (Gill 1982, Pedlosky 1987). The DGA model includes numerical routines designed to perform computations in the Great Lakes, specifically to account for sharp temperature changes in regions where the depth changes rapidly. The DGA model is fully developed and has been applied to idealized lakes and to Lake Michigan and Lake Erie.

Figures 3-1 and 3-2 provide a graphical description of the 3-dimensional nearshore circulation model. Figure 3-1 describes the structure of the nearshore model in flow chart format. Figure 3-2 is an information flow chart that outlines how data are linked between the subroutines and how information is passed between them.

Modification of the DGA model for a nested nearshore application required incorporating routines to model the atmospheric forcings and fluid dynamics:

- Cook Plant heat flux,
- Atmospheric heat flux,
- Boundary conditions for momentum,
- Boundary condition for heat,
- Turbulent mixing,
- Shoreline drag.

3.1.1 COOK PLANT EFFLUENT HEAT FLUX

The Cook Plant heat flux was incorporated by choosing the grid above the discharge and setting the advective flux ($w \frac{\partial T}{\partial z}$) in the heat equation by explicitly including the flow and the temperature gradient. The discharge for Unit 1 is placed at grid node i = 36, j = 41 and Unit 2 is places at i = 36, j = 40.

$$\text{Heat Flux at Unit 1} = w_1(T_{36,41,M-1} - T_{36,41,M})/\Delta z \quad [3.1.1]$$

$$\text{Heat Flux at Unit 2} = w_2(T_{36,40,M-1} - T_{36,40,M})/\Delta z \quad [3.1.2]$$

Where,

$w_{1,2} = \frac{Q_{1,2}}{(\Delta x \Delta y)}$, $Q_{1,2}$ is flow rate of discharge for Unit 1 or 2, Δx, Δy, and Δz are the grid spacing in the x,y, and z directions,

$T_{36,41,M}$, $T_{36,40,M}$ = temperature at Unit 1 and Unit 2, respectively, and

$T_{i,j,M-1}$ = temperature one grid above the discharge.

3.1.2 Atmospheric Heat Flux

A literature search was conducted to obtain a reference library of available heat flux models. The model approaches described in these references were evaluated and critiqued to delineate areas of improvement. In addition, physical property data and constants were researched and correlated for use in the model. From this reference analysis, a complete set of heat flux subroutines was coded and verified.

The subroutine set that describes surface heat flux in the nearshore model is derived from the 1988 heat flux model developed by M. McCormick of the Great Lakes Environmental Research Laboratory (GLERL), as applied to Lake Erie and described by Kelley (1995). The nearshore heat flux model uses standard meteorological observations and surface water temperature data as model input. The heat exchange with the atmosphere is then computed at each model grid point. The atmospheric data is typically recorded hourly requiring interpolation between observations.

The heat flux model uses a heat balance approach in which the total surface heat flux is equal to the sum of the shortwave radiation, long wave radiation, sensible heat flux, and latent heat flux. The terms are positive for energy flowing into the lake (i.e. lake warming) and negative for energy flowing out of the lake (i.e. lake cooling). In equation form, the model is:

$$H_{total} = H_{SR} + H_{LR} + H_S + H_L \quad [3.1.3]$$

Where:

H_{total} is the net heat flux with the atmosphere [W/m^2],
H_{SR} is the net incoming short wave radiation [W/m^2],
H_{LR} is the net long wave radiation [W/m^2],
H_S is the sensible heat transfer [W/m^2],
H_L is the latent heat transfer [W/m^2].

The following subsections provide the mathematical descriptions of the shortwave radiation, long wave radiation, sensible heat flux and latent heat flux terms in the nearshore model heat flux governing equation.

3.1.2.1 Short Wave Radiation

The short wave radiation term is a function of clear sky radiation. Clear sky radiation is predicted by a regression equation from the solar zenith angle, and is modified by cloud cover. The resulting equation follows Cotton (1979):

$$H_{SR} = (SR_c)(CLD) \qquad [3.1.4]$$

Where:

SR_c is the net incoming short wave radiation for clear sky conditions,
CLD is the "cloud effect" term.

SR_c is computed from the equation:

$$SR_c = a_0 + a_1\cos(Z) + a_2(\cos(Z))^2 + a_3(\cos(Z))^3 \qquad [3.1.5]$$

Where:

a_o, a_1, a_2, a_3 are regression coefficients,*
Z is the solar zenith angle (the angular distance of the sun from local vertical). †

CLD is computed from the equation:

$$CLD = c_0 + c_1S_c + c_2(S_c)^2 + c_3(S_c)^3 + c_4(RN) \qquad [3.1.6]$$

Where:

S_c is the opaque cloud cover amount‡,
$(c_o, c_1, c_2, c_3, c_4) = (0.999, -0.425, 0.922, -1.140)$,
RN = 0 if it is not raining,
= 1 if it is.

In short wave heat budget calculations, the penetration of solar radiation into the water column is an important property that needs to be addressed. The remainder of this subsection examines the quantitative assessment of the extinction coefficient for the Cook Plant site.

---

* The a- term regression coefficients have been calculated by Cotton for twenty-six U.S. stations. The term closest to the area of interest is Madison, Wisconsin. Separate terms are provided for morning and afternoon because turbidity is considered to be significantly higher in the afternoon than in the morning. The a_o term also varies by month to account for seasonal variations in turbidity, precipitable water and albedo.

† The solar zenith angle is calculated according to Guttman and Matthews (1979).

‡The opaque cloud cover amount is assumed to be equal to the total sky cover and varies from 0 to 1.

3.1.2.2 Penetration of Incoming Short Wave Radiation into the Water Column

The degree of penetration of sunlight into the water column has a significant effect on many areas of water quality. The water surface receives the maximum solar radiation and the intensity of radiation decreases approximately exponentially with depth as it penetrates through the water column. There are two principal mechanisms for such extinction of solar radiation: absorption (where short wave energy is transferred to heat), and scattering (the effect of reflection and diffraction by suspended particles). These mechanisms are illustrated in Figure 3-3. The degree of penetration depends on various factors, such as the presence and amounts of nonvolatile suspended solids, organic detritus matter and living particulates in the water column. Also, there may be a selective absorption or scattering of different regions of the solar spectrum (i.e. from infrared to ultraviolet).

Generally, a simple technique is used for the measurement of light penetration into a water body. In this technique a target (something distinctive enough to facilitate its ready recognition by the human eye) is lowered into the water until the target disappears from the view. The depth at which the target disappears can then be related to the extinction coefficient. A standardized target used in water quality work is the secchi disk. Various workers also have provided some theoretical and empirical formulations to calculate the extinction coefficients. The use of these formulations requires data for additional parameters such as total suspended solids, phytoplankton chlorophyll, and detritus.

The general approach for quantifying solar radiation extinction in a water column is based on the principle that the extinction of light is proportional to the light intensity at any depth. Therefore, a differential equation that expresses this observation is

$$\frac{dI(z,\lambda)}{dz} = -K_e(\lambda)I \qquad [3.1.8]$$

$$I = I_{0,\lambda} \ at \ z = 0 \qquad [3.1.9]$$

Where:

$I(z,\lambda)$ is the light intensity at depth z in W/m^2,
Z is the depth in m,
$K_e(\lambda)$ is the extinction coefficient in m^{-1},
I_0 is the incoming solar radiation at the surface z = 0, and
λ is the wavelength in nm.

The actual amount of solar radiation that arrives at a water surface depends on the following factors:

- the duration of sunlight throughout the day,
- latitude and longitude of the water body,

- the elevation of the sun,
- cloud cover, and
- the reflective conditions of water.

Solving equation [3.1.8] with the boundary condition described by equation [3.1.9] gives equation [3.1.10], also known as Beer-Lambert law:

$$I(z,\lambda) = I_{0,\lambda}\, e^{-K_e(\lambda)z} \qquad [3.1.10]$$

To use equation [3.4.7] for calculating the radiation at any depth requires the incoming solar radiation intensity $I_{0,\lambda}$ and light extinction parameters.

The depth dependence of the solar radiation in a well mixed water body is dictated by the optical characteristics of that water mass. Figure 3-4 shows the estimated decrease in solar radiation with depth for various water bodies, using the light extinction coefficients summarized in Table 3-1. The light intensity at the surface is assumed to be 100 W/m^2 for each water body. The clarity of some waters, such as Lake Tahoe, is remarkable where the light penetrates approximately 100 m in depth. On the other hand, turbid waters allow the radiation transfer to only a meter deep. So the attenuation of light increases greatly with turbidity.

For Lake Michigan and Lake Erie the respective extinction coefficients are similar for the visible part of the spectrum, and for the infrared region of the spectrum the extinction coefficients are the same. The clarity of some of the waters is contrasted with turbid waters, where the extinction coefficients may even be an order of magnitude greater.

3.1.2.3 Long Wave Radiation

The long wave radiation term is a function of the water temperature, air temperature and cloud cover. The equation follows Wyrtki (1965):

$$H_{LR} = -(S_{SB})(T_W)^4(0.39-0.05e_a^{1/2})[1.0-(k)(S_c^2)] - 4.0(S_{SB})(T_W)^3(T_W-T_A) \qquad [3.1.11]$$

Where:

S_{SB} is the Stefan-Boltzmann constant, 5.67051E-8 watts/(m^2 K^4),
T_W is the water temperature in degrees Kelvin,
e_a is the vapor pressure of air in millibars,
k is a parameter that increases linearly with latitude from 0.5 at the equator to 0.8 at 70° of latitude,
T_A is the air temperature in degrees Kelvin.

Long wave radiation is a function of emissivity, although this term is not included explicitly in Equation [3.1.11]. Emissivity is defined as the relative emission power of a radiating surface, expressed as a fraction of the emissive power of a black body radiator at the same temperature. The long wave radiation formula provided by Wyrtki assumes

emissivity equal to one; however, the literature search indicated emissivity values ranging from 0.97 to 1.0. Wyrtki's formula was modified slightly by multiplying equation [3.1.11] by an emissivity value equal to 0.97.

3.1.2.4 Sensible Heat Flux

The sensible heat flux term is the amount of heat exchanged across the air-water interface due to a temperature differential. It is a function of air density, heat capacity, wind speed, and water temperature and air temperature. The calculation uses a bulk transfer approach according to McBean et al. (1979):

$$H_S = (\rho_a)(C_p)(C_H)(U)(T_W - T_A) \qquad [3.1.12]$$

Where:

ρ_a is the density of air, [kg/m^3]
C_p is the specific heat of air at constant pressure, [J/(kg K)],
C_H is the bulk heat transfer coefficient from the momentum model [dimensionless],
U is the wind speed [m/s],
T_W is the water temperature [K], T_A is the air temperature [K].

The method used to calculate the dimensionless bulk heat transfer coefficient (C_H) is presented in section 3.1.2.6.

3.1.2.5 Latent Heat Flux

The latent heat flux term is the amount of heat lost or gained by evaporation or condensation and also is calculated using the bulk heat transfer approach. It is a function of air density, water latent heat of vaporization, wind speed, water temperature, and air humidity. The equation presented by Kelley (1995) is:

$$H_L = (\rho_a)(L_V)(C_D)(U)(q_A - q_W) \qquad [3.1.13]$$

Where:

L_V is the latent heat of vaporization at the temperature of water surface T_W [J/kg],
C_D is the bulk transfer coefficient for momentum [dimensionless],
q_A is the specific humidity of the air [dimensionless],
q_W is the specific humidity of the air at the water surface [dimensionless].

The q_A and q_W functions are calculated by:

$$q_A = 0.62185e_A/(P - 0.37815e_A) \qquad [3.1.14]$$

$$q_W = 0.62185e_W/(P - 0.37815e_W) \qquad [3.1.15]$$

Where:

e_A is the saturation vapor pressure,
P is the air pressure,
e_W is the saturation vapor pressure of water at T_W.

The method used to calculate the dimensionless bulk transfer coefficient for momentum (C_D) is presented in section 3.1.2.6.

3.1.2.6 Calculation of the C_D and C_H Coefficients

This section summarizes the procedures used to calculate the dimensionless bulk transfer coefficient for momentum (C_D) and the bulk transfer coefficient for heat (C_H). The C_D and C_H coefficients are used in the calculations of the latent and sensible heat transfer terms, respectively. Both C_d and C_h are dependent on the stability of the lowest few meters of the atmospheric boundary layer, the height of wind measurement and the wind speed. These coefficients also include the effects of surface roughness.

The bulk transfer coefficient for momentum, C_D, (also known as drag coefficient over water) is used in the latent heat transfer term and is a function of wind speed and boundary layer stability. It is described by the equation

$$C_d = \frac{u_*^2}{u_z^2} \qquad [3.1.16]$$

Where:

u_* is the friction velocity,
u_z is the surface wind speed at a specific height, z.

The variable u_* is not a readily measured parameter; therefore, an empirical method is used to obtain u_* from measurements of u_z and air-lake temperature difference. The air-lake temperature difference is calculated by taking the difference of air temperature and the water surface temperature.

GLERL has developed a profile method to estimate u_* (Schwab 1978; Liu and Schwab 1987). This method to estimate u_* is based on Monin-Obukhov (M-O) similarity theory (Monin and Obukhov, 1954) and on the works of Businger et al. (1971), Long and Shaffer (1975) and Smith and Banke (1975).

3.1.3 Boundary Conditions for Momentum

3.1.3.1 Plume Momentum

The high velocity diffusers from Units 1 and 2 impart a substantial amount of moment into the flow domain. Early tests with the numerical model demonstrated that it was necessary to include the exit momentum in order to correctly model the plume shape. Including the plume momentum required modification of the nearshore model, and some study of the Unit 1 and 2 diffuser schematics.

The offshore component of velocity was multiplied by the flow rate and the fluid density to compute the amount of momentum flux entering the control volume next to the discharge.

$$M_{in} = \rho\ (u\ Q)\ \ [\text{kg m/s}^2] \qquad [3.1.17]$$

This momentum was added into the grid cell adjacent to the discharge grid, and the nearshore circulation model transferred the momentum throughout the model domain in accordance with the Navier-Stokes equations.

3.1.3.2 Momentum from Lake Michigan

The boundary conditions to incorporate momentum from Lake Michigan were chosen so that the information needed from the far field model was incorporated at the same ti me that the important effects of the wind stress on the computational domain were included. The boundary conditions applied for the performance assessment are shown in Figure 3-5 and summarized in Table 3-2. In Figure 3-5 the shoreline boundary is labeled as boundary A, the northern boundary perpendicular to the coastline is called boundary B, the boundary in the lake and parallel to the coastline is called boundary C, and the southern boundary perpendicular to the shoreline is labeled boundary D.

The wave radiation condition applied to boundaries B and C allows for the free surface wave to propagate out of the computational domain with minimal reflection. The method of wave radiation has been well documented in the literature, including many applications (Camerlengo and O'Brien 1980, Matano et. al. 1998, Orlanski 1976, Roed and Smedstad 1987, Wurtele et. al. 1971).

The momentum boundary conditions used for the 1995 simulation are shown in Table 3-3. Velocities from the LMMBS model were used to form the boundary conditions for boundaries B and D.

3.1.4 Lake Michigan Boundary Condition for Heat

Heat from the far field LMMBS-HMP model domain was exchanged with heat in the nearshore model domain by two processes, advective and diffusive. The diffusive process depends on the temperature gradient at the boundary, as given below;

$$\text{Diffusive heat flux at B and D} = A_Y \frac{\partial T}{\partial y} \qquad [3.1.18]$$

$$\text{Diffusive heat flux at C} = A_X \frac{\partial T}{\partial x}\text{, and Diffusive heat flux at A} = 0. \qquad [3.1.19]$$

where, A_X, and A_Y are the turbulent diffusivites of heat in the x and y directions respectively.

Advective heat transport across the nearshore model boundaries is controlled by the velocity at the model boundary. When flow is entering the model domain, the incoming water is given the boundary condition temperature. When flow is leaving the model domain, the exiting water temperature is set to the temperature of the internal node that it is leaving from.

3.1.5 TURBULENT MIXING

3.1.5.1 Background

Turbulence models are used to estimate the extent of mixing that occurs in a fluid. Even though there are many different types of turbulence models, they all have the common goal of quantifying the amount of mixing that is generated by turbulence in the flow field. Turbulent diffusion of mass and momentum is not a property of the fluid, but rather a property of the flow of the fluid, which is why a turbulence model has to be closely linked with the fluid flow.

Turbulence is created by shear in the fluid, which occurs at the boundaries of the flow domain, and at internal regions of fluid where there is a velocity gradient. Turbulence is destroyed, or dissipated naturally by the resistance to flow due to molecular viscosity. Turbulence is dampened if there is a density stratification in the fluid due to the work that is required in order to lift dense water into regions that are less dense. This work drains energy from the turbulence field, therefore inhibiting turbulent mixing.

The turbulent mixing parameter for momentum is analogous to molecular viscosity and is referred to as eddy viscosity. The turbulent mixing parameter for scalar properties like temperature, salinity and concentration is analogous to molecular diffusivity and is called the eddy diffusivity. The reference to eddies is based on the concept that turbulence consists of eddies of many different widths. These eddies deform and mix the fluid properties. Turbulent eddies are described by two features, kinetic energy and length scale. The speed (κ) of the eddy rotation and the width (λ) of the eddy are considered to be the two major factors that control the turbulent mixing.

A review of the development and application of turbulence models can be found in American Society for Civil Engineers (ASCE) 1988. The ASCE 1988 articles follow the convention set by Mellor and Yamada (1974) who created a framework for comparing turbulence models based on the number of transport equations that are used in the model. Table 3-4 lists the various levels, variables used, and some comments about each. Level 0

models consist of a parameterization of mixing based on field data. As such there are no transport equations to be solved. Often the Level 0 model will include the effects of density stratification by scaling down the mixing appropriately. Level 1 models solve a transport equation for a quantity known as turbulent kinetic energy (κ). Level 2 models solve a transport equation for κ, and for a variable know as the mixing length scale (λ). The Level 2.5 equations solve for both κ and λ, and include anisotropy in the mixing field by solving a set of algebraic equations. A Level 3 turbulence model requires at least 9 transport equations, which is why there have been no applications on a geophysical scale reported in the literature.

3.1.5.2 Nearshore model application

The nearshore model uses a zero equation turbulent mixing model that is based on the Pacanowski and Philander (1981) approach with the constants adjusted for Great Lakes data (Aubert 1981) by Podber (1997).

The eddy diffusivity and viscosity are functions of vertical gradient of density as described by the gradient Richardson number (**Ri**). An expression for **Ri** is given below

$$Ri = \frac{\beta g \frac{\partial T}{\partial z}}{(\frac{\partial u}{\partial z})^2 + (\frac{\partial v}{\partial z})^2}, \qquad [3.1.20]$$

where;

T is the water temperature in °C, g is the acceleration due to gravity,

β is the thermal expansion coefficient of water, $\beta \sim 8.75 \times 10^{-6}$ (T + 9.),

u, and v are the horizontal components of velocity.

The vertical eddy viscosity (A_z) and the vertical eddy diffusivity (K_z) are given in the equations below;

$$A_z = \frac{\nu_0}{(1+\alpha\, Ri)^n} + \nu_b, \qquad [3.1.21]$$

$$K_z = \frac{A_z}{(1+\alpha\, Ri)} + \kappa_b, \qquad [3.1.22]$$

where, ν_0, is the maximum shear driven mixing (**Ri** = 0), α and n are constants derived from field data, and ν_b, κ_b are background mixing levels.

An analysis of the sensitivity of current fields to these parameters was performed by Pacanowski and Philander (1981). The mixing model was studied by Nunez Vaz and Simpson (1994) who found the model compared well with the higher order turbulence schemes. Nunez Vaz and Simpson set the parameters as follows; $\nu_0 = 0.01$ m^2/s, $\alpha = 5$,

and n = 2. Figure 3-6 shows the eddy viscosity and diffusivity as a function of **Ri** for the parameters set by Nunez Vaz and Simpson.

The nearshore model used a lower value of ν_0, $\nu_0 = 10^{-4}$ which is more typical of observed values in the Great Lakes (Aubert 1981). The mixing model using the smaller ν_0 value lead to a more realistic vertical representation for the thermal plume for the Cook Plant. This is discussed further in Chapter 4, Model Performance Assessment.

3.1.6 SHORELINE DRAG

The presence of a shoreline will cause drag on the flow. When modeling flow with a large grid spacing (i.e. 1 km or more) the effect of the shoreline drag is small and is generally ignored. However, using a high resolution grid (i.e. 100 meters) the shoreline drag should be incorporated. A standard skin friction approach was chosen following Schlichting (1951), where the friction factor C_f is based on laboratory studies. A value of $C_f = 0.005$ was chosen based on the flow characteristics of the nearshore model. The wall stress is then computed using the following equation (Schlichting 1955):

$$\tau_w = C_f \frac{\rho}{2} U_\infty^2 \qquad [3.1.23]$$

Where,

τ_w is the wall stress [Pa],

ρ is density of water [kg/m^3],

U_∞ is the free stream velocity [m/s]
(the velocity that is outside of the wall boundary layer).

3.2 NEARSHORE GRID CONSTRUCTION.

A nearshore model grid was constructed by examining the flow domain and the plume charts that were made using the 1978-1979 data. Because none of the measured plumes extended farther than 3.8 km from the discharge in any direction, a computational domain of 8 km along the coast and 4 km out into the lake was established, along with a uniform horizontal grid spacing of 100 meters. This domain is appropriate because it is large enough to contain the entire plume and still is small enough to be computationally feasible with a 100 meter horizontal resolution.

Figure 2-2 illustrates the 8000 meter by 4000 meter nearshore model grid. This figure illustrates that the model grid is symmetrical with Cook Plant, with the long axis of the grid trending northeast-southwest (parallel to the shore and rotated approximately 18° from true north). The grid consists of 40 columns (numbered 1 through 40) and 80 rows (numbered 1 through 80). The origin of the grid is located on the southwest corner at node [1,1]. Cook Plant is located at grid node [41, 40].

Metric Cartesian coordinates were assigned to each grid node and to the center of each grid block. These numbers were obtained by using the latitude and longitude coordinate of the Cook Plant, by converting this coordinate to a metric equivalent, and by calculating the distance of each grid node and each block center relative to the Cook Plant metric. Metric grid locations also were assigned to relevant features, such as the plant intake and discharge lines and the temperature and current meter stations. These features are depicted on Figure 2-3.

3.3 NEARSHORE BATHYMETRY

Water depth data were obtained from a compact disk of Lake Michigan bathymetric information compiled by NOAA GLERL 1998. Local bathymetry data were added to the nearshore model, as depicted in Figure 2-2.

3.4 WATER VELOCITY OPEN BOUNDARY CONDITIONS

The LMMBS database for Stations 24-9 and 24-10 (Figure 2-4) were used to derive water current forcing functions for the southern and northern edges, respectively, of the nearshore model grid cells. The approach used to develop the water current velocity forcing functions assumed that the north-south component of flow from the LMMBS model is directly parallel to the Cook Plant shoreline (i.e. parallel to the north-south trending gridlines in the nearshore model).

The LMMBS model used twenty depth intervals at each station, which needs to be merged into the thirteen evenly-spaced layers in the nearshore model grid. The LMMBS current data are presented as the northern and eastern components of the resultant current vector in meters per second (m/sec), and are referenced from the midpoints of the southern and western edges of the LMMBS grid blocks, respectively. For each of the northern and eastern components, the data are presented by depth at 3 hour increments. For each of the twenty LMMBS depth intervals, the velocity data were linearly interpolated to provide hourly data for the thirteen layer nearshore model. The current velocity profiles from the twenty layer LMMBS model were merged into the thirteen layer nearshore model by a squeezing method that maintains the shape of the LMMBS velocity profiles. This method is based on a percent of total depth for each of the layers. For example, if the third layer of the thirteen layer nearshore model is located at 25% of the total depth interval for a given grid block location, then layer three of the nearshore model grid would be assigned a velocity value from the LMMBS layer located at 25% of its total depth. If the 25% depth for the LMMBS block is located between two layers, then the current velocity was calculated by linearly interpolating the two adjacent velocity values.

The east-west velocity component at the western boundary was determined by applying the radiation boundary condition at the western boundary.

3.5 WATER TEMPERATURE BOUNDARY CONDITIONS

The LMMBS water temperature database for Stations 23-9, 23-10, 24-9 and 24-10 were used to derive water temperature forcing functions for the northern, southern and western boundaries of the nearshore model grid. The LMMBS water temperature data are provided by depth at 6 hour increments for each day (i.e. hours 0, 6, 12 and 18), and are referenced to the midpoints (centers) of the four LMMBS blocks. As with the velocity data, the water temperature data were linearly interpolated for each of the twenty LMMBS depth intervals to provide hourly data for the thirteen layer nearshore model.

The water column temperature data for LMMBS block 24-9 were used to develop water temperature forcing functions for the south boundary of the nearshore grid. The water column temperature data for LMMBS block 24-10 were used to develop water temperature forcing functions for the north boundary of the nearshore grid. The easternmost boundary of the grid coincides with the shoreline where a zero flux condition was employed.

For the western boundary of the nearshore model grid, a spatially weighted average temperature was calculated for each westernmost nearshore grid block using the data from LMMBS blocks 23-9, 23-10, 24-9 and 24-10. An equation was developed for each of the nearshore blocks along the western boundary by calculating the distance of the center of each block from the centers of LMMBS blocks 23-9, 23-10, 24-9 and 24-10. The inverse values of these four distances were normalized and used as coefficients to multiply with the corresponding temperature profiles from the four LMMBS blocks.

As with the current velocity data, the LMMBS model used twenty depth intervals at each station to determine water temperature. These temperature data needed to be merged into the thirteen evenly-spaced layers in the nearshore model grid by a method that maintained the shape of the LMMBS temperature profiles relative to depth. The LMMBS water temperature data were correlated by depth to the horizontally equivalent layer in the nearshore model. For example, if layer three of the thirteen layer nearshore model grid is located at a depth of 5 meters, then a temperature would be assigned to this layer equal to the value from the appropriate LMMBS block temperature profile at a depth of 5 meters. If the 5 meter depth for the LMMBS block is located between two layers, then the water temperature was calculated by linearly interpolating the two adjacent water temperature values. The water temperature profiles were truncated at locations where the LMMBS depth exceeded the bathymetry of the nearshore model grid. Through this method, the water temperature profile relative to depth is maintained between the LMMBS grid and the nearshore grid.

3.6 CONVERTING WATER TEMPERATURE INTO PLUME SIZE

This section describes the process of turning water temperature, which is the output of the nearshore model into plume size, which is the concern of the regulatory agency. Two methods were chosen;

- A point by point method for April – August, and November,

- A field survey method for September and October.

The results from both methods were comparable to the data gathered in 1978-79. The good comparison with field data was the criterion for judging the methods to be valid. The seasonally changing thermal conditions, wind conditions, and circulation patterns precluded the applicability of using a single method for all months.

The point by point method requires the computation of an ambient temperature field, which is defined as the nearshore model computed with the plant heat flux set to zero. The model was then run with the identical forcings and the plant heat on. Plumes were computed by subtracting the model results with the plant on, point by point, from the model results with the plant off. This definition of ambient water conditions, and the plumes computed by using this definition will lead to plumes sizes that are conservative in the following sense. When plumes are measured in the field it is necessary that the plant be operating, which means that the "ambient" conditions determined during the field survey may be affected by the plant operation which would lead to the delineation of smaller plumes.

The field survey method to compute plumes size, was designed to simulate the way in which the field survey crew would define ambient water. The idea was to sample water temperatures from a set of points that formed a ring around the discharge. The points were chosen to be outside of the influence of the plume and the maximum temperature from the ring was chosen as the ambient temperature. The plumes would then be determined by subtracting off the ambient temperature.

The use of the field survey method was required because the point by point method did not always lead to plumes that were reasonable. For certain cases, especially during the fall turn over in September and October, the point by point comparison lead to plumes that included water entering from the Lake Michigan boundary condition. These plumes were not centered on the discharge and were large rectangular regions near the boundary. In these cases the buoyant thermal discharge influenced the circulation pattern in the nearshore model relative to the simulations with no thermal discharge, and the point by point method counted the mismatched regions as plume water.

The two methods computed plumes that appeared reasonable and look similar to the plumes measured in 1978-79. In addition, the point by point method and the field survey method both compared well to the field data of 1978-79. The comparison is explained in detail in Chapter 4, Model Performance Assessment.

4.0 MODEL PERFORMANCE ASSESSMENT

In order for the numerical model to be useful for regulatory decision making, the model performance must be assessed and deemed acceptable. This process has three steps;

- vertical turbulent mixing parameters were set to match site specific conditions,
- a comparison between model behavior for the 1995 simulation and measured data from 1978-79, on the seasonal time scale was performed,
- and a detailed comparison between modeled and measured plumes was performed with a three day simulation.

The performance analysis of the nearshore model indicates that the model results are highly credible. The major internal parameter, vertical turbulent mixing, was adjusted so that the nearshore model results agree to within 0.2 °C of the CORMIX model results. The seasonal analysis shows that the model results are consistent with the data gathered in the 1978-79 field survey. The short term performance analysis shows that the model is able to compute plume shape, and area accurately. The model has a high level of reliability.

For the nearshore model, the vertical mixing due to turbulent fluid motions was adjusted based on comparing nearshore model runs with 1978-79 field data to create a vertical temperature structure that qualitatively agrees with the data. The details of the strong mixing that occurs near the high velocity discharge structures at the Cook Plant were addressed by applying the CORMIX nearfield mixing model, and adjusting the nearshore model appropriately.

Once the vertical mixing was determined, the model performance was assessed by comparing model results to seasonal averages of the observed data, and by running a three day simulation from November 1 – 3, 1978 and comparing the results to six plumes that were measured over that period. The following sections describe in detail the adjustment of the vertical mixing, the seasonal comparison with data, and the three day simulation.

Recall that the 1978-79 thermal plumes were measured, but there is not enough available boundary data to run a circulation model for the periods when the data were collected. The LMMBS study of 1995 has sufficient boundary data to support long term circulation models, but no plumes were measured in 1995. The mismatch of measured plumes and availability of boundary circulation data required that model performance be assessed by comparison of plume size and checking that the model results and measured data provide consistent characterizations of the plumes.

4.1 ADJUSTING VERTICAL MIXING

Adjusting the vertical mixing coefficient based on site specific information as well as CORMIX model results lead to the proper incorporation of the mixing induced by the high rate diffusers of the Cook Plant. The vertical mixing plays an important role in the modeling of oceans, estuaries, lakes, and nearshore regions. This is due to the fact the horizontal scales are often two to three orders of magnitude larger than the vertical scales. This leads to grid boxes that are quite thin, as in the case of the nearshore model.

The horizontal grid spacing in the nearshore model is 100 meters with 13 layers in the vertical where the depths range from 2 meters to 20 meters. Some grid boxes are as thin as 15 cm and larger in spatial extent than a soccer field. Such a box has 20,000 m^2 of surface area across the top and bottom faces, and there is 60 m^2 of surface area along the horizontal faces. Therefore changes in vertical mixing will have a dominant effect on the computed solutions.

The amount of vertical mixing that occurs in a body of water is determined by the amount of turbulent energy available for mixing which in the Great Lakes is related to wind stress on the surface of the lake. Aubert (1981) describes field studies that were performed on Lake Ontario to measure the amount of vertical mixing of dye. The maximum shear driven vertical mixing, ν_0 from Equation [3.1.7], exhibited a wide range of values ($10^{-4} \leq \nu_0 \leq 10^{-2}$). Therefore, the nearshore model was run with $\nu_0 = (10^{-4}, 10^{-3}, 10^{-2})$ for a period of 72 hours with idealized forcings to test the effect of the ν_0 plume computation. The time trace of the area of the plume at the surface, 1 m, 2m, and 4m for the three different settings of ν_0 is shown in Figures 4-1 through 4-3.

Figure 4-1 shows that the plume area at the surface, 1m, 2m, and 4m are almost identical, which implies that the water is well mixed for this case. When ν_0 was set to 10^{-3} (Figure 4-2), the top two meters were well mixed, and there was some mixing down to the 4 meter level. Figure 4-3, shows that when ν_0 was set to 10^{-4}, significant vertical variability in the plume was computed. This variability agrees qualitatively with the vertical variability observed in the measured plumes from 1978-79. As a result the value of ν_0 was set to 10^{-4} for the entire model domain, except for the region near the high flow rate diffusers for the Cook Plant discharge.

The Cook Plant discharge structures are high flow rate diffusers that induce complex flow fields close to the outfall which numerical circulation models are unable to directly compute. The U.S. E.P.A. CORMIX (Jirka et. al. 1996) modeling system is designed to combine empirical and analytic techniques to estimate the effects of the nearfield physics on dilution factors of jets and plumes. CORMIX was applied to the Cook Plant discharge structure and the following were computed; dilution factors, surface temperature, and distance traveled until the plume reached the surface. A detailed description of the application can be found in Attachment A.

The CORMIX model was given input data to represent the November 3, 1978 10:00 am plume. The input data consisted of variables such as ambient water temperature, wind speed, discharge temperature, background current. CORMIX predicted that the plume would reach the surface within 5 meters of the discharge and have a temperature of $19\,^{o}C$. Using this information, the parameter ν_0, was set to $\nu_0 = 0.01$ m^2/s for the grid cells above the discharges (cells i = 36, j = 40 and i = 36, j = 41). This caused the water properties to mix top to bottom, within the first grid, as predicted by CORMIX. For the cells adjacent to the discharge grid cells ν_0 was set to 10^{-3}, and it was unchanged at 10^{-4} elsewhere.

This choice for the vertical mixing parameter helped the nearshore model to produce temperature results that are in close agreement with the CORMIX. Figure 4-4 shows a time series of the water temperature at the surface above the discharge from the numerical model. The line at $19\,^{o}C$ represents the CORMIX steady state prediction of water temperature at the surface. After about 24 hours the dynamic model attains a surface temperature similar to that of the CORMIX model, the $\pm 0.5\,^{o}C$ line was drawn to aid in the visual interpretation of the results. At hour 66, the time for the CORMIX steady state solution, the nearshore model predicts a temperature of $18.8\,^{o}C$. Based on this comparison the adjustment to the vertical mixing allowed the nearshore model to perform in accordance with the CORMIX model.

4.2 SEASONAL ASSESSMENT

The seasonal assessment compared the results of the 1995 simulation with the 1978-79 field data to determine if the model results were consistent. The model and data showed plume sizes that were similar, with mean values within a standard deviation of each other.

The 1978-1979 field survey measured 29 plumes during the four months of sampling (see Table 4-1). The months of July 1979, September 1978, and November 1978 were chosen for seasonal assessment, while August 1978 was disregarded since there were only three plumes measured during that month. The field data for plume area at the one meter depth were averaged by month for, July 1979, September 1978, and November 1978.

The nearshore model simulation was performed for April through November of 1995. An average of the computed plumes was performed, for the months of July, September, and November, that excluded plumes when wind speeds were higher than the maximum or lower than the minimum wind speeds observed when the plumes were measured in 1978. Plumes at higher and lower wind speeds were excluded so that the model results could be compared with measured plumes without bias. Figures 4-5 through 4-7 show comparison between the plume areas at 1 meter depth for the measured and computed plumes. The error bars represents one standard deviation.

Figure 4-5 shows the measured July 1979 plumes in dark gray and the modeled 1995 plumes in lighter gray. The error bars are larger for the modeled plumes, because the model computed a wider variety of plumes than was typically measured. The average

plume size for the 1979 data was 200 hectares, and the average for the July 1995 simulation was 219 hectares.

Figure 4-6 shows the comparison between the September 1978 measured plumes and the September 1995 modeled plumes. The 1978 plumes averaged 364 hectares, while the 1995 plumes averaged 384 hectares. Figure 4-7 shows the comparison between the November 1978 measured plumes and the November 1995 modeled plumes. The measured plumes from 1978 averaged 373 hectares, while the modeled plumes from 1995 averaged 280 hectares.

The comparison shows that the model computed plume areas are close on average to the observed plume areas which means that on a seasonal basis the model reproduces what has been observed. This provides a sufficient comparison given that the model and data are not contemporaneous. The measured plumes from 1978-79 should not be identical to the modeled plumes of 1995, because the weather and lake conditions were likely to be different. However, it is necessary that the model reproduce the seasonal trend in plume size, e.g. smaller plumes in the summer, and produce plume sizes that are consistent with observation. The model has both reproduced the seasonal trend and produced results that are consistent with observation.

4.3 SHORT TERM ASSESSMENT: DAILY RUNS

The short term assessment showed that the model predicted both plume shape and plume size accurately. The plots of the plume size computations show that the model bounds the measured plume in size and shape. This is important because the uncertainties in the forcing functions and boundary data for 1978 will lead to uncertainty in the plume size. However, the fact that the model results bound the measured plume is remarkable given that the far-field boundary conditions along with the local wind records were unavailable for the 1978 simulations. The model performance is consistent with the measured data, and that deviations shown in this comparison are explainable by the uncertainties associated with 1978 model simulation.

The short term assessments were based on simulating a three day run from November 1 through November 3, 1978. Six plumes were surveyed during this period, one in the morning and one in the afternoon for each day. There were no boundary conditions measured at the time of the survey, and continuous atmospheric measurements were unavailable. Even so, the nearshore model did exceptionally well at predicting plume area and plume shape. The model computations bounded the measured plumes both in shape and size.

Current meters and thermisters were deployed relatively close to the outfall (see Section 2.4) during the 1978-79 field survey which required that the boundary conditions for the nearshore circulation model had to be extrapolated out 4 kilometers. The atmospheric conditions were derived from measurements taken at the Benton Harbor Airport approximately 18 km from the Cook Plant (Figure 4-8). The 72 hour run used a uniform initial temperature of 12.17 °C (53.9 °F) which was based on the observations.

The boundary conditions for this simulation consist of an imposed alongshore current on the southern boundary, and a wave radiation condition on the northern and western boundaries. The along shore current was set to .05 m/s based on typical flows reported by the current meter during the time period of the simulation. A logarithmic boundary layer was applied to the alongshore current.

4.3.1 Plume Area

The results from the plume area analysis show that the model predicts a highly dynamic system, which also points out the field data of 1978-79 represent a snap-shot of the system. The model results pass directly through some of the data points and are very close to most of them. The measured plume area is bounded by the model results for the area enclosed by the 2°C contour, and the 1 °C contour. This means that modeling system accurately represents plume areas within a temperature variation of $\pm 0.5\ ^{o}C$.

The simulation from November 1–3 was performed using the available data as thoroughly as possible. The results from the simulation demonstrate that the model is behaving credibly and does have predictive power. Figure 4-9 shows the time trace of the plume area at 1 meter depth. The plume measurements in 1978 took roughly two hours to complete. While the field crew was measuring the plume, the plume was evolving. This is expressed by the horizontal error bars attached to the plume measurements. Hours 18 – 22 were the morning and afternoon plumes for November 1. The simulation shows a dip in plume area around hour 18, and rises to pass through the error bar of the November 1 pm plume area. The model then predicts a peak in the plume area around hour 30. The plume area then drops down and passes very close to the data points for November 2. The model then predicts an increase in the plume size, but under predicts the plume size relative to the data.

The shape of plume area curve can be accounted for by comparing the plume area to the wind speed as in Figure 4-10. For the first ten hours the model is ramping up. After that, dips in the wind speed lead to rises in the plume area. For hours 23 to 26 the wind speed is zero, which is precisely when the plume area ramps up. Steady winds after hour 26 lead to a decay in the plume area, and the wind spike at hour 40 causes the plume are a to approach zero. The plume begins to rebuild and holds a relatively constant volume from hour 50 to hour 72. The response of the plume area to the wind speed underscores the importance of the atmospheric data and may explain the discrepancy at hours 65 -70. Wind data used in the simulation were from the Benton Harbor Airport, and may not be representative, in speed and direction, of the over lake winds. The importance of wind direction is also examined in Chapter 6 Sensitivity Analysis.

Table 4-2 shows the measured area for each of the 6 plumes, and the area enclosed by the 2°C contour, the 1.67°C contour, and the 1°C contour. Survey 1 shows that the model over-predicted the plume area. However, for surveys 2,3,4,5, and 6 the measured plume area is between the area of the 2°C and 1°C contours of the modeled plume. This means that modeling system accurately represents plume areas within a temperature variation of $\pm 0.5\ ^{o}C$.

4.3.2 PLUME SHAPE

The nearshore model simulated the plume shape accurately. In general, all of the computed plume shapes were similar to those measured, and many of the measured plumes fell inside of the 1°C contour and outside of the 1.67°C contour.

It is important to note that comparing the computed plume shapes with the measured plume shapes is the most exacting type of comparison. There were many judgment calls made about the data while it was being collected, and later when it was compiled into plume maps. The data collection team had to make an estimate of what the ambient water temperature was to draw the plume outline. In the model, the plume outline was drawn by subtracting the results of a model run with the plant running, from a model run without the plant running. This is a different definition of plume from that used by the field crew, but it is the best method for the model to determine ambient temperature.

The field crew took approximately two hours to measure a plume, which means that there are two model data points to compare with each measured plume, since the model results are hourly. Figures 4-11 through 4-16 show the plume plots for the six measurement data points shown in Figure 4-9. Figures 4-11 through 4-16 consist of two panels, each one being a computed plume for the hour shown on the plot. The panels are the rectangular model domain. The measured plume from the 1978 survey is shown as the thick solid line, and the computed plume is shown as a blue scale contour plot with dashed lines. The Cook Plant discharge is indicated by an asterisk placed at x = 3 600 m, y = 4000 m. There is a wind gage in the upper left hand corner of the plot, which shows wind speed in meters per second, and wind direction. The circle on the wind gage represents a wind speed of 5 m/s. The simulation date and time appears in the lower left region of the Figures. The computed and measured plume areas are reported in hectares (10^4 m^2). The 1.67 °C contour has been made solid and is the first region to be shaded since 1.67 °C (3 °F) is the regulatory delineation of a plume. The dashed 1°C line is informative in that it shows the extent of the computed plume. Discrepancies of ½ °C could extend or contract the plume, and the 1°C line indicates what the expansion would like.

Figure 4-11 shows that the computed plume is larger than the measured plume. Figure 4-12 shows that the plume areas are quite close. Although the measured plume shape is different from the computed plume, the extent of the 1 °C line indicates that the general plume direction is correct. Figure 4-13 shows a much smaller plume, and the computed and measured plumes are almost coincident. Figure 4-14 shows the plumes to be similar in size and orientation. The measured plume is bounded between the 1.67 °C contour and the 1 °C contour. Figure 4-15 shows that the modeled and computed plumes have grown and deformed in roughly the same manner. Also these figures show that the model has bounded the observations. Figure 4-16 again shows remarkable agreement in terms of plume shape and orientation. The measured plume is again bounded by the modeled plume.

A qualitative assessment of the model performance for the short duration plumes shows that the model does well at predicting the measured plumes of 1978. The general shape and plume direction is accurately portrayed. The growing and shrinking nature of the

plume is also well portrayed. The ability to pass these performance tests indicates that model results are credible.

4.4 CONCLUSIONS OF THE MODEL PERFORMANCE ANALYSIS

The performance analysis of the nearshore model indicates that the model results are highly credible. The major internal parameter, vertical turbulent mixing, was adjusted so that the nearshore model results agree within 0.2 °C of the CORMIX model results. The seasonal analysis shows that the model results are consistent with almost all of the data gathered in the 1978-79 field survey. The short term performance analysis shows that the model is able to compute plume shape, and area accurately. The overall model has a high level of reliability.

5.0 NEARSHORE MODEL RESULTS

The power levels and associated temperature changes that were simulated are listed in Table 5-1. The model results showed the system to be highly dynamic. The dynamic nature of the circulation of Lake Michigan was passed into the nearshore model by application of the LMMBS data through the boundary conditions. Strong wind fronts generated wind driven currents in the nearshore model that transported the plume in all possible directions. The conditions rarely remained stable enough for a steady plume shape to take form, and for those instances when the plume shape was steady, it did not last for more than a few hours.

For the fall months, a strong diurnal signal was detected in the computed plumes indicating a rapid heat loss at night when the atmosphere was significantly cooler than the lake. Plumes tended to be smaller and have 6 to 8 °C maximum temperature increases right above the Cook Plant discharge. The opposite was noted for the spring months where the atmosphere was warmer than the plume water. In this case, the atmosphere acted like a blanket to trap the heat. The plumes were observed to be larger in spatial extent, but less intense in temperature increase with 4 to 5 °C being typical of the maximum temperature deflection.

The summer plumes were on average the smallest plumes. This is due to the fact that for some periods of June, July, August, and September a thermal bar was in place. The thermal bar is a nearshore region of water that is heated faster than the offshore water because it is shallow. The fine grid resolution (100 meters) of the nearshore model meant that the depths along the shoreline were set to 2 meters. This allowed the nearshore model to compute a thermal bar.

The presence of the thermal bar means that at times the Cook Plant discharge was actually cooler than the receiving water. This model result, was at first seen as unlikely, but was later corroborated as observed by AEP biologists and consultants who were aware of the 1978-79 survey. Conditions that can lead to this phenomenon are the presence of the thermal bar, and the Cook Plant intakes being below the thermocline. For example, the Cook Plant intakes may draw water from below the thermocline that is 15 °C cooler than the water in the thermal bar. After circulating through the plant and gaining approximately 12 °C of temperature, the water is discharged water into the thermal bar, which is actually 3 °C warmer than the effluent. In this case there is no thermal plume. Temperature variations of 15 °C between the epilimnion and hypolimnion water have been measured in Lake Ontario (Aubert 1981), and are known to occur in Lake Michigan.

5.1 FREQUENCY ANALYSIS OF PLUME SIZE

A frequency analysis of the model results was performed by creating a histogram with 38 bins in 50 hectare intervals. For instance, the first four bins toll the number of plumes that ranged between 0 – 49 ha, 50 –99 ha, 100 – 149 ha, and 150 – 200 ha (see Figure 5-1).

The frequency analysis shows that over the course of the simulation, there was no significant effect due to operating the plant at higher energy levels. The biggest difference noted was that at the higher energy levels there were 7% fewer small plumes (0-49 hectares). The frequency of occurrence of larger plumes for the low, medium, and high power levels converged asymptotically.

The results from all of the model runs were combined to form a frequency analysis shown in Figure 5-1. For all three power levels, 50 hectare bins were created and each of the 5,856 (244 days times 24 hours/day) plumes were assigned to one of the bins. The x-axis of Figure 5-1 shows the 50 hectare bins, and the primary y-axis shows the number of plumes in each bin. Each of the bins has three bar charts, one for each power level. The line plot and secondary y-axis show the percent of plumes with areas greater than the current bin.

Figure 5-1 shows that the 0-49 bin contains approximately 57% of the plumes for the low power level, 53% of plumes for the medium level, and 50% of the plumes for the high power level. The range of 0-249 hectares accounts for 80% of all plumes at the low power level, 77% at the medium power level, and 74% at the high power level. The 0 - 449 range accounts for 91% of the low power level plumes, 88% of the medium power level plumes, and 85% of the high power level plumes. Several of the larger observed plumes in 1978 were 450 hectares or larger.

Of all of the bins, this initial bin shows the largest difference between the high and the low power level simulations. The bar charts for the 50-99 range, show that the high, medium, and low simulations had roughly the same number of plumes in this range. The bar charts that follow indicate that while there are more plumes noted at the high power levels, the number of extra plumes is small.

Qualitatively the frequency plot shows that when the plant is operating at higher power levels there are fewer very small plumes in the 0-49 bin, with the excess plumes from the high output being spread over the range of observed plumes. The percent curves approach each other asymptotically indicating that the extreme behavior does not vary between the low and the high energy levels.

5.2 AVERAGE MONTHLY PLUMES

Hourly model results were compiled in a database, leading to 720 plume areas for months with 30 days and 744 plume areas for months with 31 days. The average of the plume areas at 1 meter depth for the low, medium, and high runs are reported in Table 5 -2. The hourly model results for each month were examined to find plumes that had areas close to the monthly average. A single plume was selected as representative of the average conditions for that month. Figures 5-2 through 5-9 are contour plots of the thermal plume at 1 meter depth for the representative plume for April through September 1995 for the high power level simulation.

These figures are similar to the ones shown in the Model Performance Assessment chapter and are described as follows. The rectangular region represents the model

domain. The temperatures above ambient are contoured in a blue scale. The first contour drawn is the 1.67 °C (3 °F) contour. The next contour drawn is at 2 °C, and subsequent contours are drawn at 1 °C intervals. The plots have a wind gage in the upper left hand corner indicating wind speed and direction. The simulation date and time are no ted on the plot. The plume area in hectares is reported on the plot.

The April plot (Figure 5-2) shows the plume center to have migrated to the south of the discharge and has a maximum temperature of 5 °C. The wind was blowing from the north prior to when the image was plotted. The wind turned and began to blow from the southwest with relatively strong intensity. The plume here is beginning to double back on itself.

The May plume (Figure 5-3) is a southerly directed plume. The wind has died off and is beginning to turn to an easterly wind. Again the maximum plume temperature is 5 °C above ambient. Figure 5-4 is the representative June plume. It is smaller in extent than are the April and May plumes. Figure 5-5 is the July plume. The small size of this plume is partly determined by the large number of days in July when there was no plume due to the appearance of the thermal bar and the thermocline. The number of days with a zero plume held the average values down.

Figure 5-6 is the August representative plume. This plume was experience an easterly wind and relatively calm background lake circulation. The result is a symmetric plume. Figure 5-7 is the representative September plume. This plume has similar wind and circulation conditions to the August plume. The plume is about the same size as the August plume, but the maximum temperature is 6 °C. The thermocline is eroding so that the effluent is relatively more buoyant. Figure 5-8 is the October representative plume. This plume is small in area but relatively warmer, with an 8 °C rise above ambient. Figure 5-9 shows the November representative plume. This plume is larger in spatial extent than the October plume, and has a cooler maximum temperature at the surface of 6 °C.

5.3 MAXIMUM PLUMES

Although not required by the permit, an analysis was performed to evaluate the maximum simulated plume size for each of the eight simulated months. Initial assessment revealed unrealistically large plume sizes, substantially larger than the average or typical condition. However, closer examination revealed that many of the "computed" conditions were not in fact true plumes, but anomalies related to converting computed water temperatures into plume sizes. These anomalies were caused by transient conditions such as changing winds, changing circulation, upwelling and/or the formation of the thermal bar.

Displayed in Table 5-3 are the maximum plume areas after anomalous plumes were discarded. The maxima are not representative of the system, but are very short term transients. Often these plumes last for but a few hours, are typically confined to the upper two meters, and generally represent a transition condition that resulted from changing winds or circulation. Often the maximum plumes were a combination of two plumes, a

recently formed plume and a remnant plume from a previous condition, which quickly dissipated.

An illustration of these transient conditions can be seen in the computed November maximum plume. The model computed the maximum area as 1,975 hectares at 1 meter depth. However, this is a shallow plume extending only 72 hectares at 3 meters depth. Additionally, the maximum area of 1,975 hectares lasts at that magnitude but a couple of hours, and drops to 500 hectares 3 hours after the maximum level, and then to 78 hectares after 6 hours. These maximum conditions are transient and not representative plume conditions.

5.4 CONCLUSIONS

The monthly average plume sizes are larger when the plant operates at higher energy output levels. The frequency analysis of the plumes sizes and the power output levels shows that the distribution of plumes does not change much between the low, medium, and high power levels. There are fewer small plumes at the higher energy levels, but the frequency of large plumes converges for all of the power levels.

The maximum plumes are transient, often thin, and the result of transient atmospheric or lake circulation conditions.

6.0 SENSITIVITY ANALYSIS

A sensitivity analysis was conducted to examine the performance of the model when the atmospheric forcing functions varied. The five atmospheric variables used in the heat flux computation, wind speed and direction, air temperature, relative humidity, and cloud cover, are subject to uncertainty, variability, measurement error, and error associated with spatial projection. The sensitivity analysis quantifies the effects that uncertainty in the forcing functions has on the model predictions of plume area.

6.1 WIND SPEED

The first of the five tests performed was to vary the wind speed. The 72 hour performance analysis model run was recomputed with wind speed multiplied by a factor of 1.5 and by a factor of 0.5. All of the other variables remained the same as they were for the performance analysis test. Figure 6-1 shows the time trace of the plume area at 1 m for the three model runs. The figure also shows the measured data points from the November 1 – November 3, 1978. All of the simulations showed the same qualitative behavior. The higher wind speed runs computed plumes with consistently lower areas. The run with decreased wind speed had the plume areas ramp up more quickly, peak at a lower level, and then look similar to the other runs.

6.2 WIND DIRECTION, CLOUD COVER, AIR TEMPERATURE, AND RELATIVE HUMIDITY

The next four sensitivity tests were computed for a 24 hour period using idealized conditions. The wind direction was westerly and the wind speed was set to 3.7 m/s, which is the average wind speed of the November 1 - November 3, 1978 period. Figure 6-2 shows the model sensitivity to wind direction. The wind was rotated $\pm 45^{o}$ relative to westerly. The effect on plume size was large. This is due to the fact that the performance analysis model used a constant alongshore velocity unlike the 1995 model simulations, which computed the velocities based on the LMMBS currents and winds. When the wind had a component inline with the along shore current the plume areas tended to be smaller. When the wind opposed the alongshore current the plume areas were larger. This test shows two things; first the importance of computing currents that are consistent with the wind field, and second the sensitivity of plume areas to transitional events such as shifts in wind direction.

Figure 6-3 shows that the model is relatively insensitivity to cloud cover. This is a good result, because cloud cover is a subjective measurement and cloud cover can vary spatially at a distance from the observation point. Figure 6-4 shows that the computed plume areas are relatively insensitive to air temperature. Variations of 3 °C caused very little difference in the computed plume areas. Figure 6-5 showed that the computed plume areas did not vary as relative humidity was altered from 10% to 50%, but that

when the relative humidity was set to 100% some variation in plume size occurred after 15 hours into the simulation.

6.3 SENSITIVITY FINDINGS

The sensitivity analysis shows that the plume size is not greatly affected by variations in wind speed, cloud cover, air temperature, or relative humidity. The wind direction however had a significant effect on the model results. Fortunately wind direction can be reliably measured. The sensitivity of plume area to wind direction implies that wind shifts can lead to dramatic plume growth and decay, as was observed the 1995 model simulations.

7.0 CONCLUSIONS

A numerical modeling system was created that computed the thermal discharge from the Cook Plant. The model computed plumes that compared well to 1978-79 field data both on the seasonal and daily time scales. The numerical model was run to simulate April through November of 1995, using boundary forcing from the LMMBS-HMP model. Monthly averages were computed from the model runs and plumes representing the monthly average for the high power level were plotted.

The model results showed that there is not a significant difference between the plumes generated by the Cook Plant operating at the current level and the plumes generated by operating at the uprated levels. A frequency analysis showed that the when the plant was running at high output there were 7% fewer small plumes, plumes in the 0-49 hectare range. In the next largest plume sizes classes, 50-99, 100-149, and 150-199 hectares, all three power levels had roughly the same number of plumes. The frequency analysis also showed that the current plant operation and the plant operation at the higher power levels converge asymptotically in frequency for the larger plume sizes, meaning that they produce a similar number of large plumes.

8.0 REFERENCES

American Society of Civil Engineers Task Committee on Turbulence Models in Hydraulic Computations (1988). Turbulence modeling of surface water flow and transport: Parts I-V, *Journal of Hydraulic Engineering* **114**:(9) 970-1073.

Aubert, E. and Richards, T. (eds.), 1981. IFYGL – The international field year for the Great Lakes. National Oceanic and Atmospheric Administration, Great Lakes Environmental Research Laboratory, Ann Arbor, Michigan.

Bedient, P. B. and Huber, W. C., 1992. Hydrology and Floodplain Analysis, 2nd Ed. Addison-Wesley Publishing.

Blumberg, A. and G. Mellor. 1987. Three-Dimensional Coastal Ocean Models, A Description of a three-dimensional coastal ocean circulation model. *American Geophysical Union.* pp. 1-16.

Businger, J. A., J. C. Wyngaard, Y. Izumi and E. F. Bradley, 1971. Flux-Profile Relationships in the Atmospheric Surface Layer. J. Atmos. Sci., 28, 181-189.

Camerlengo, A.L. and J.J O'Brien. 1980. Open Boundary Conditions in Rotating Fluids. *Journal of Computational Physics.* **35**:12-35.

Charnock, H., 1965. Wind Stress on a Water Surface. Q.J.R. Meteorol. Soc., 81, 639.

Cotton, G. F. (1979). ARL models of global solar radiation, SOLMET, Volume 2 – Final Report. Research Triangle, NC, EPA, Air Resources Laboratories, pp. 165 – 184.

Deardorff, J. W., 1980. Stratocumulus-capped Mixed Layers Derived from a Three-Dimensional Model. *Boundary Layer Meteorol.* **18**: 495-527.

Deardorff, J.W. 1973. The Use of Subgrid Transport Equations in a Three-dimensional Model of Atmospheric Turbulence. *Journal of Fluids Engineering.* **95**: 429-438.

Denbo, D. and E. Skyllingstad. 1996. An Ocean Large-eddy Simulation Model with Applications to Deep Convection in the Greenland Sea. *Journal of Geophysical Research.* **101**: 1095-1110.

Galperin, B., Kantha, L., Hassid, S. and Rosati, A. (1988). A quasi-equilibrium turbulent energy model for geophysical flows, *Journal of the Atmospheric Sciences,* **45:** No. 1, 55-62.

Gill, A. 1982. *Atmosphere-Ocean Dynamics.* Academic Press, Dan Diego.

Great Lakes Environmental Research Laboratory (GLERL 1998), Office of Oceanic and Atmospheric Research, National Environmental Satellite, Data, and Information

Service, National Geophysical Data Center, Bathymetry of Lake Michigan, compact disk, digital data.

Guttman, N. B. and Matthews, D. J., 1979. Computation of extraterrestrial solar radiation, solar elevation angle and true solar time of sunrise and sunset. SOLMET, Volume 2 – Final Report. Asheville, NC, National Climatic Center, pp. 47 – 54.

Jirka, G.H., R.L. Doneker, and S.W. Hinton (1996). User's Manual for CORMIX: A Hydrodynamic Mixing Zone Model and Decision Support System for Pollutant Discharges into Surface Waters. Office of Science and Technology, U.S. Environmental Protection Agency, Washington D.C.

Kelley, J. G. W. (1995). One way coupled atmospheric-lake model forecasts for Lake Erie, Ph.D. dissertation, Ohio State University.

Liu, P. C. and D. J. Schwab, 1987. A Comparison of Methods for Estimating u* from a given uz and Air-Sea Temperature Differences. J. Geophys. Res., 92, 6488-6494.

Long, P. E. and W. A. Shaffer, 1975. Some Physical and Numerical Aspects of Boundary Layer Modeling. NWS TDL-56 (COM75-10980). National Weather Service, Techniques Development Laboratory, 37 pp.

Matano, R.P., E.D. Palma, J.M. Mesias, and P.T. Strub. 1997. Open Boundary Conditions for use in Coastal Models. *Proceedings of the Fifth International Conference. American Society of Civil Engineers.* pp. 541-555.

McBean, G. A., Bernhart, K., Bodin, S., Litynska, Z.,Van Ulden, A. P. and Wyngaard, J. C. (1979). The Planetary Boundary Layer. World Meteorological Organization Technical Note No. 165, U.D.C. 551.510.522

Mellor, G., and Yamada, T. (1974). A Hierarchy of Turbulence Closure Models for Planetary Boundary Layers. *Journal of the Atmospheric Sciences* **31**: 1791-1806.

Monin, A. S. and A. M. Obukhov, 1954. Basic Laws of Turbulent Mixing in the Atmosphere near the Ground. Tr. Akad. SSSR Geofiz. Inst., 24, 163-187.

National Oceanic and Atmospheric Administration, National Weather Service, Surface Weather Observation Reports for November 1978 and July 1979, Benton Harbor Tower, Michigan.

Nunes Vaz, R., and J. Simpson. 1994. Turbulence Closure Modeling of Estuarine Stratification. *Journal of Geophysical Research.* 99(C8): 16, 143-16, 160.

Orlanski, I. 1976. A Simple Boundary for Unbounded Hyperbolic Flows. *Journal of Computational Physics*. 21: 21-269.

Pacanowski, R. and S. Philander. 1981. Parameterization of Vertical Mixing in Numerical Models of Tropical Oceans. *Journal of Physical Oceanography.* 11: 1443-1451.

Panofsky, H. A., 1963. Determination of Stress from Wind and Temperature Measurements. Quat. J. Meteorol. Soc., 89, 85-94.

Paulson, C. A., 1970. The Mathematical Representation of Wind Speed and Temperature Profiles in the Unstable Atmospheric Surface Layer. J. Appl. Meteo., 9, 857-861.

Pedlosky, J. 1987. *Geophysical Fluid Dynamics,* second edition. Springer-Verlag, New York.

Podber, D.P. (1997). Modeling Strongly Stratified Flow with the Dynamic Grid Adaptation (DGA) Technique, Ph.D. Dissertation, The Ohio State University, Columbus, Ohio.

Podber, D.P. and K.W. Bedford (1998). An Analysis of Grid Convergence for the Dynamic Grid Adaptation Technique Applied to the Propagation of Internal Waves. Estuarine and Coastal Modeling, Proceedings of the Fifth International Conference. Eds. Spaulding, M.L. and Blumberg, A.F. American Society of Civil Engineers. pp.834- 849.

Podber, D.P., Yen, C.C., Regenmorter, L., Bedford, K.W., and Wai, W.H. (1994). A nearshore model for Cleveland CSO remediation design selection, in Hydraulic Engineering: Proceedings of the 1994 Conference in Buffalo N.Y. American Society of Civil Engineers. Eds. Cotroneo, G.V. and Rumer, R.R. pp. 222-226.

Roed, L.P, and O.M. Smedstad. 1984. Open Boundary Conditions for Forced Waves in a Rotating Fluid. *Siam J. Sci. Stat. Comput.* Vol. 5, No. 2, June, pp. 414-426.

Schlichting, H., 1951. Boundary Layer Theory, Seventh Edition, McGraw-Hill, Inc.

Schwab, D. J., 1978. Simulation and Forecasting of Lake Erie Storm Surges. Mon. Wea. Rev., 106, 1476-1487.

Schwab, D. J. (National Oceanic and Atmospheric Administration, Great Lakes Environmental Research Laboratory) and Beletsky, D. (University of Michigan, Department of Naval Architecture and Marine Engineering), (October 1988). Lake Michigan Mass Balance Study: Hydrodynamic Modeling Project, NOAA Technical Memorandum ERL GLERl-108.

Smith, S. D. and E. G. Banke, 1975. Variation of the Sea Surface Drag Coefficient with Wind Speed. Q. J. R. Meteorol. Soc., 101, 665-673.

Stull, R. B., 1988. An Introduction to Boundary Layer Meteorology. Dordrecht, The Netherlands, Kluwer Academic Publishers, 666 pp.

Wurtele, M.G., J. Paegle, and A. Sielecki. 1971. The use of Open Boundary Conditions with the Storm-Surge Equations. *Monthly Weather Review*. Vol. 99, No. 6, pp. 537-544.

Wyrtki, K. (1965). The average annual heat balance of the North Pacific Ocean and its relation to ocean circulation. *J. Physical Oceanography*, 70/18, pp. 4547 – 4559.

FIGURES

Figure 1-1 Study Approach

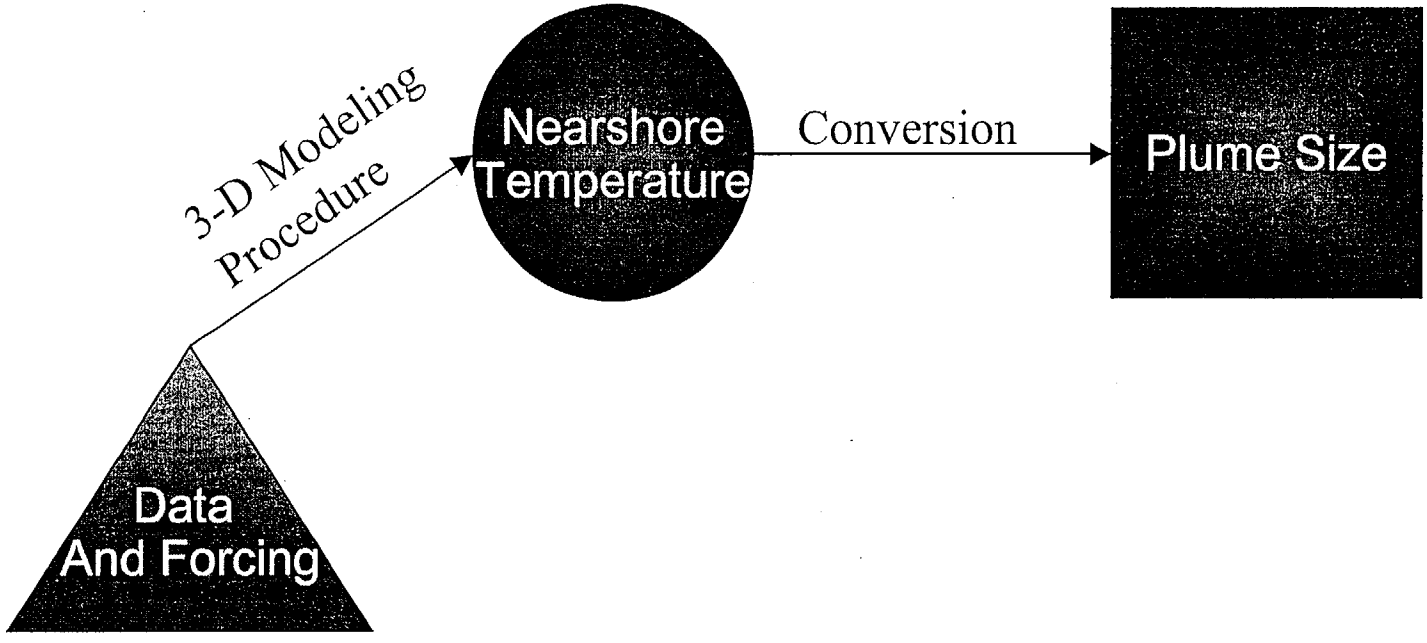

Figure 1-2 Model Approach

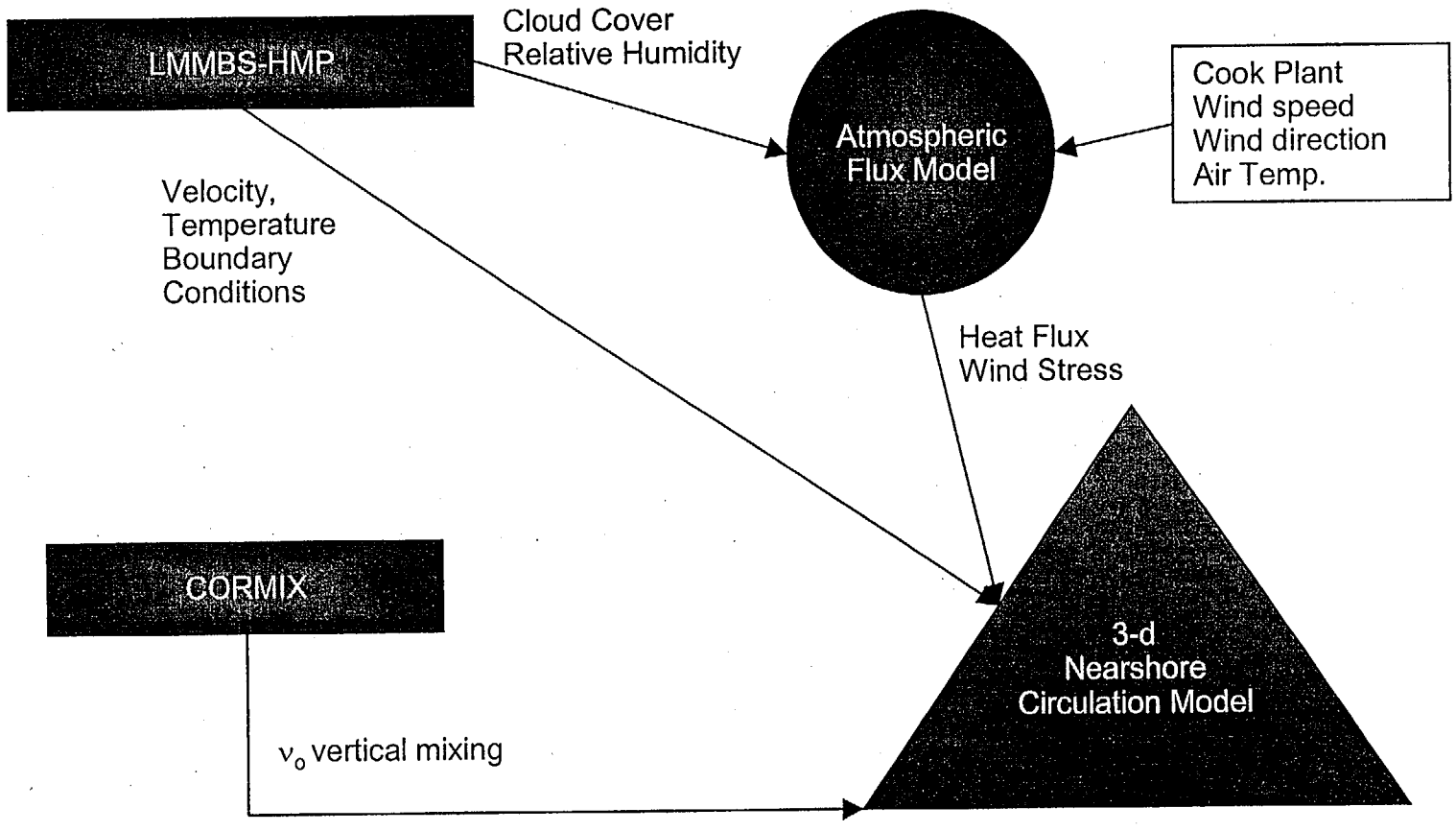

Figure 2-1. Southern Lake Michigan with a 5 Kilometer Grid and the Nearshore Model Grid Centered on the Cook Plant.

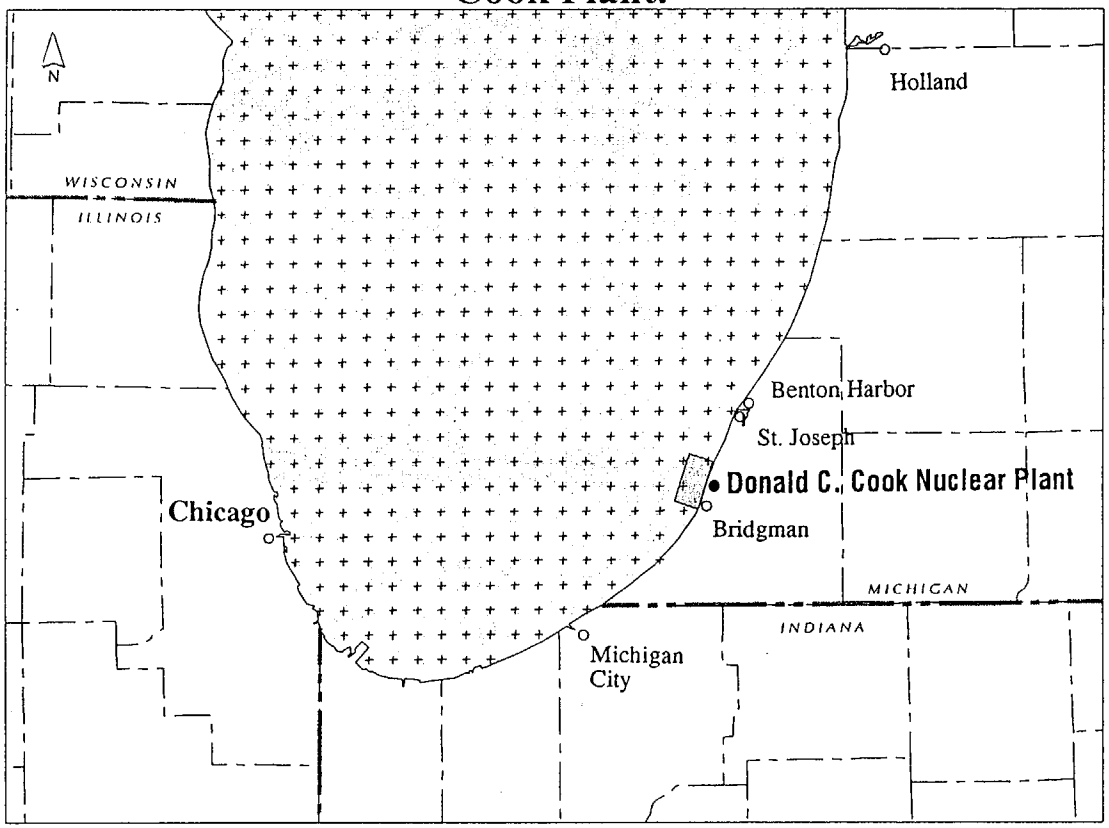

Figure 2-2. Cook Plant Nearshore Map.

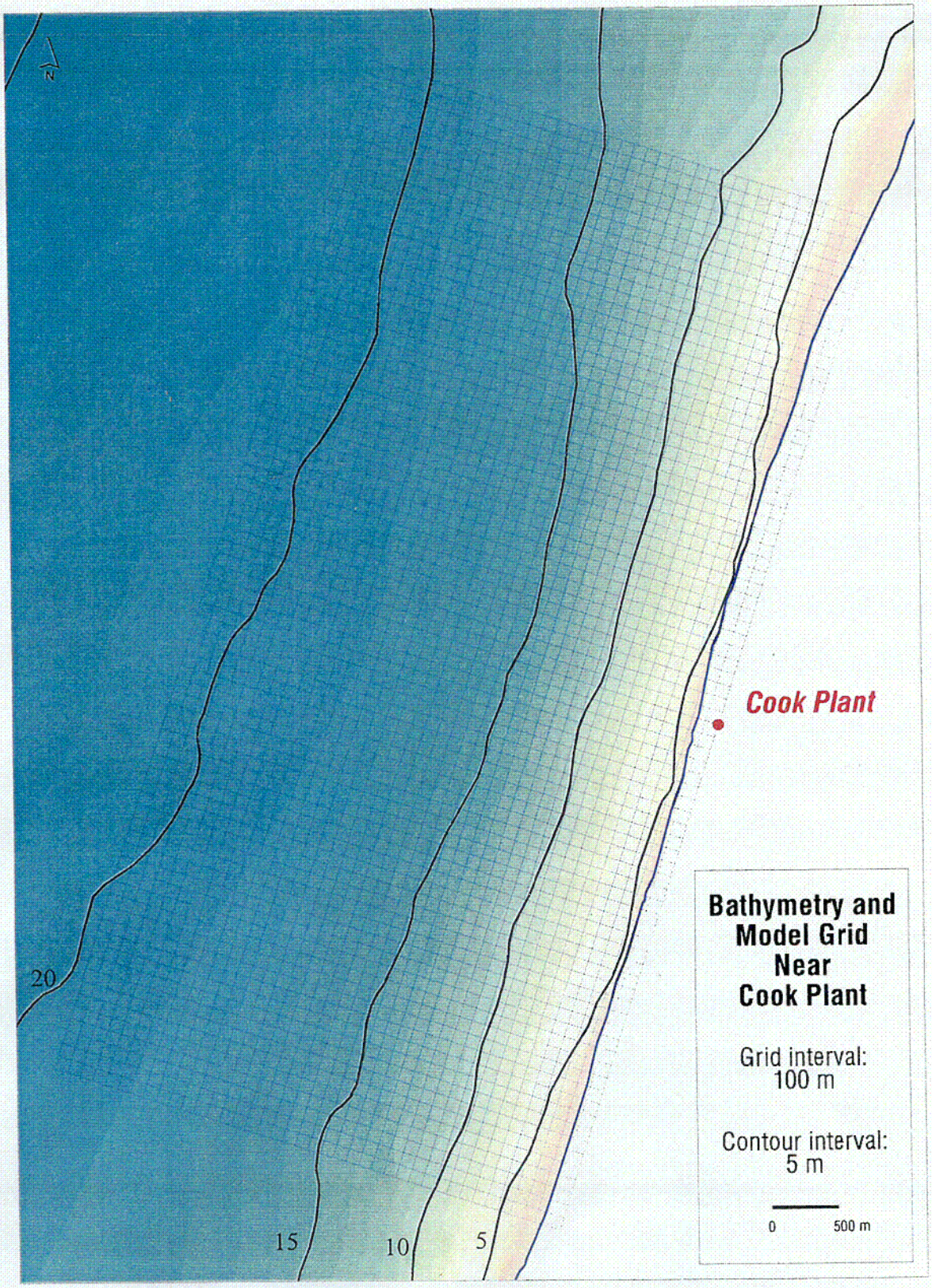

C01

Figure 2-3. Nearshore Model Grid in Vicinity of Cook Plant, Showing Local Features.

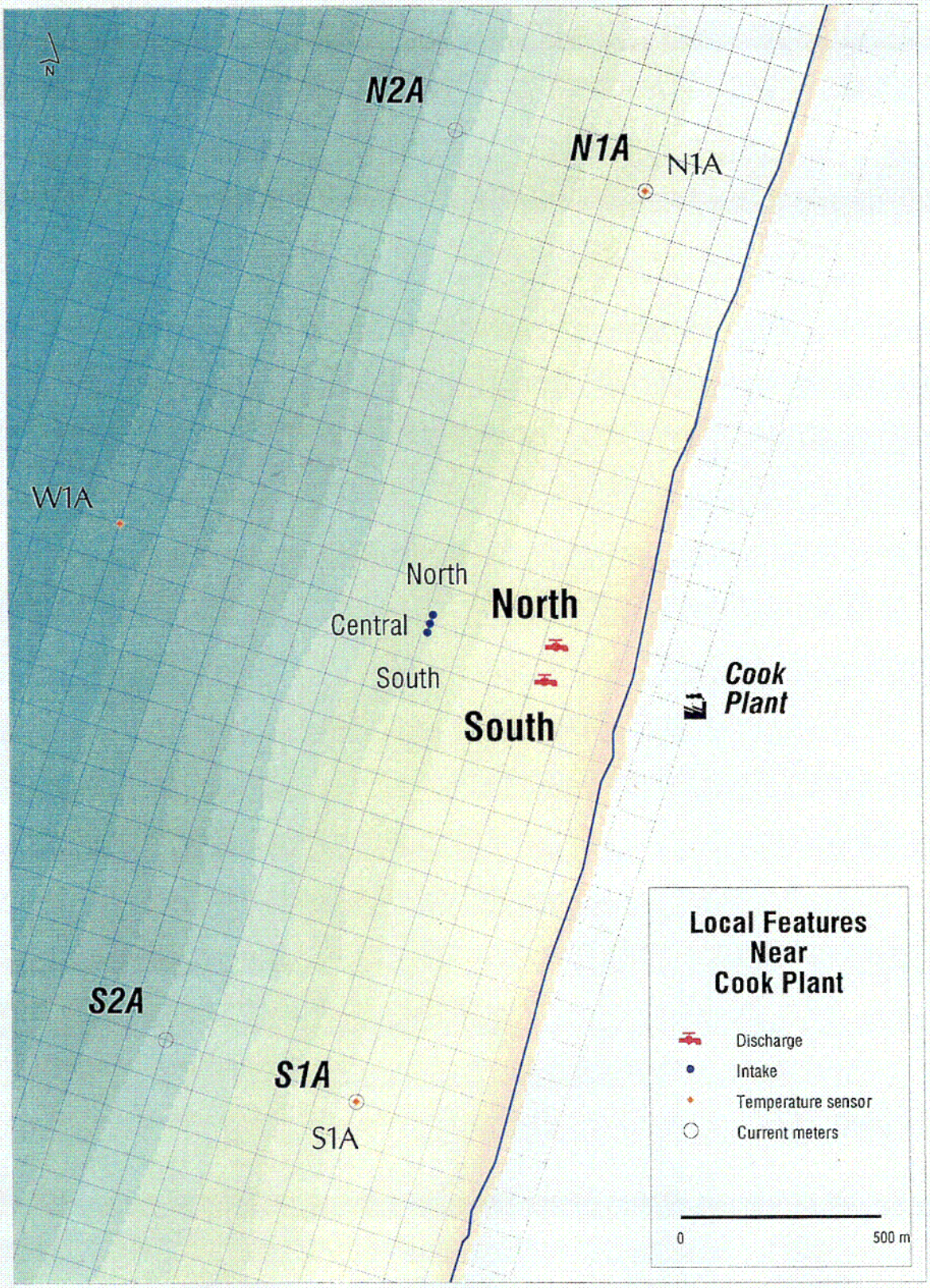

C02

Figure 2-4. LMMBS Model Grids near the Cook Plant Model Domain.

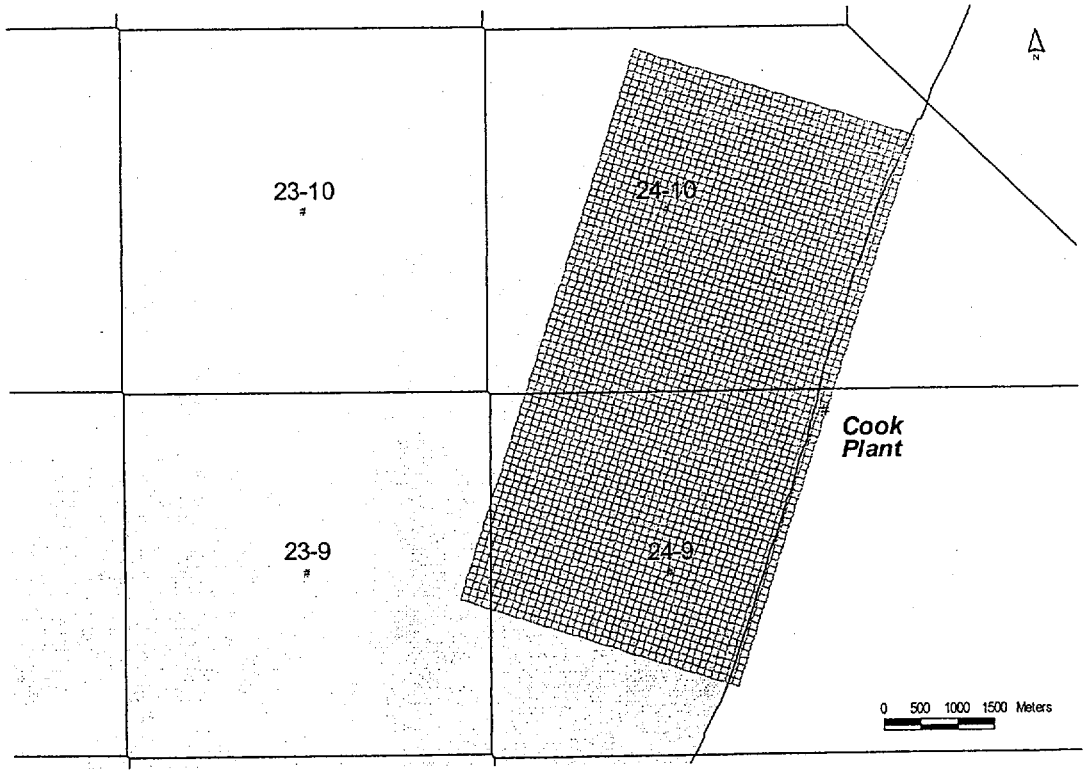

Figure 3.1. Flow Chart for the 3-Dimensional Nearshore Circulation Model.

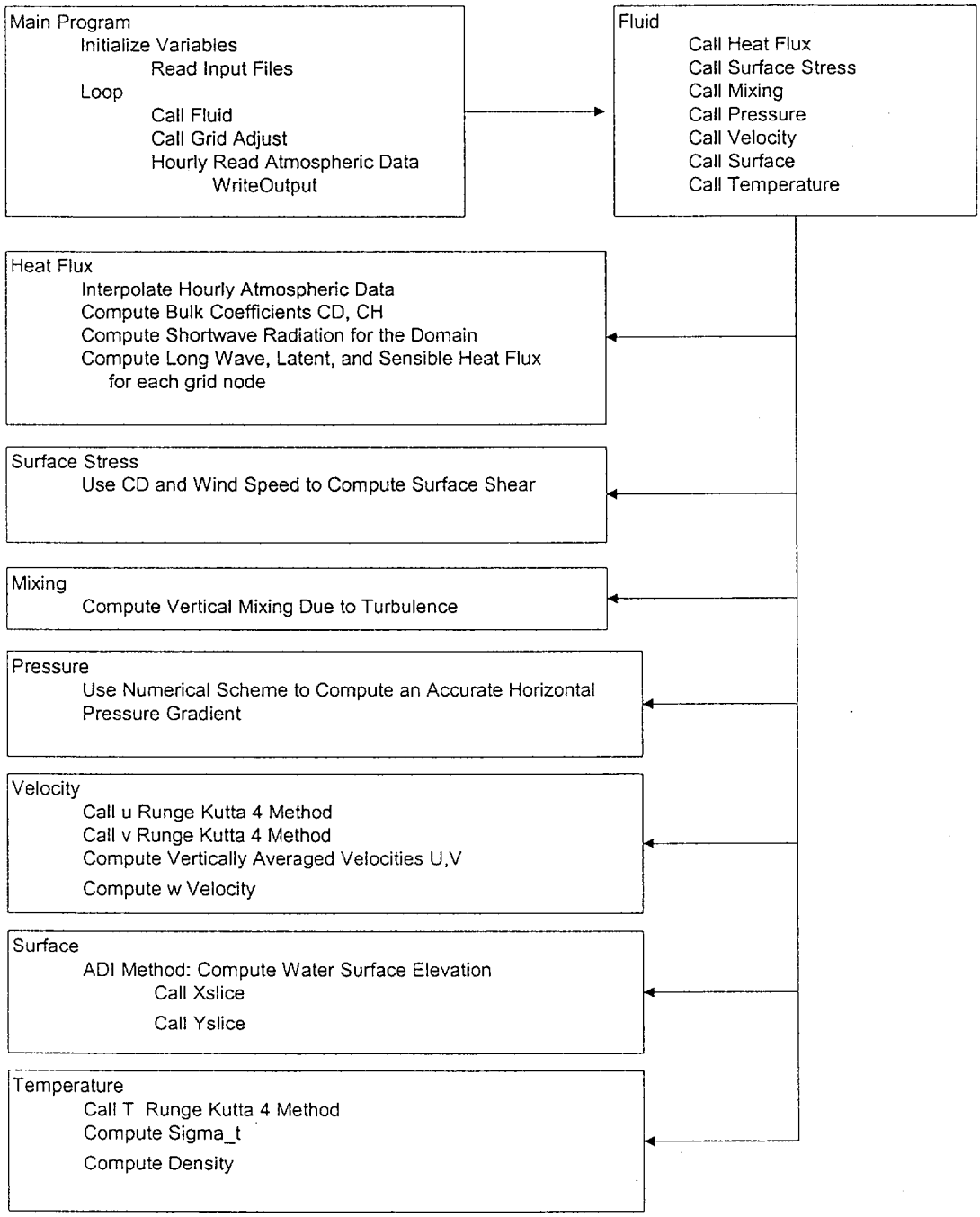

Figure 3-2. Nearshore Model Information Flow Chart.

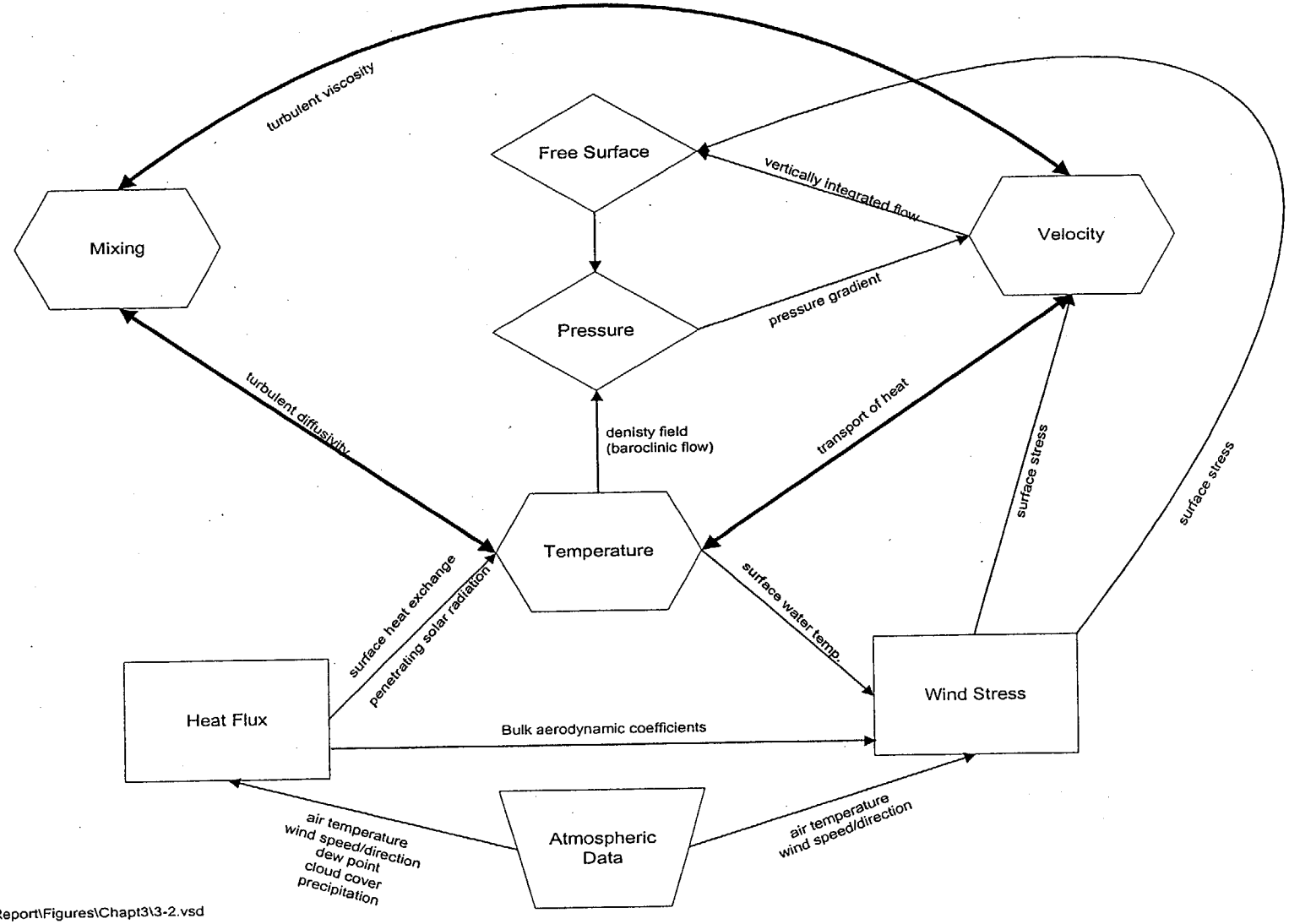

s:\cook1\FinalReport\Figures\Chapt3\3-2.vsd

Figure 3-3. Principal Mechanisms of Light Extinction.

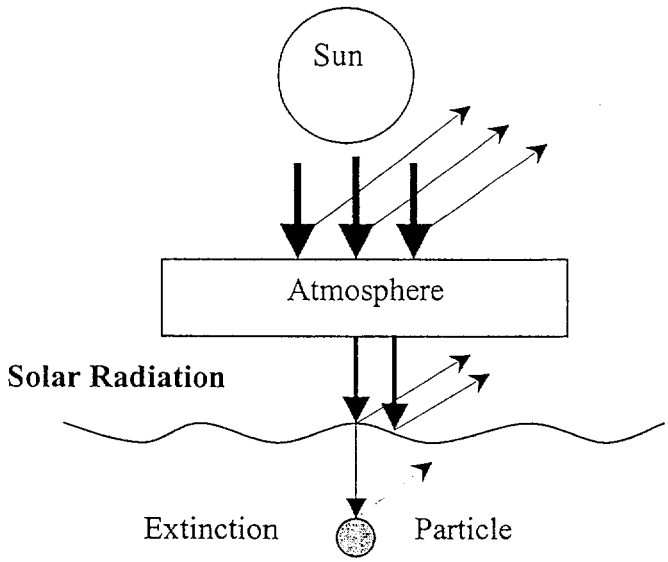

Figure 3-4. Solar Radiation Versus Depth for Various Water Bodies.

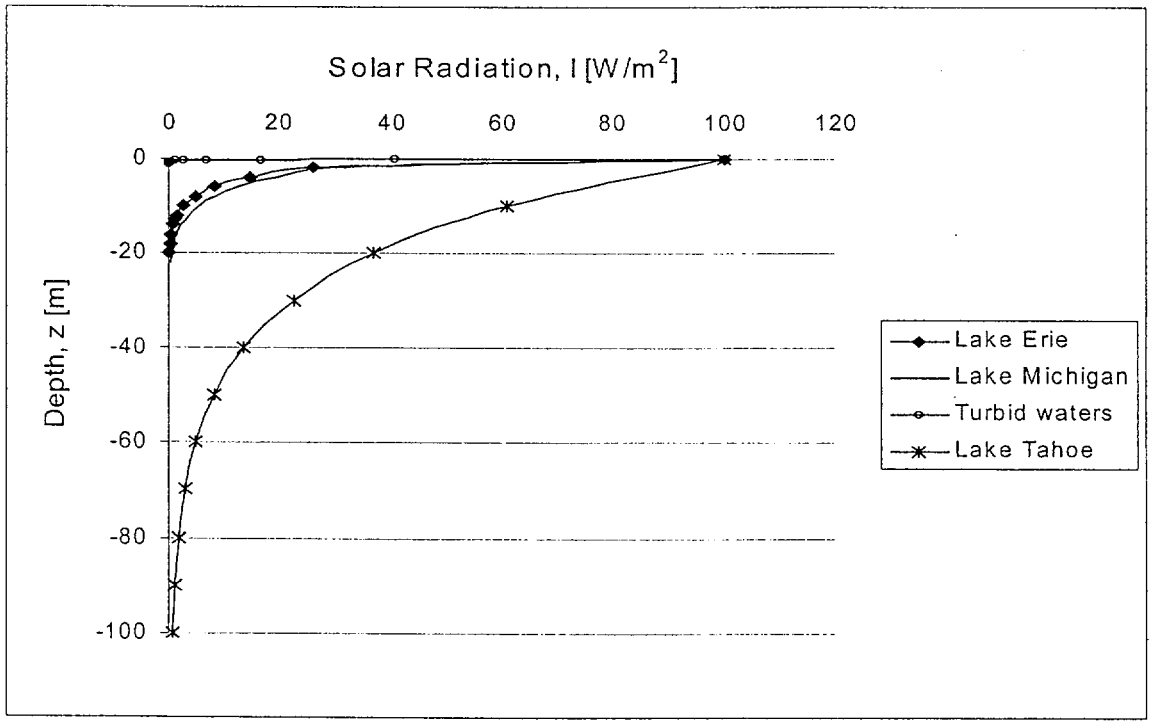

Figure 3-5. Momentum Boundary Conditions for the Performance Assessment.

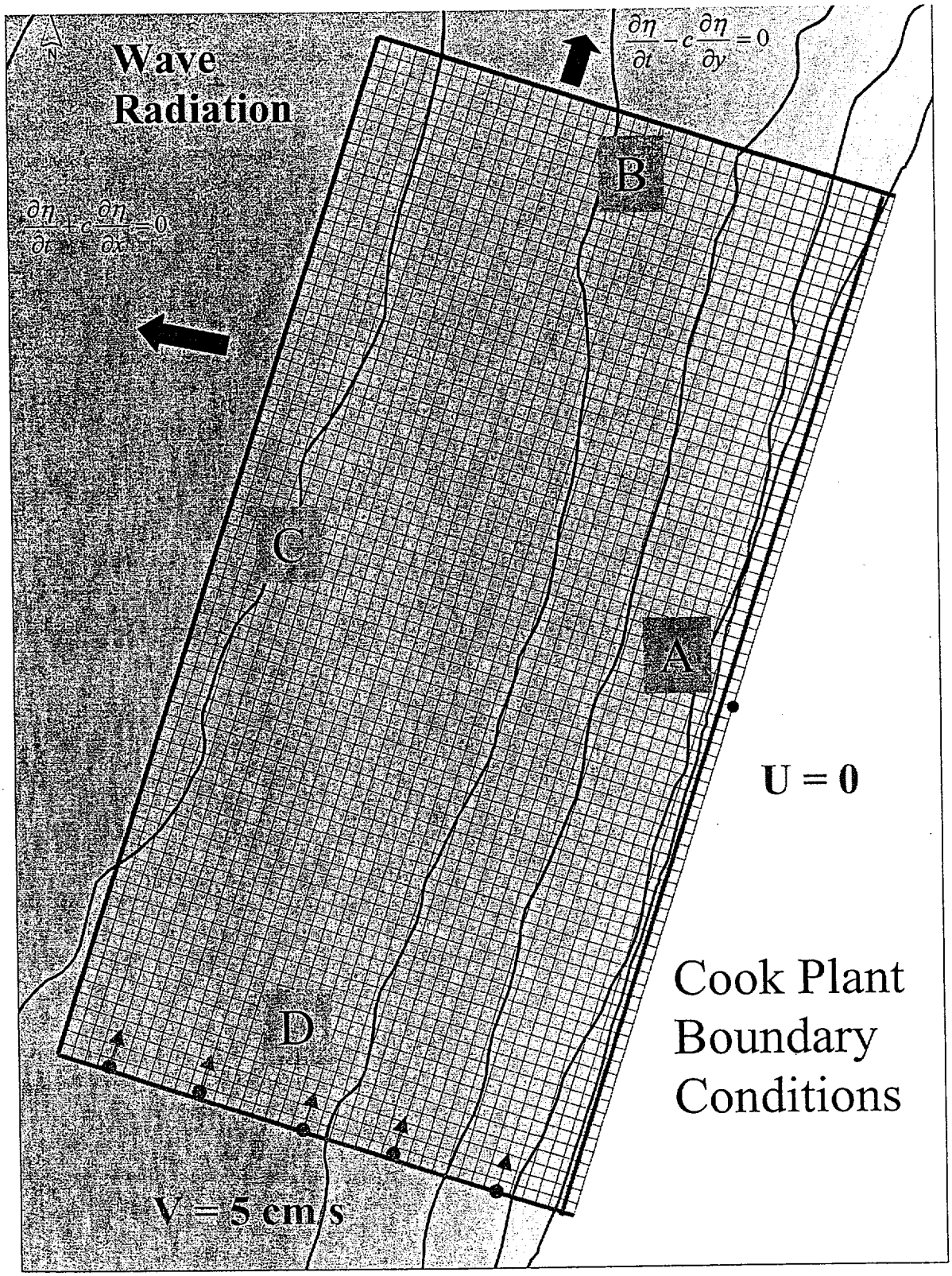

Figure 3-6. Vertical Mixing as a Function of Ri.

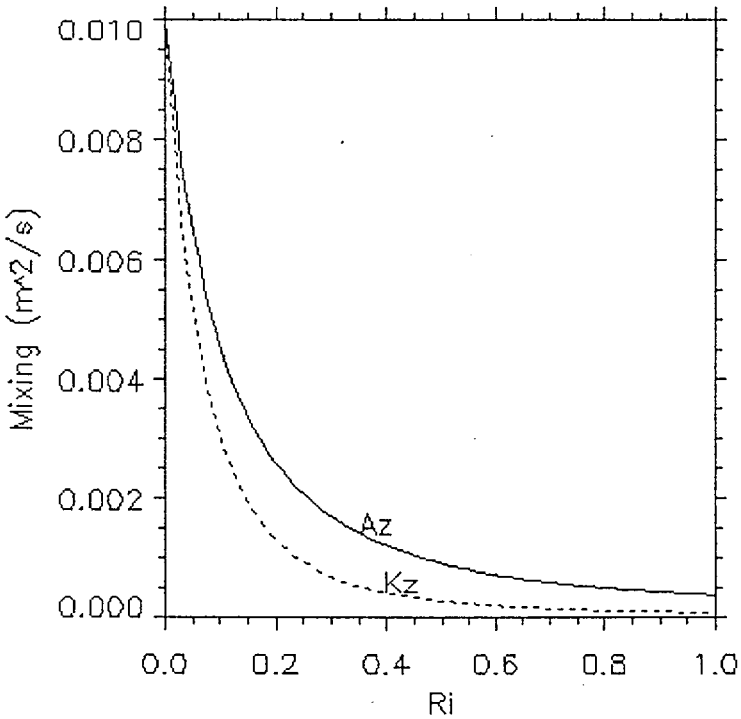

Figure 4-1. Plume Areas at the Surface, 1m, 2m, and 4m for a 72 Hour Test Run with $\nu = 10^{-2}$.

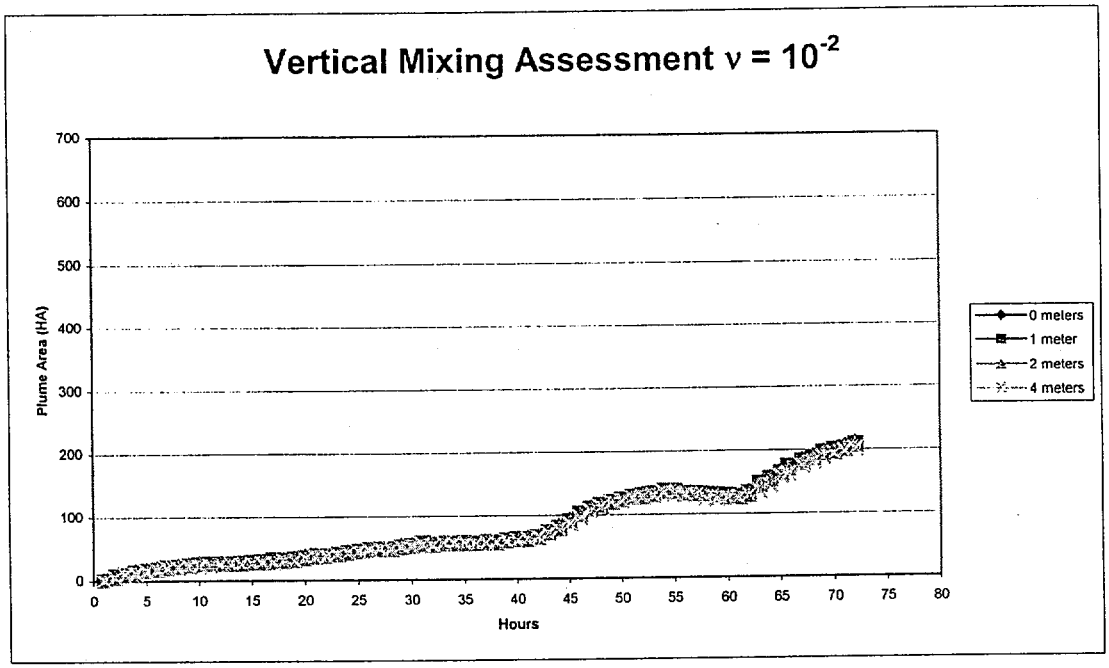

Figure 4-2. Plume Areas at the Surface, 1m , 2m, and 4m for a 72 Hour Test Run with $\nu = 10^{-3}$.

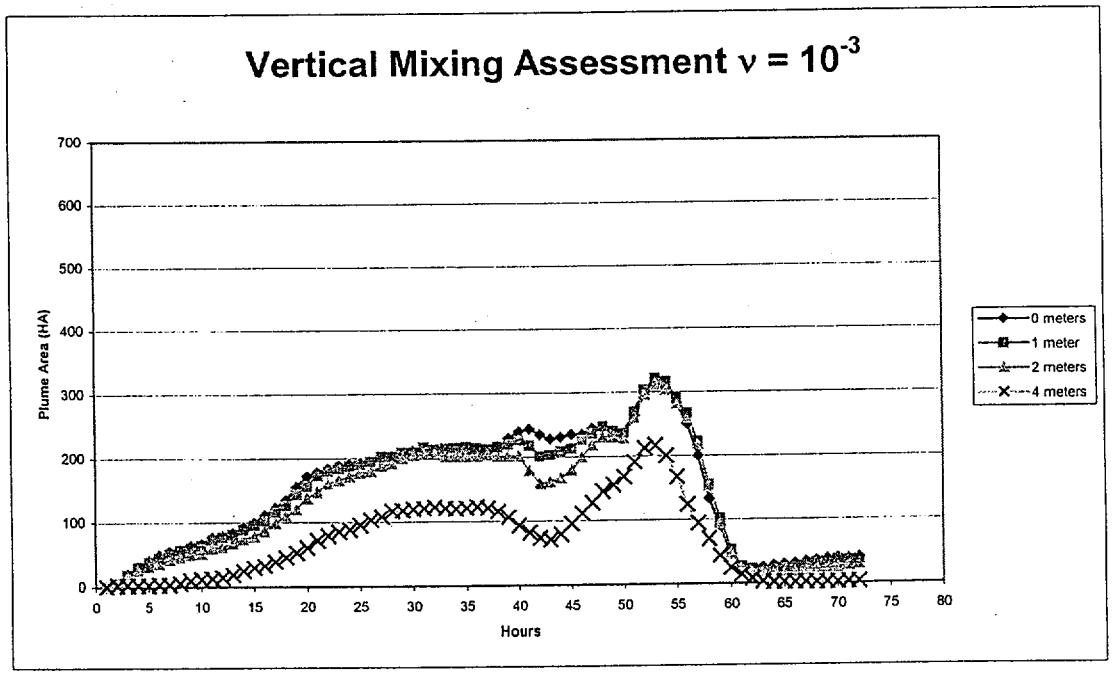

Figure 4-3. Plume Areas at the Surface, 1m, 2m, and 4m for a 72 Hour Test Run with $\nu = 10^{-4}$.

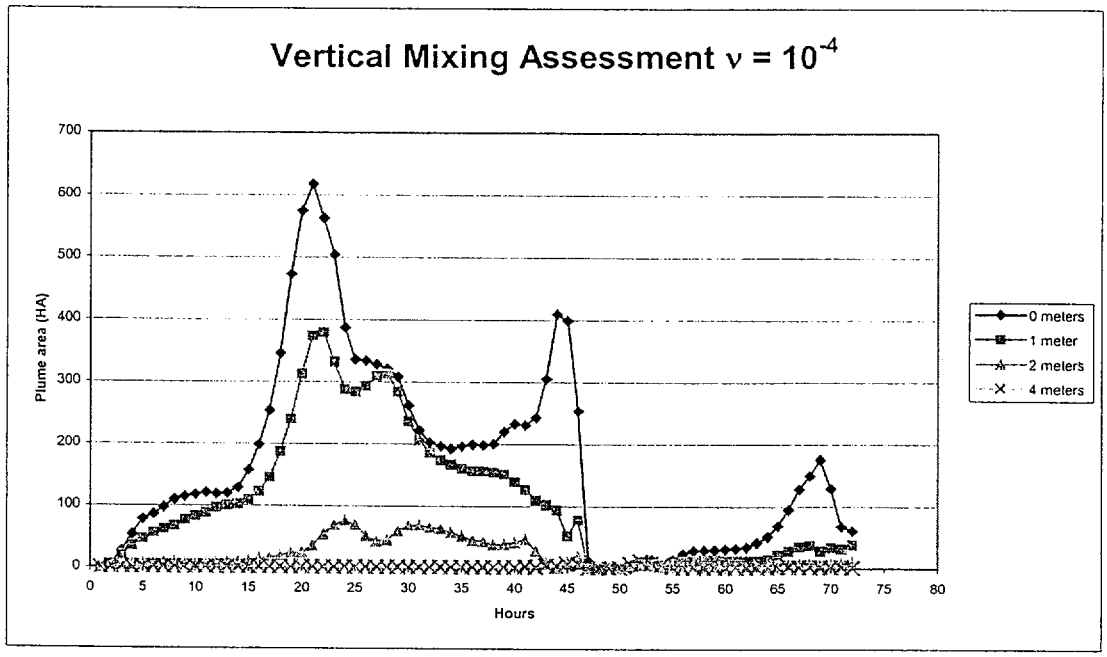

Figure 4-4. Nearshore Model Surface Temperature Compared to CORMIX Steady State Prediction.

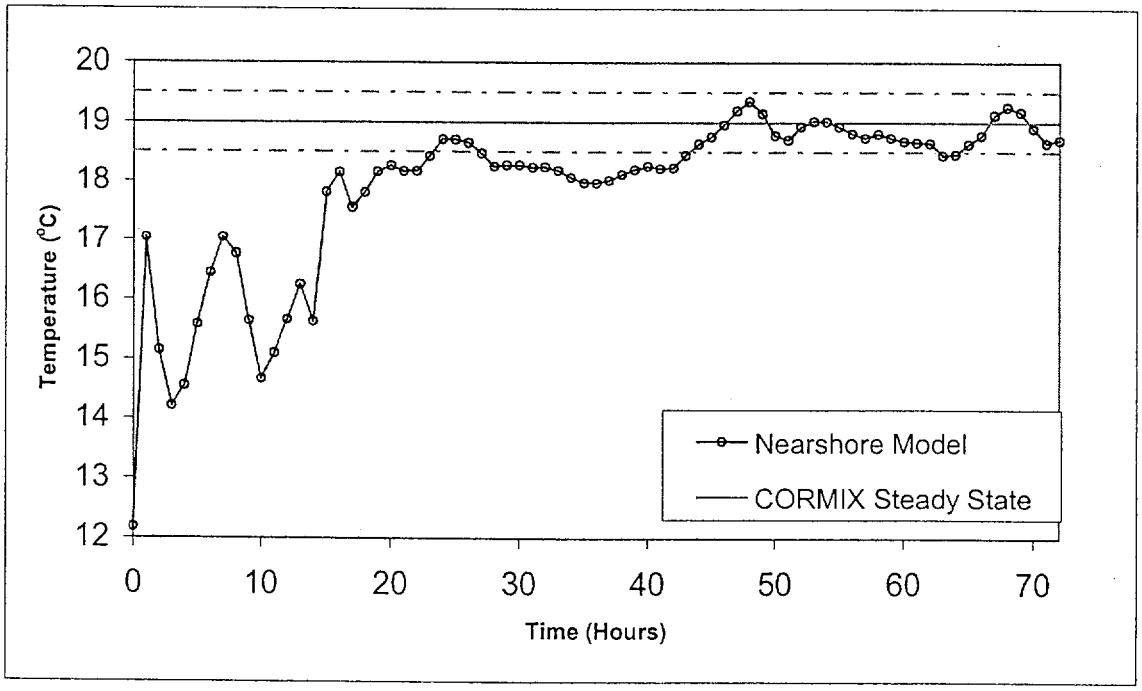

Figure 4-5. Plume Comparison for July 1995 Modeled Plumes and July 1979 Measured Plumes.

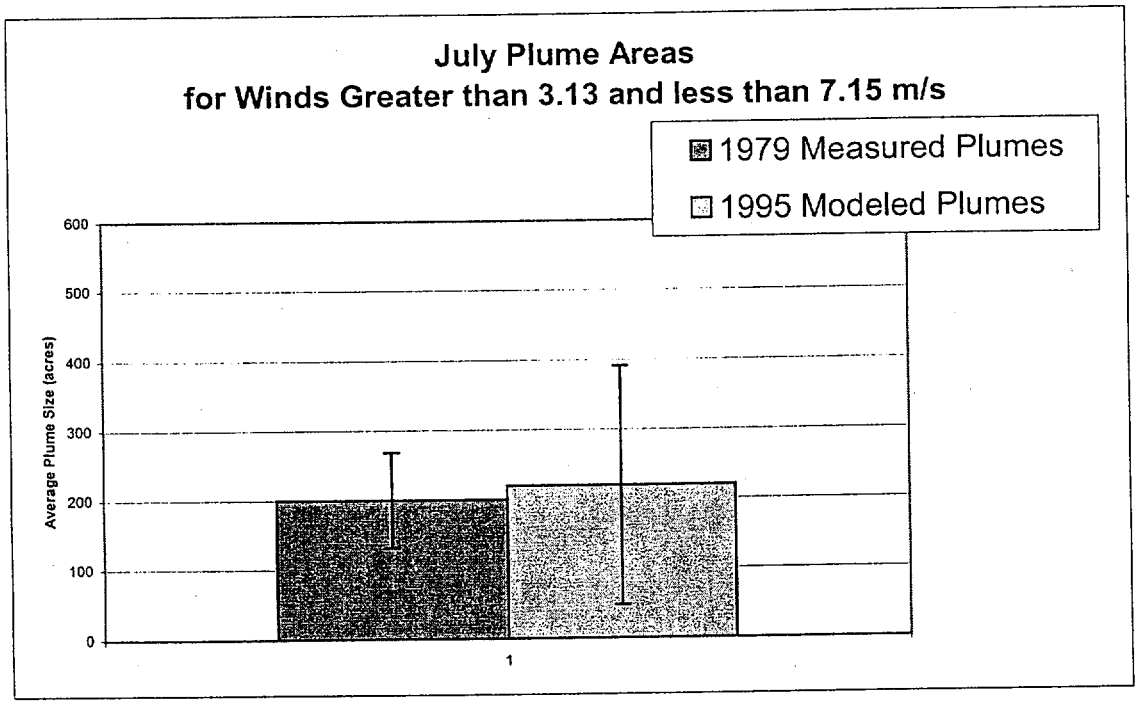

Figure 4-6. Plume Comparison for September 1995 Modeled Plumes and September 1978 Measured Plumes.

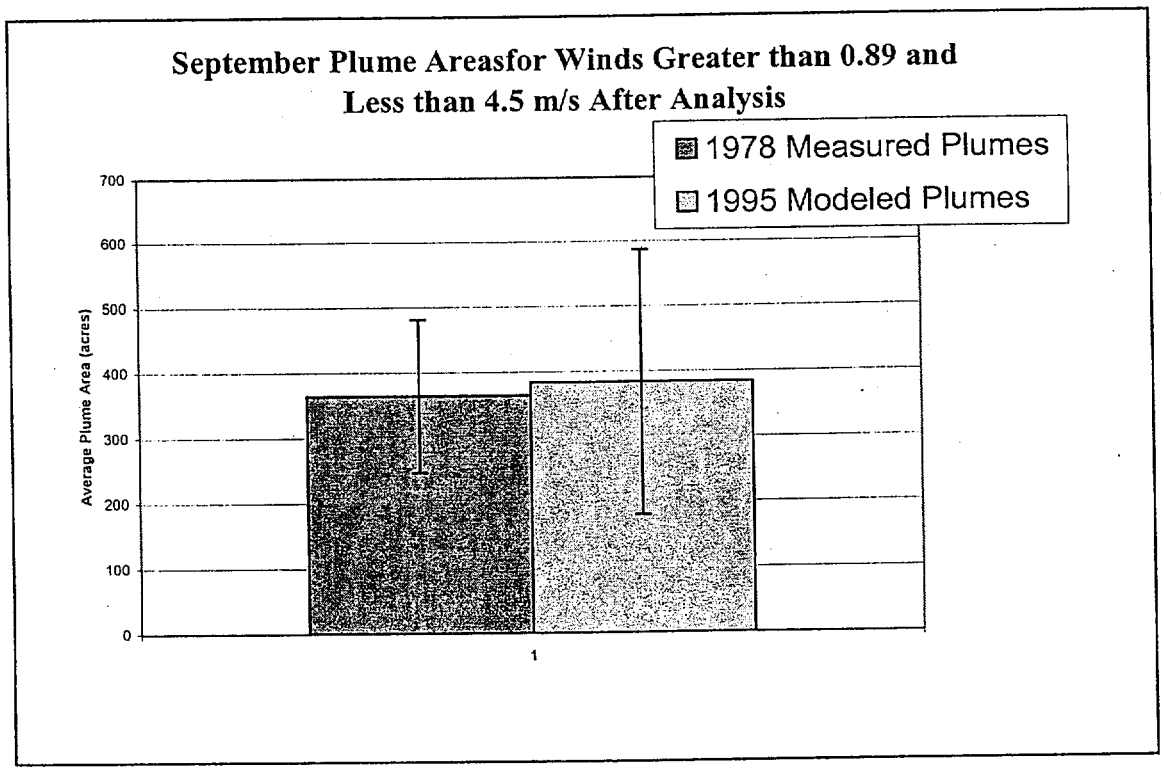

Figure 4-7. Plume Comparison for November 1995 Modeled Plumes and November 1978 Measured Plumes.

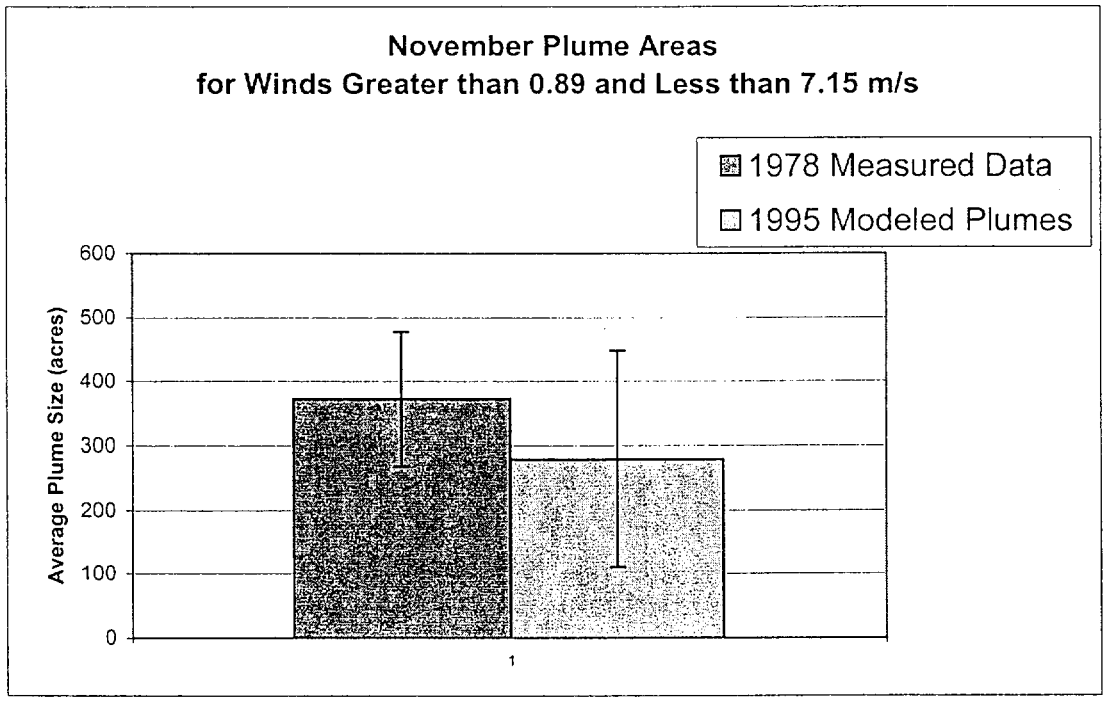

Figure 4-8. Map of Study Domain and the Benton Harbor Airport.

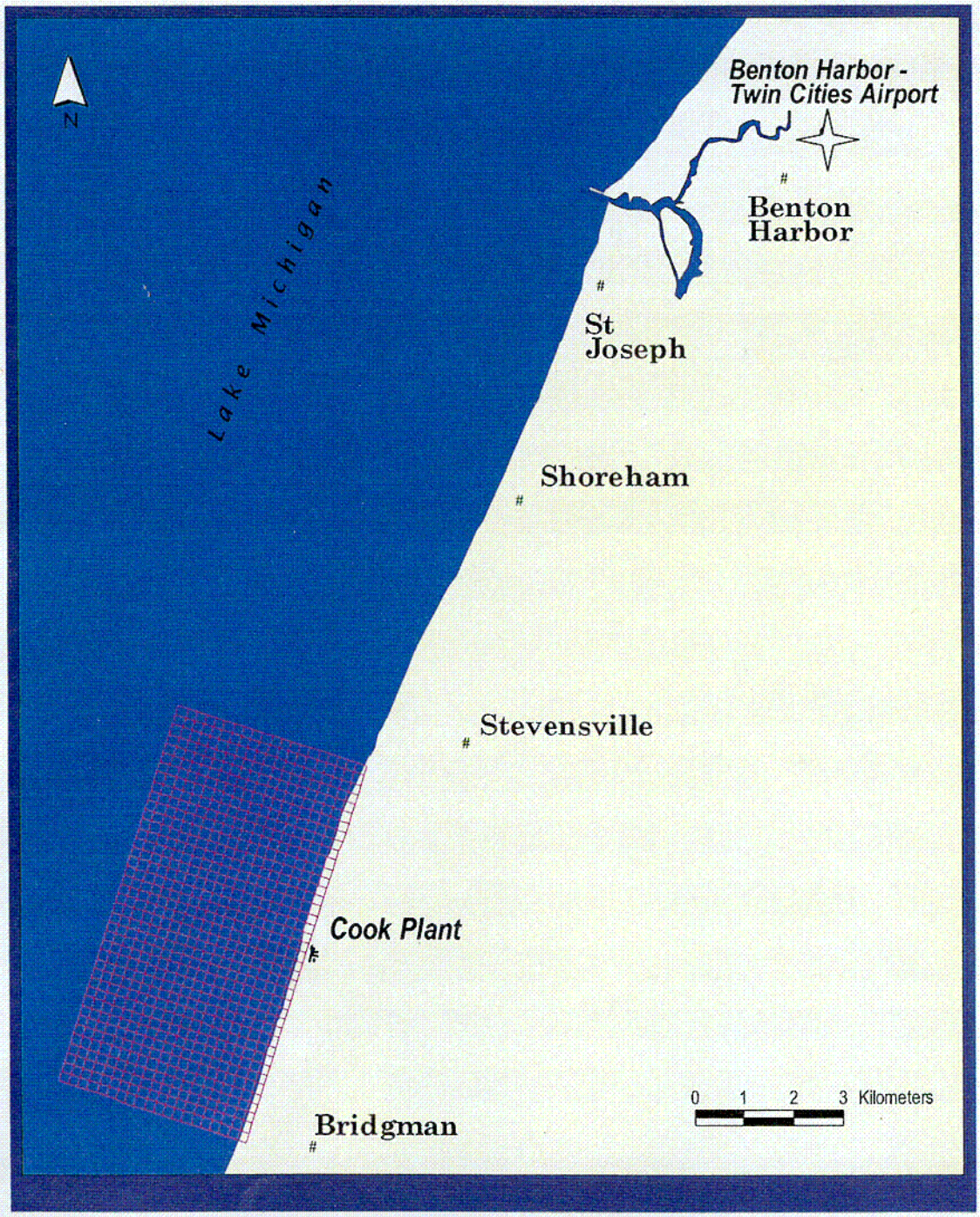

C03

Figure 4-9. Short Term Performance Assessment.

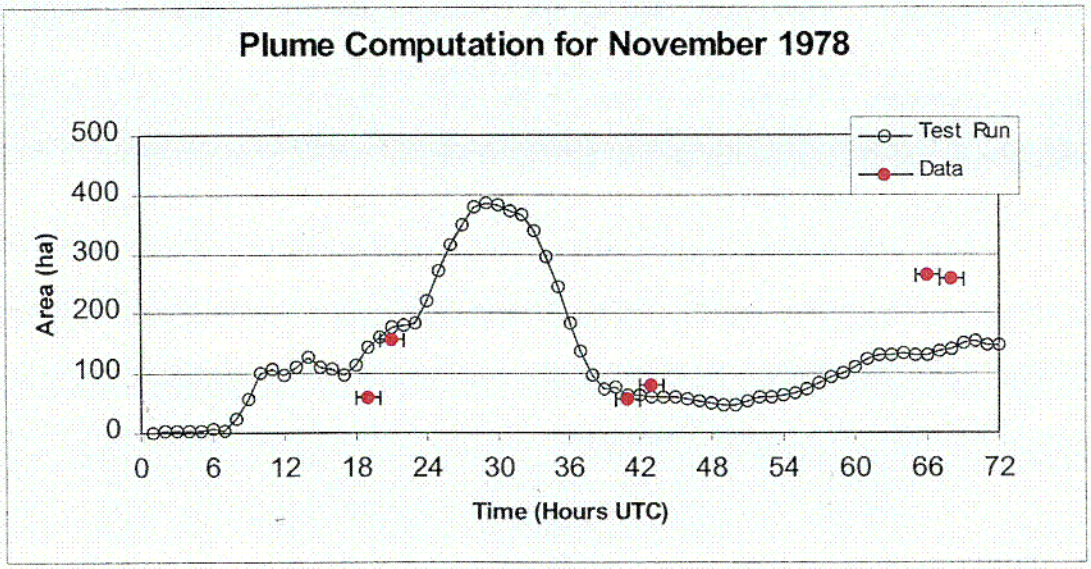

Figure 4-10. Plume Area and Wind Speed.

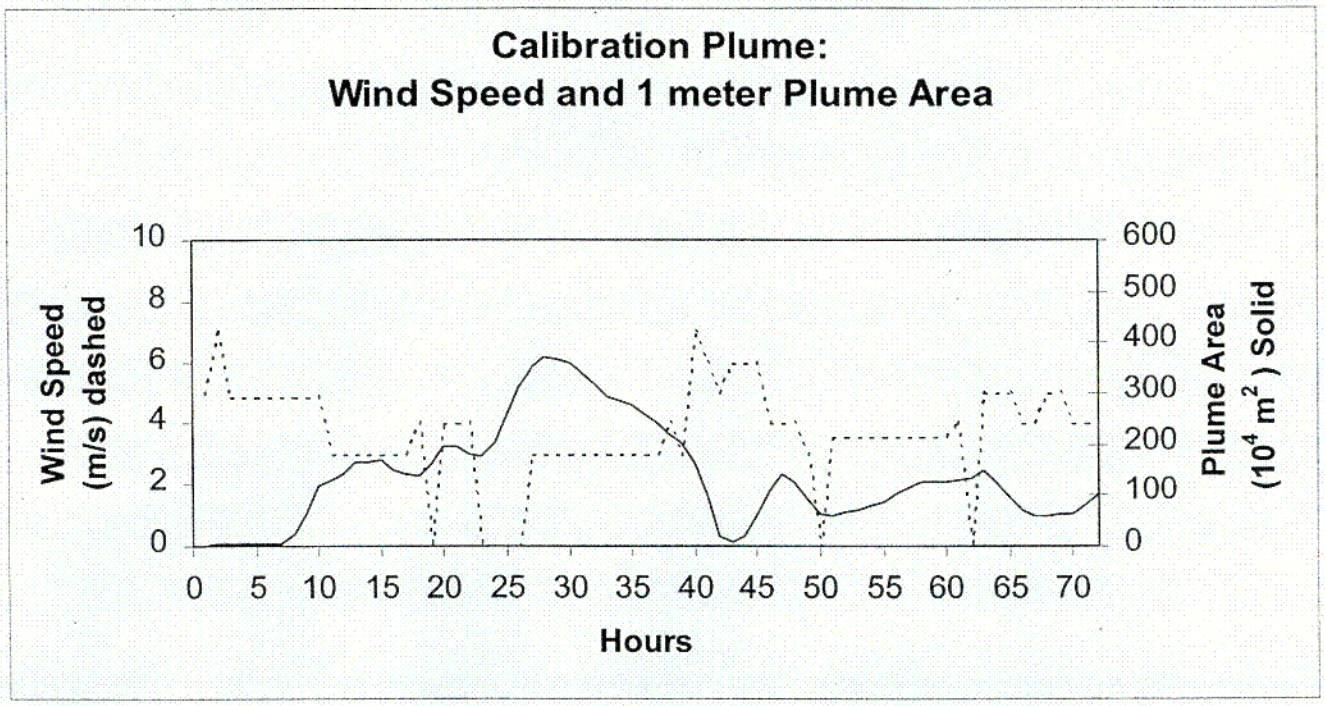

C04

Figure 4-11. Computed Plume for November 1 am.

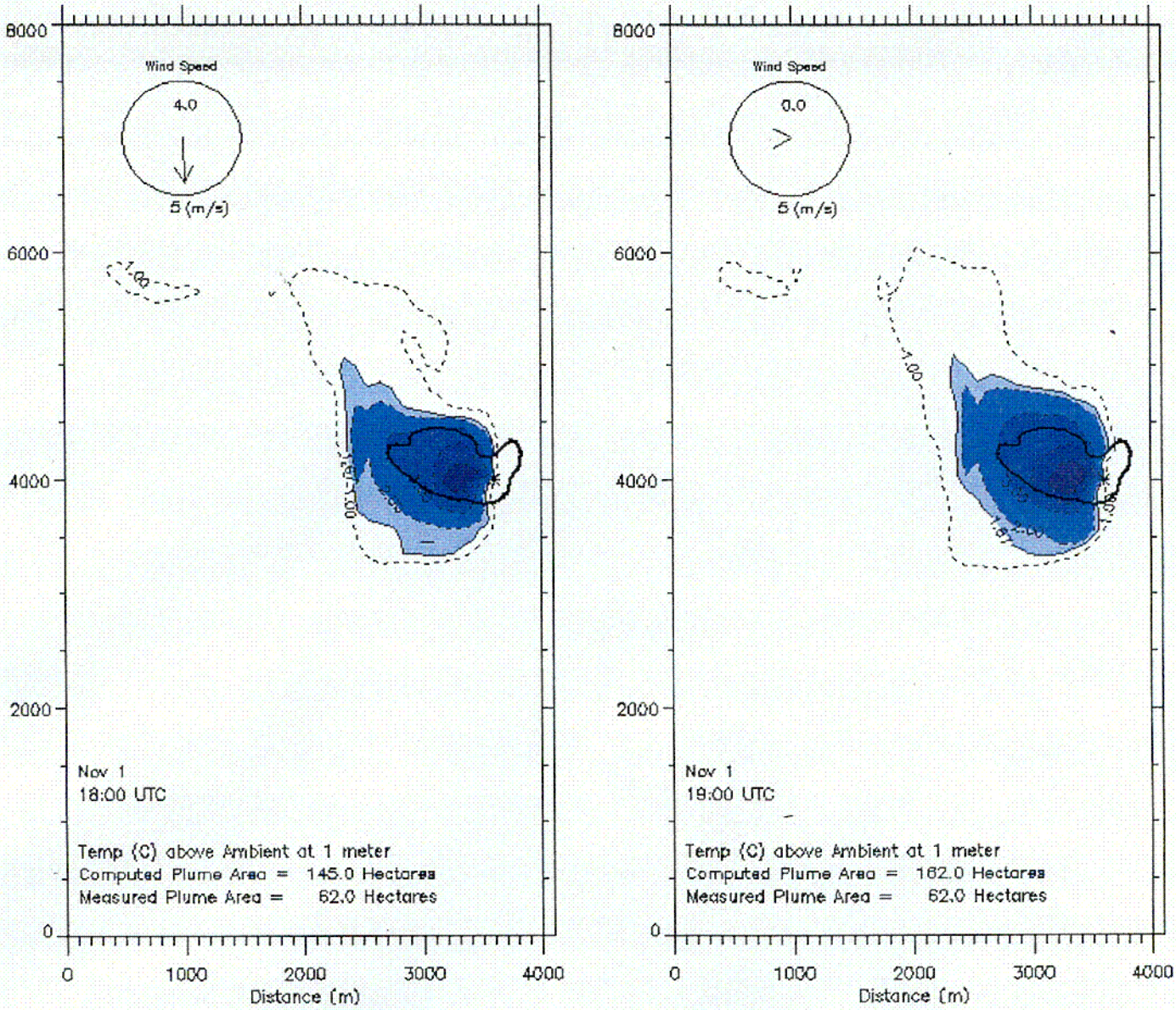

C05

Figure 4-12. Computed Plume for November 1 pm.

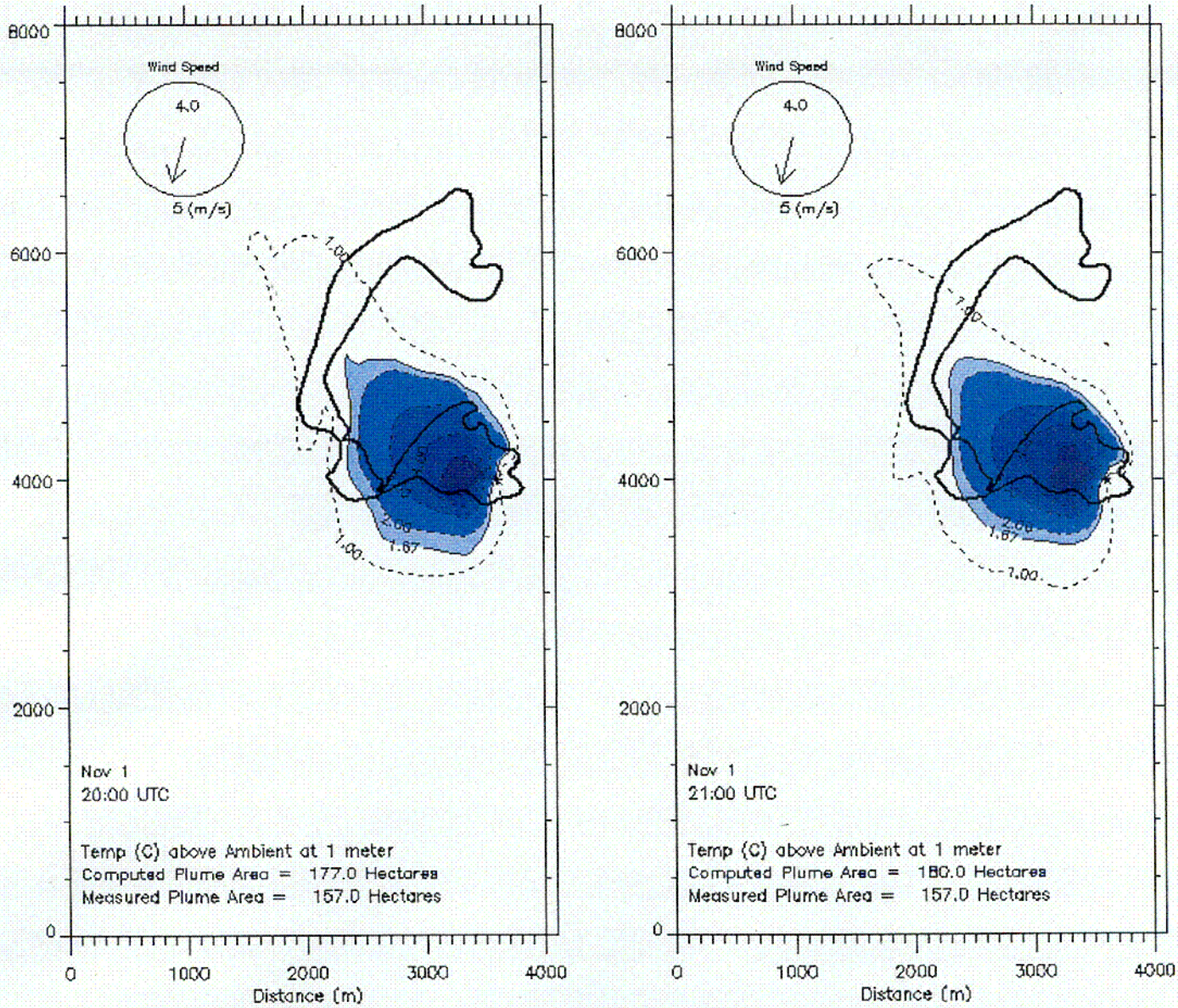

C06

Figure 4-1.3 Computed Plume for November 2 am.

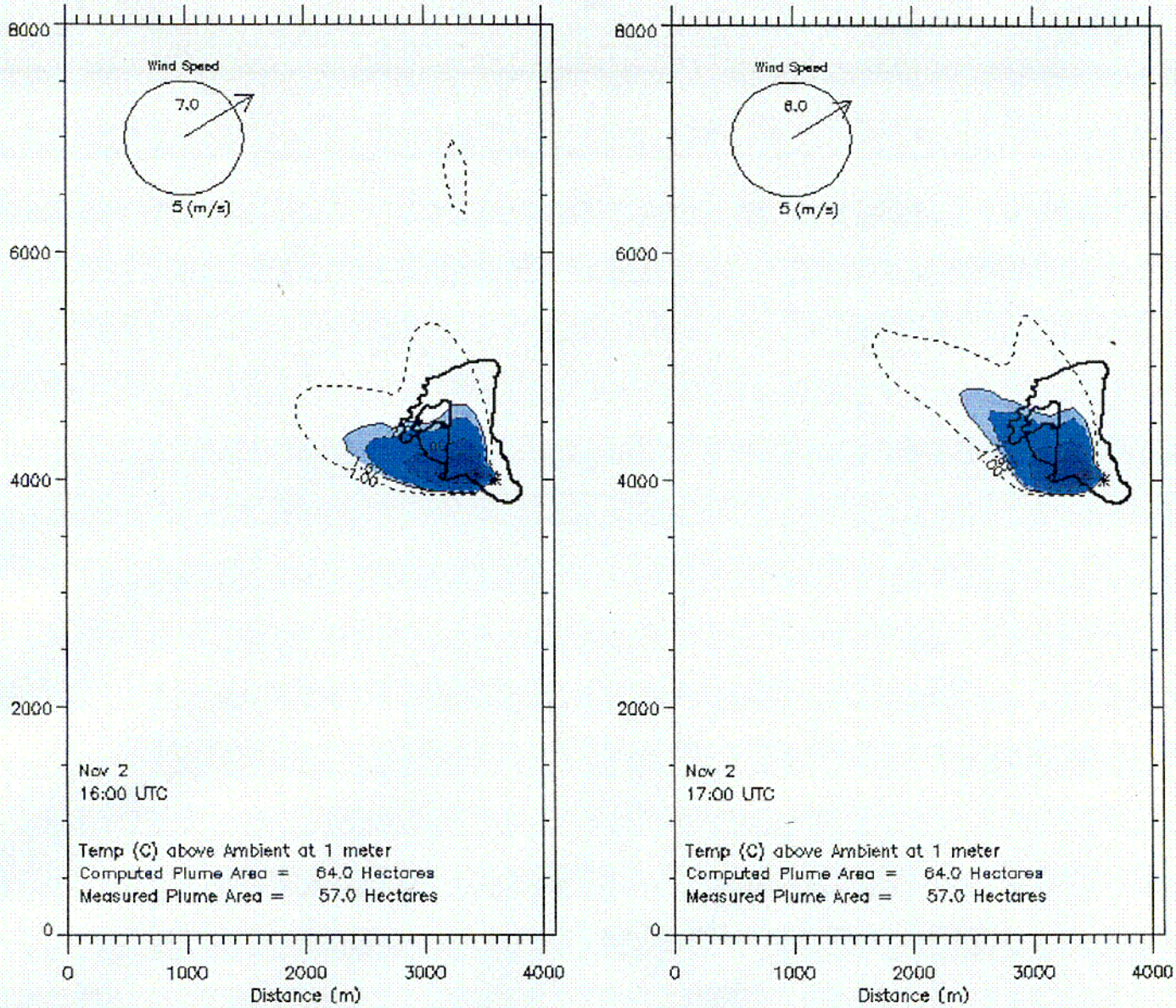

Figure 4-14. Computed Plume for November 2 pm.

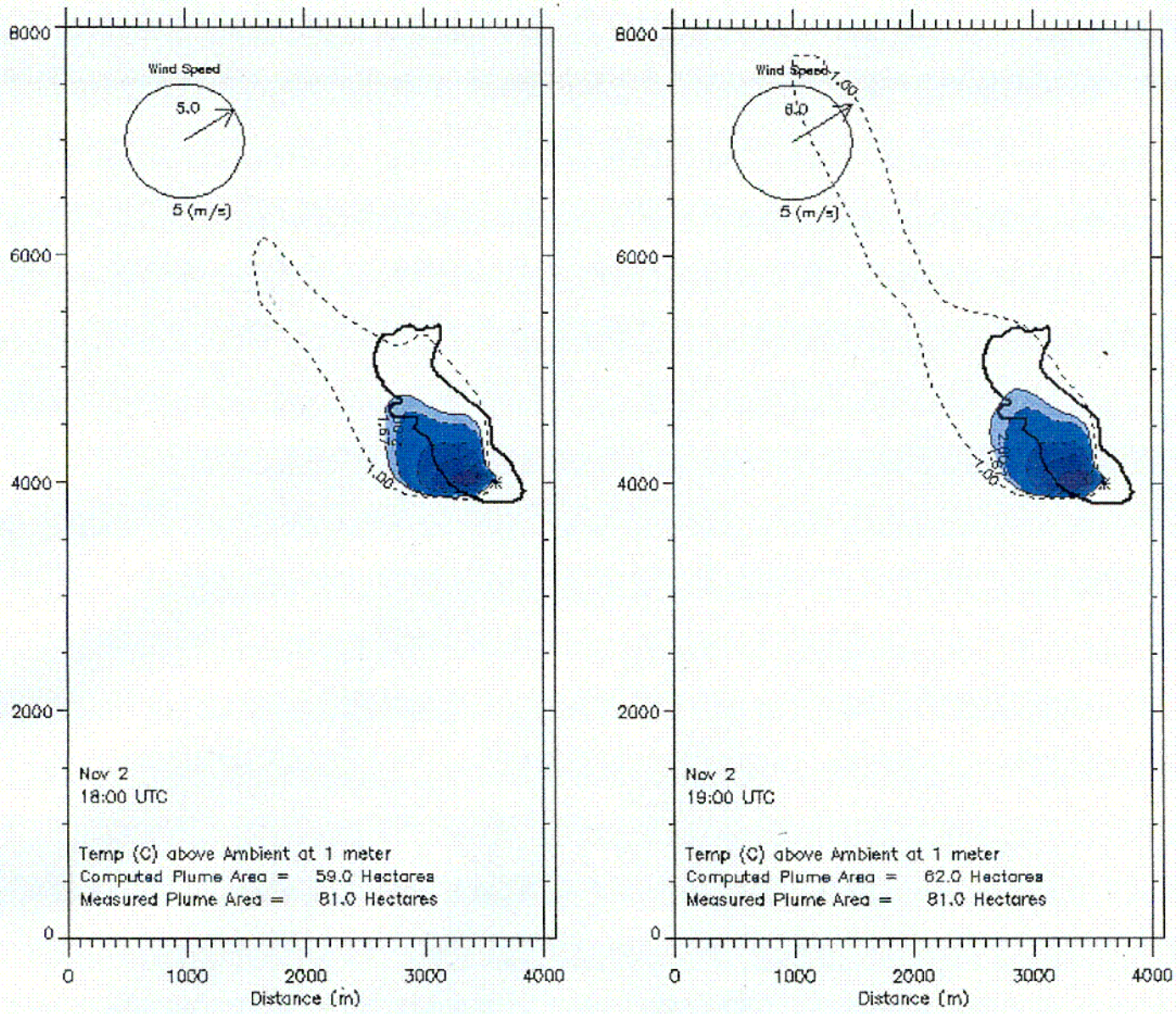

C08

Figure 4-15. Computed Plume for November 3 am.

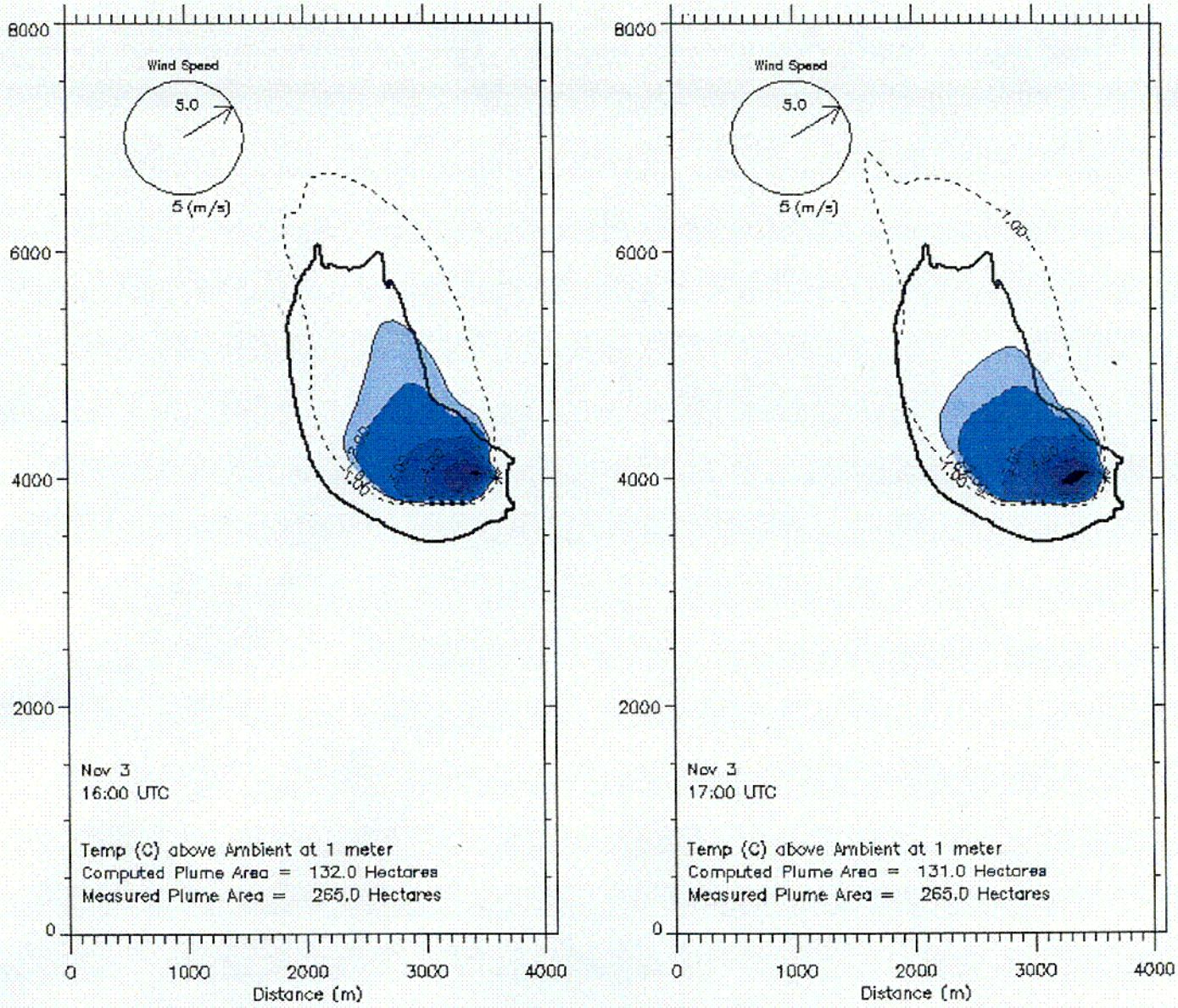

Figure 4-16. Computed Plume for November 3 pm.

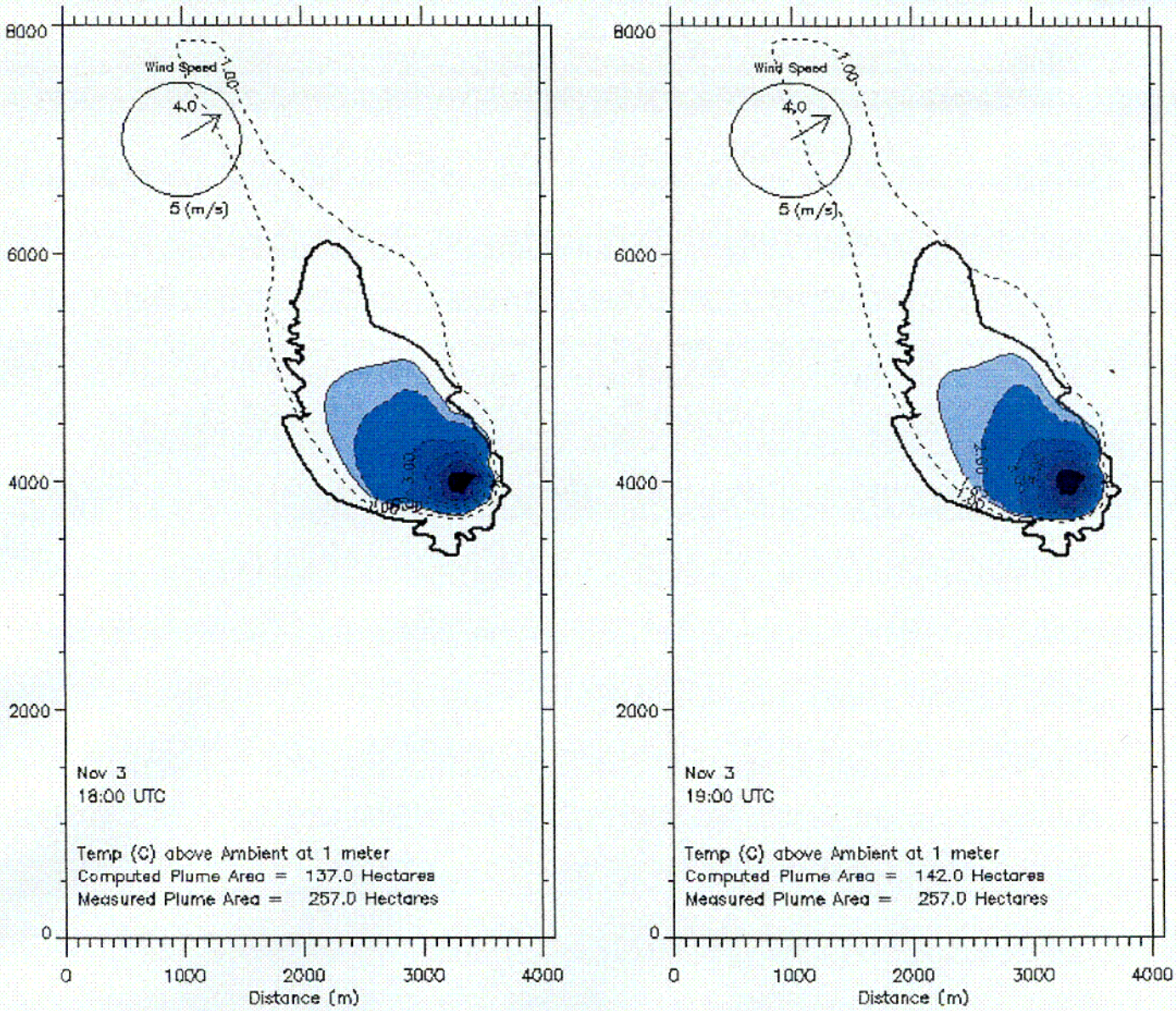

Figure 5-1. Frequency Distribution for all of the Computed Plumes.

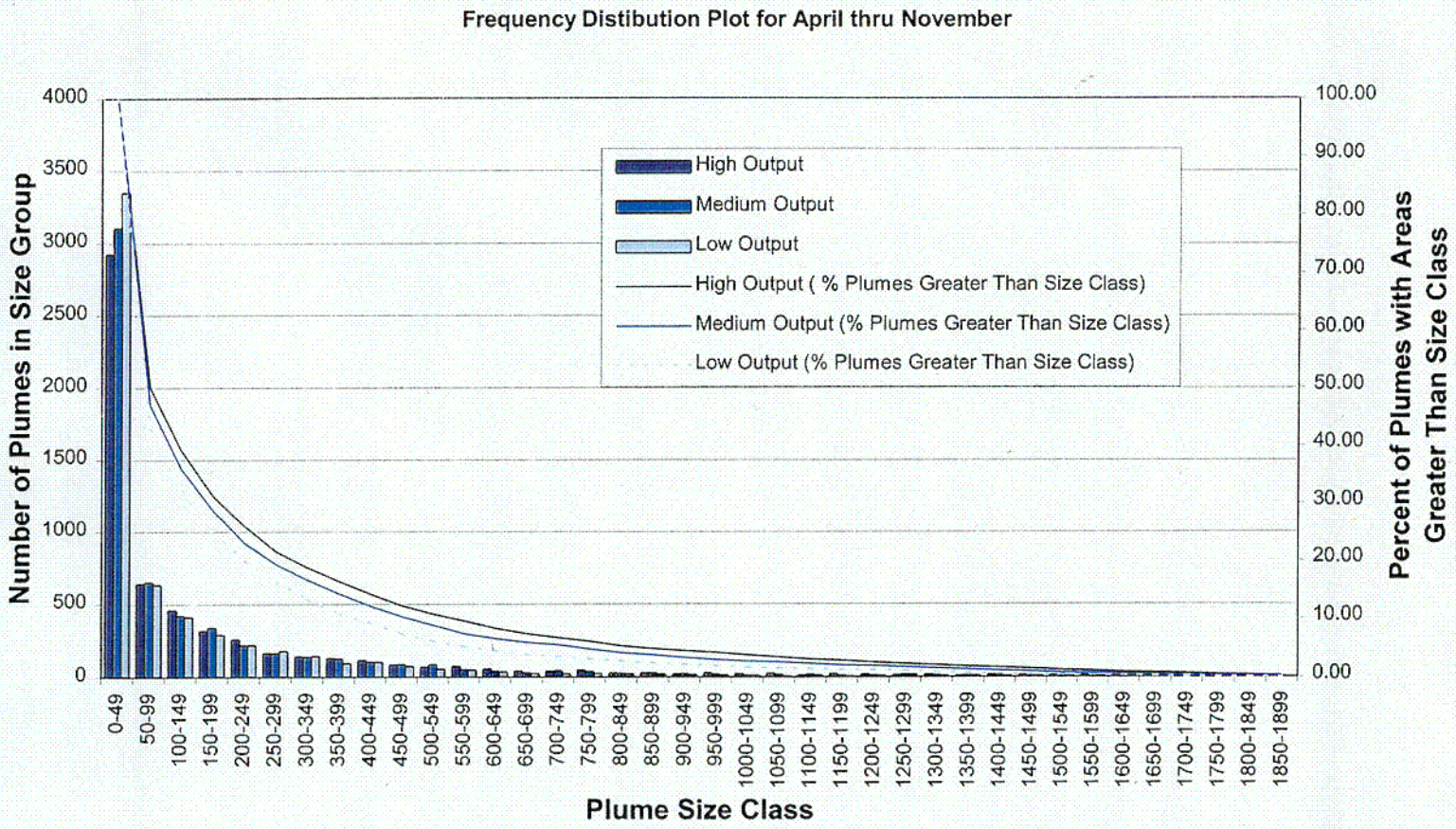

C11

Figure 5-2. April Average Plume with High Plant Output.

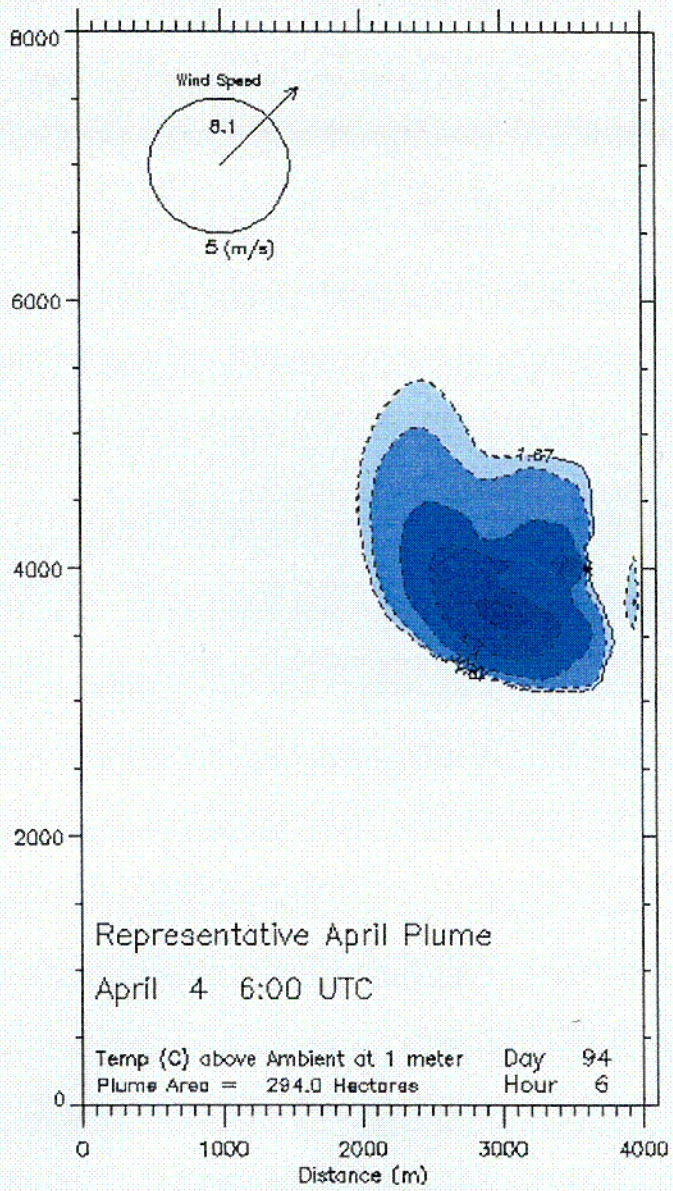

Figure 5-3. May Average Plume with High Plant Output.

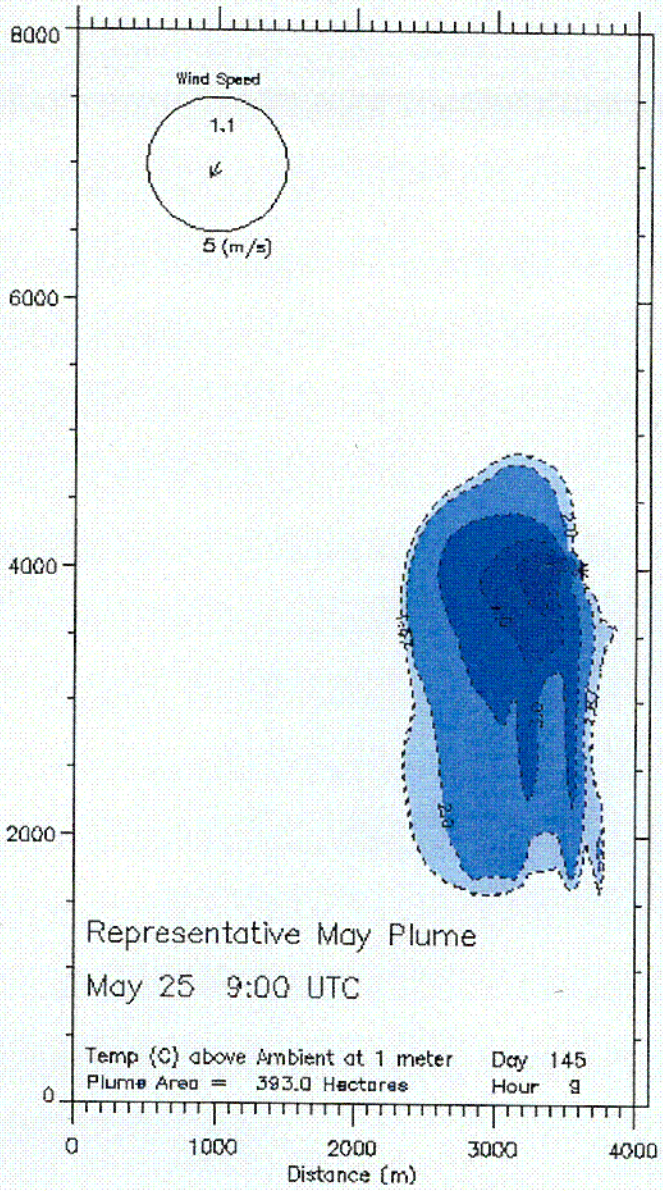

Figure 5-4. June Average Plume with High Plant Output.

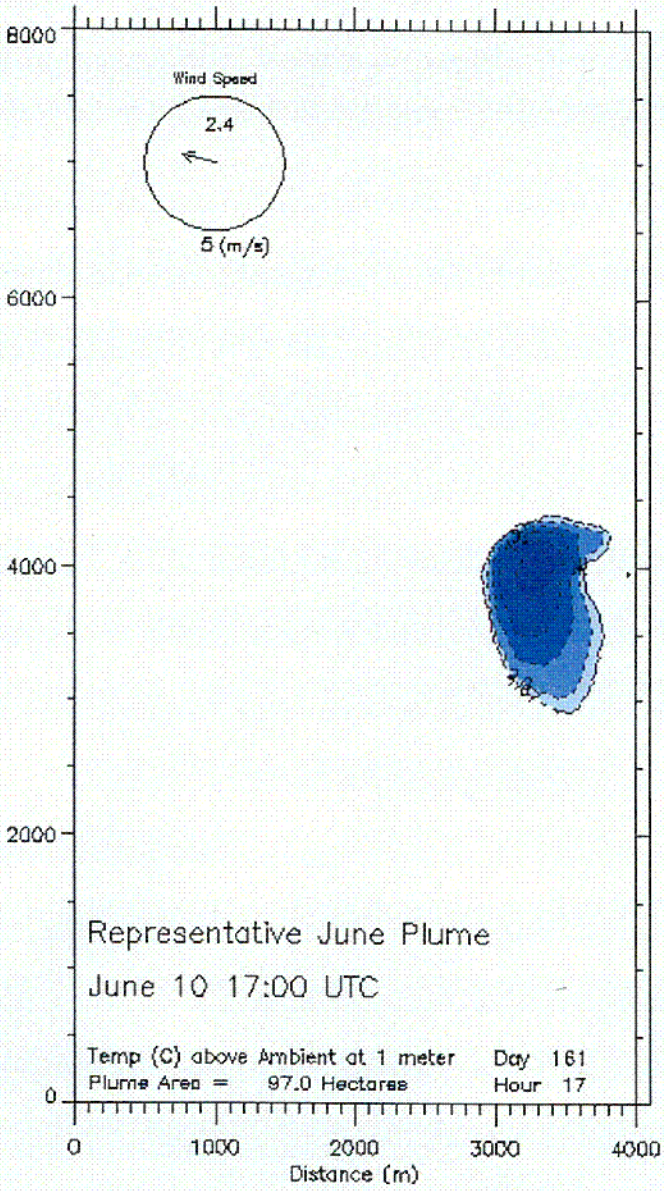

Figure 5-5. July Average Plume with High Plant Output.

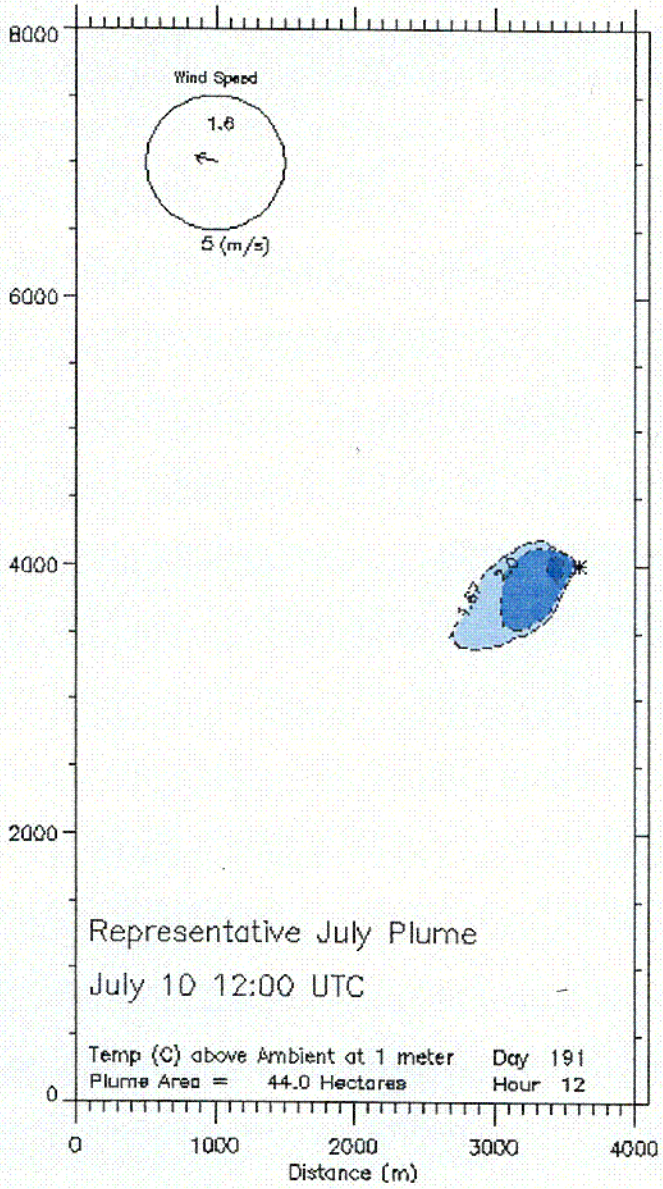

Figure 5-6. August Average Plume with High Plant Output.

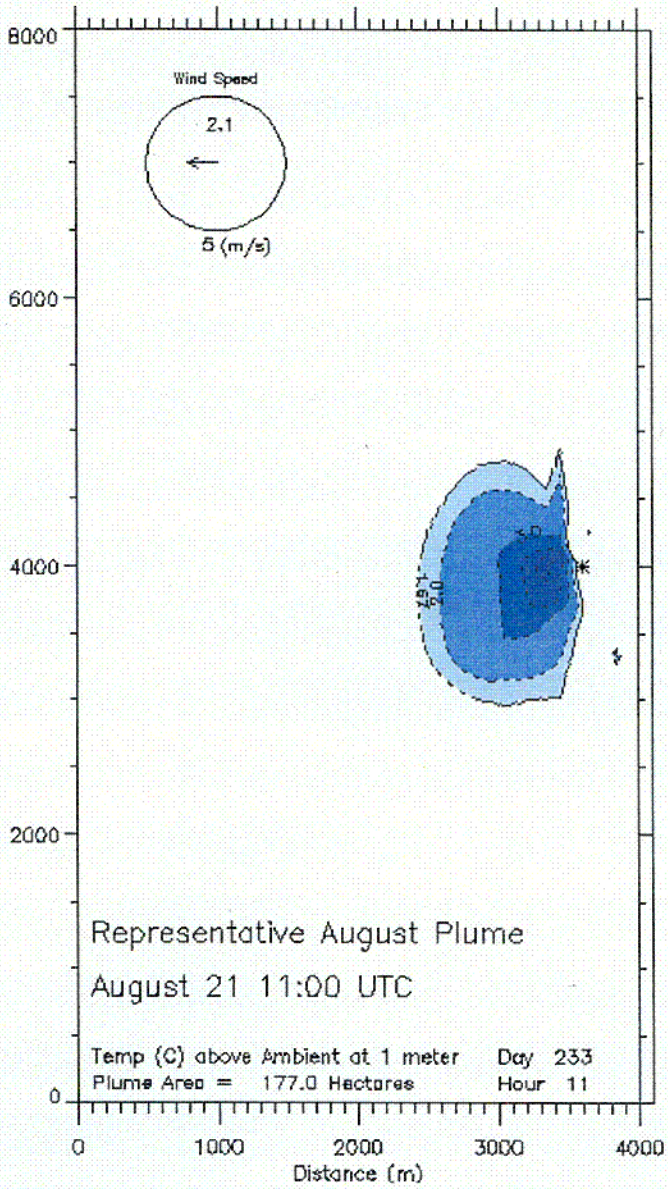

Figure 5-7. September Average Plume with High Plant Output.

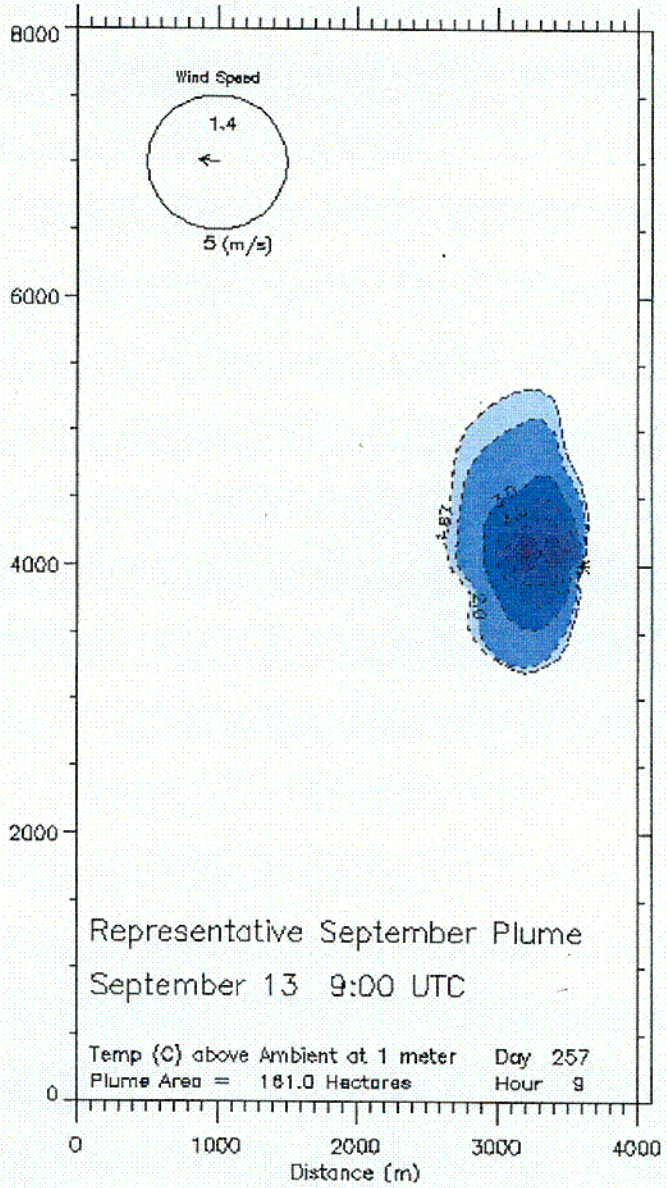

Figure 5-8. October Average Plume with High Plant Output.

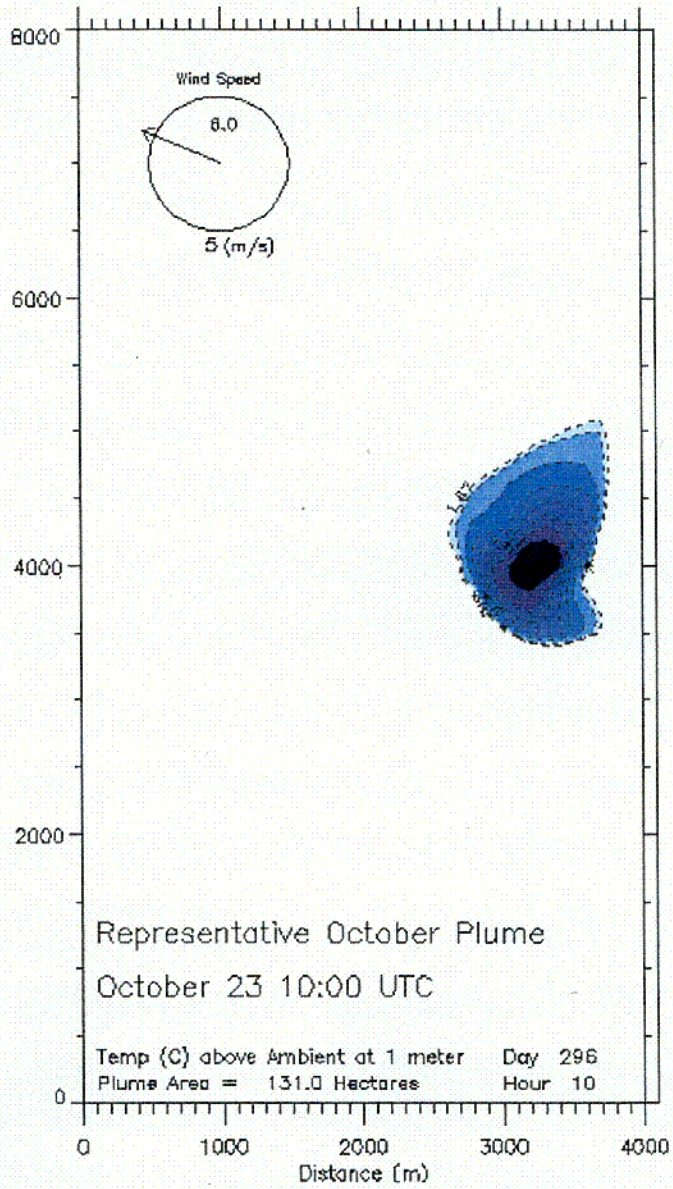

Figure 5-9. November Average Plume with High Plant Output.

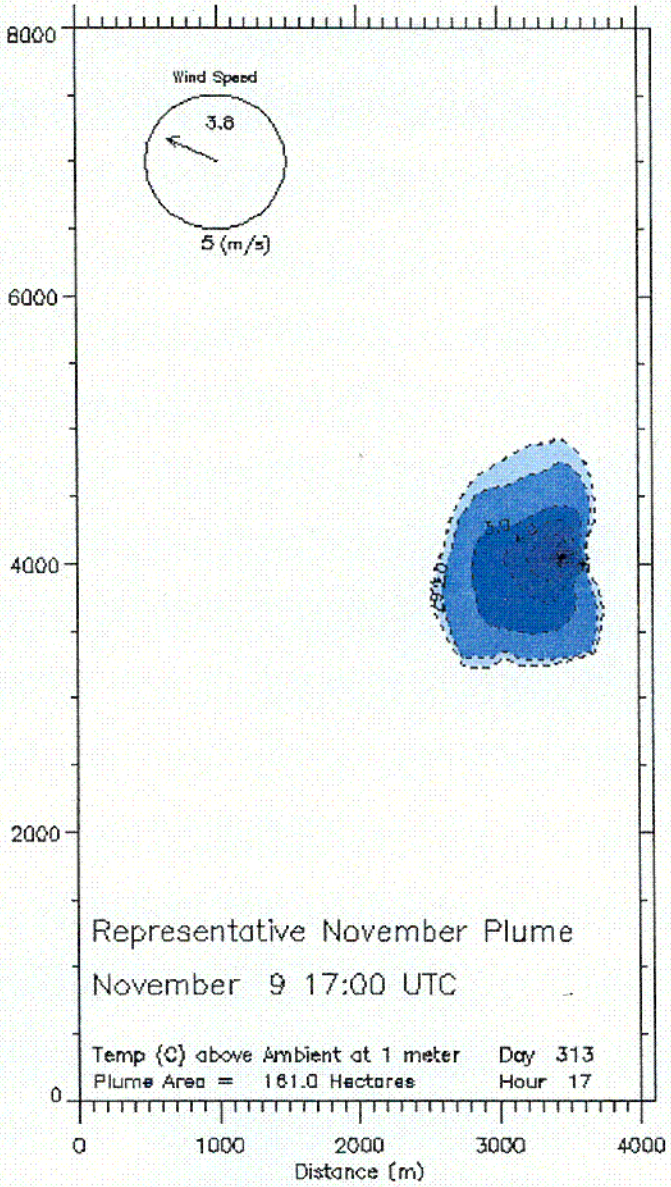

Figure 6-1. Plume Area Sensitivity to Wind Speed.

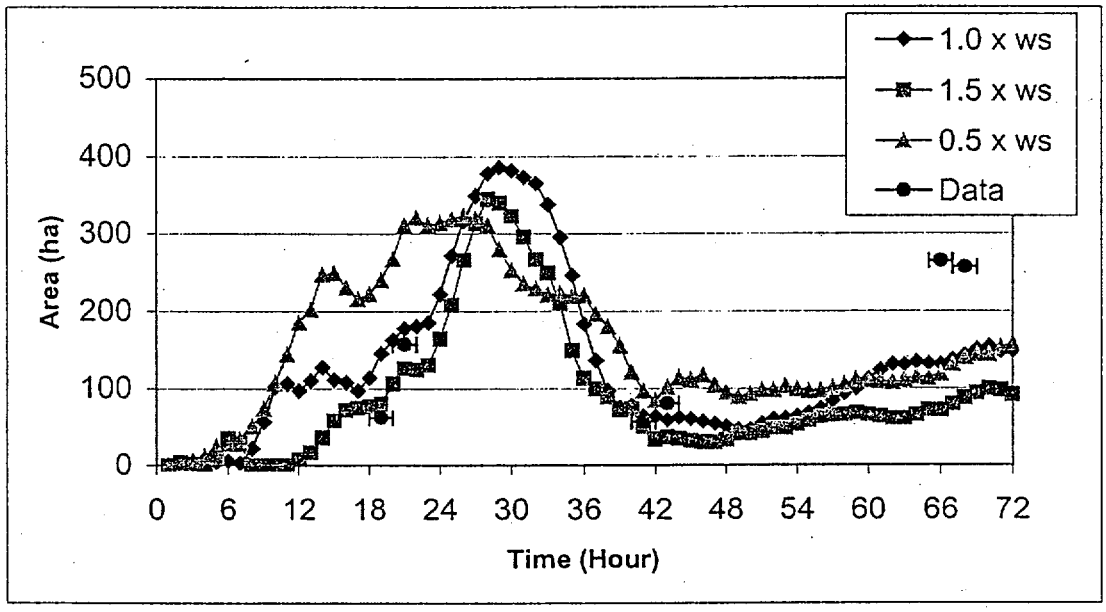

Figure 6-2. Plume Area Sensitivity to Wind Direction.

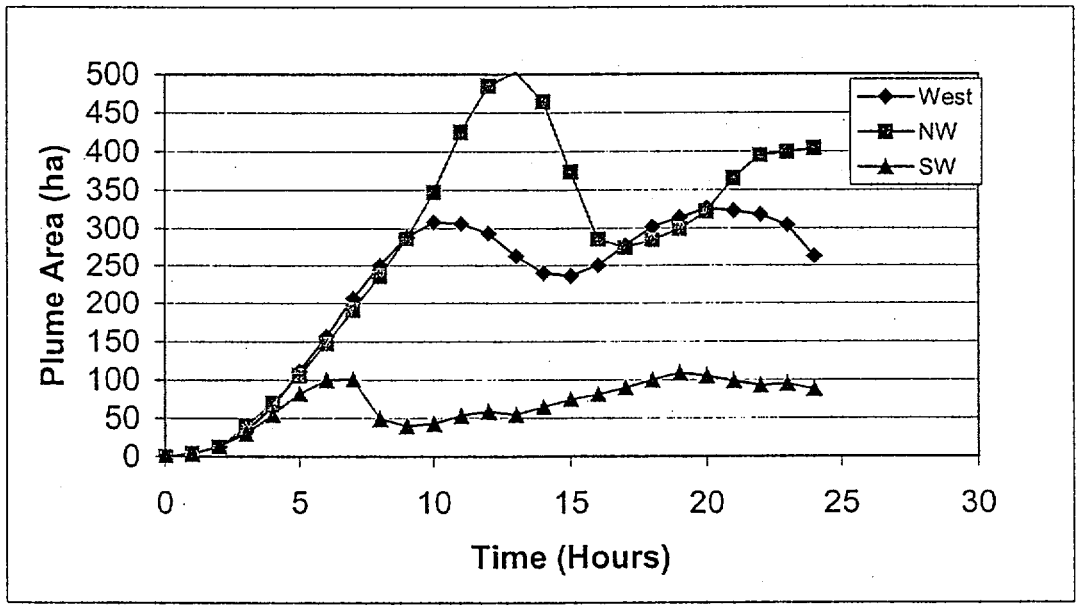

Figure 6-3. Plume Area Sensitivity to Cloud Cover.

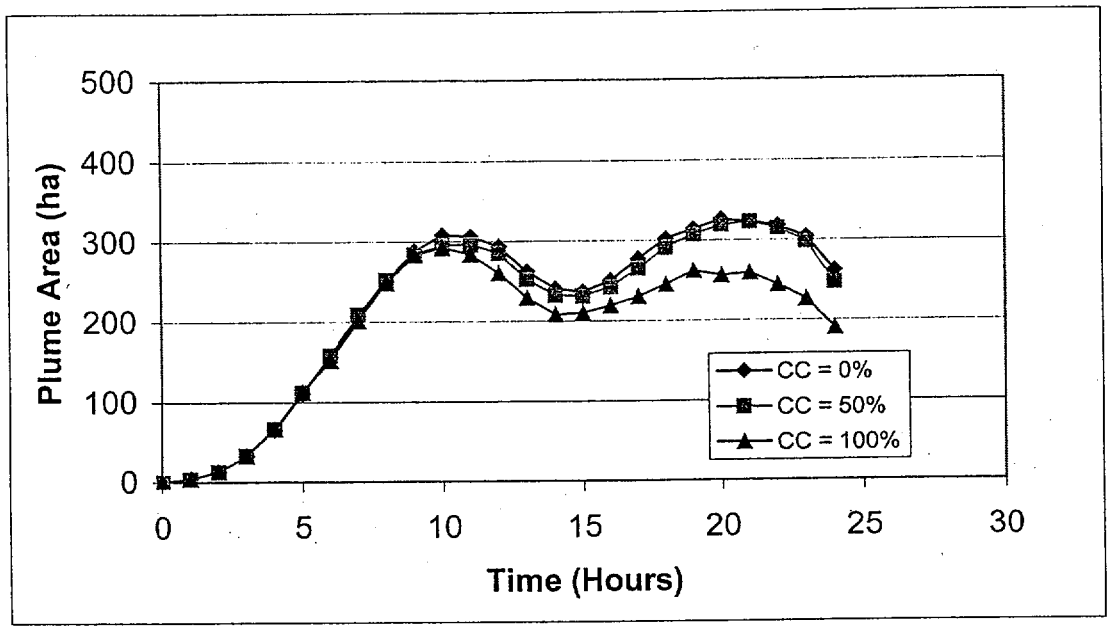

Figure 6-4 Plume Area Sensitivity to Air Temperature.

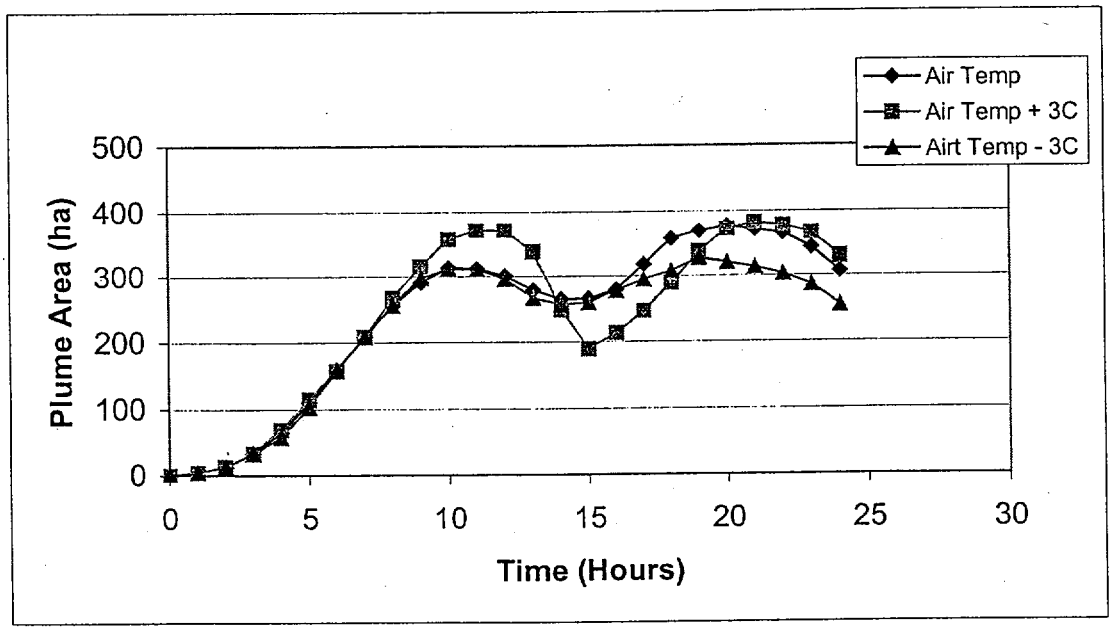

Figure 6-5. Plume Area Sensitivity to Relative Humidity.

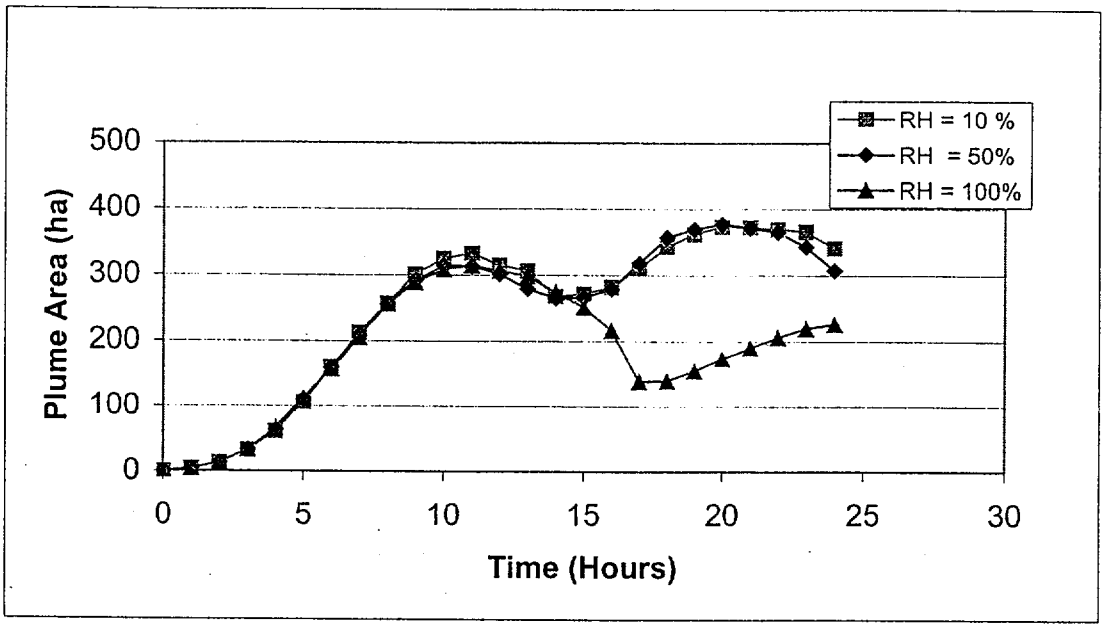

Table 1-1 Forcing Data and Field Data Used for the Model Runs.

Model Run	Forcing Data		Field Data
	Atmospheric	Boundary	
Performance Analysis; Short Term	78-79 Observation + Benton Harbor Airport	Estimated From 1978-79 Data	Nov 1 – 3, 1978 Measured Plumes
Performance Analysis; Long Term	1995 LMMBS* + Cook Plant Met. Tower	1995 LMMBS*	July 1979, Sept. and Nov. 1978 Measured Plumes
1995 Simulation	1995 LMMBS + Cook Plant Met. Tower	1995 LMMBS	Not Available
Sensitivity Analysis: Wind Speed	78-79 Observation + Benton Harbor Airport	Estimated From 1978-79 Data	Not Available
Sensitivity Analysis: Other Variables	Idealized	Estimated From 1978-79 Data	Not Available

* LMMBS is the abbreviation for the Lake Michigan Mass Balance Study.

TABLES

TABLE 2-1 SUMMARY OF 1978 - 1979 THERMAL PLUME MAPPING EVENT CHARACTERISTICS AND RESULTS
COOK NUCLEAR PLANT, BRIDGMAN, MI

Plumes Mapped on Relatively Calm Lake Days

Date	Time	Wind Speed (mph)	Wind Direction (°)	Air Temp. (°F)	Plant Reactor Power Unit 1	Plant Reactor Power Unit 2	Unit 1 Water Temp (°F) Intake	Unit 1 Water Temp (°F) Discharge	Unit 2 Water Temp (°F) Intake	Unit 2 Water Temp (°F) Discharge	Plume Area* (acres) Surface	Plume Area* (acres) 1 m	Plume Area* (acres) 2 m	Plume Area* (acres) 3 m	Plume Area* (acres) 4 m	Max Width @ 1 m (feet)	Plume Volume (acre-ft)
23-Aug-78	15:53 - 16:42	5 - 6	235 - 250	82 - 84	99.5% - 99.7%	25.5% - 60.6%	74 - 75	94.0 - 96.1	73.2 - 74.0	86.2 - 87	142	24	26	5	0	984	413
5-Sep-78	11:19 - 14:36	5 - 9	300 - 305	75 - 80	99.4% - 99.8%	88.4% - 90.6%	75.2 - 77.3	96.2 - 98.6	73.2 - 75.2	87.9 - 90.2	191	237	98	64	30	2230	1720
5-Sep-78	14:51 - 17:42	2 - 5	300 - 320	80 - 83	99.4% - 99.8%	90.0% - 90.5%	77.3 - 77.6	98.5 - 98.9	74.7 - 75.4	89.7 - 90.5	330	80	88	51	25	1148	1342
7-Nov-78	12:30 - 14:30	6 - NDA	110 - NDA	NDA	99.0% - 99.2%	80.0% - 80.8%	58.1 - 58.8	79.0 - 80.1	62.0 - 62.5	75.0 - 75.6	972+	294	56	25	18	2066	2883+
7-Nov-78	14:39 - 16:30	NDA	NDA	NDA	99.0% - 99.1%	80.0% - 81.9%	58.8	80.1 - 80.4	62.0 - 63.0	75.0 - 76.1	722	515	250	117	8	6724	4103

Date	Ambient Temperature Range (°F) Surface	Surface min	Surface max	1m	1m min	1m max	2m	2m min	2m max	3m	3m min	3m max	4m	4m min	4m max	Surface Current (1640 ft offshore) Speed (fps)	Direction (°)^	Surface Current (3280 ft offshore) Speed (fps)	Direction (°)^
23-Aug-78	75.9	75.6	76.5	75.0	74.5	75.4	74.5	74.0	75.1	73.7	72.9	74.2	72.7	72.6	73.5	0.23	26	0.23	151
5-Sep-78	74.5	73.9	74.8	73.5	73.2	74.6	72.3	71.9	72.7	71.5	70.4	72.3	70.6	70.0	71.9	0.23	199	0.2	25
5-Sep-78	77.4	76.0	77.9	75.8	75.0	76.9	74.4	72.9	75.3	73.0	71.2	74.8	71.8	71.0	72.6	0.36	138	0.52	143
7-Nov-78	54.6	54.4	54.7	54.5	54.4	54.7	54.4	54.0	54.6	54.4	54.2	54.5	54.3	54.1	54.3	0.2	208	0.16	226
7-Nov-78	54.5	54.3	54.6	54.4	53.6	54.7	54.4	54.0	54.6	54.1	53.8	54.3	53.9	53.6	54.1	0.33	184	0.33	156

Plumes Mapped on Days When Swell/Waves Were Less than or Equal to Two Feet.

Date	Time	Wind Speed (mph)	Wind Direction (°)	Air Temp. (°F)	Plant Reactor Power Unit 1	Plant Reactor Power Unit 2	Unit 1 Water Temp (°F) Intake	Unit 1 Water Temp (°F) Discharge	Unit 2 Water Temp (°F) Intake	Unit 2 Water Temp (°F) Discharge	Plume Area* (acres) Surface	Plume Area* (acres) 1 m	Plume Area* (acres) 2 m	Plume Area* (acres) 3 m	Plume Area* (acres) 4 m	Max Width @ 1 m (feet)	Plume Volume (acre-ft)
7-Sep-78	09:34 - 11:06	8 - 10	280 - 285	73 - 75	99.6% - 99.8%	96.7% - 96.9%	75.0 - 75.2	96.6 - 97.0	73.2 - 73.8	89.3 - 89.8	247+	336	92	57	0	4100	1996+
7-Sep-78	11:12 - 12:54	9 - 10	285 - 290	75 - 78	99.6% - 99.7%	96.9% - 97.3%	75.1 - 75.6	96.1 - 97.0	73.8 - 74.3	89.7 - 90.3	623+	568	305	44	0	4838	4029+
1-Nov-78	12:34 - 14:22	4 - 7	135 - 355	49 - 52	89.9 % - 99.1%	89.2 % - 89.8%	57.8 - 58.8	79.0 - 79.8	60.1 - 61.5	73.7 - 75.3	836+	154	101	51	12	1771	2414
1-Nov-78	14:28 - 16:19	2 - 5	15 - 355	51 - 52	99.1 % - 99.7%	85.9 % - 89.8%	57.6 - 58.9	79.0 - 80.1	60.1 - 61.5	73.6 - 75.3	1091+	389	129	53	26	2854	3747
3-Nov-78	09:50 - 11:26	13 - 14	250 - 255	55 - 59	98.7 % - 99.1%	79.5% - 79.7%	59.8 - 60.3	81.0 - 81.6	62.3 - 63.1	74.9 - 75.7	745	655	434	122	1	3838	5197
3-Nov-78	11:40 - 13:17	14 - 15	255 - 265	59 - 65	89.0 % - 99.2%	79.5% - 80.0%	59.4 - 60.3	80.7 - 81.5	62.4	75.0 - 75.3	1064+	634	428	98	20	4658	5615+
24-Jul-79	11:46 - 13:08	12	180 - 195	74 - 77	78.3% - 80.9%	99.3% - 100%	75.4 - 75.6	91.1 - 92.1	75.6 - 76.8	91.0 - 91.8	345	297	211	34	6	2034	2363
24-Jul-79	13:30 - 14:51	12 - 15	185 - 200	77 - 78	78.7% - 80.9%	100% - 100.1%	75.4 - 75.6	90.9 - 92.1	76.7 - 77.0	90.7 - 91.2	533	450	250	38	0	3182	3295
25-Jul-79	11:37 - 12:38	12 - 16	240 - 260	71 - 73	80.5% - 83.4%	99.5% - 100%	76.1 - 77.0	92.8 - 93.9	76.4 - 77.2	91.5 - 92.0	242+	109	39	21	0	700	951+
25-Jul-79	12:34 - 13:39	12 - 16	250 - 260	72 - 73	82.6% - 83.4%	99.8% - 100%	76.7 - 77.0	93.6 - 93.9	76.5	91.5 - 91.7	442+	161	64	27	0	950	1551+
27-Jul-79	11:28 - 12:45	7 - 8	240 - 300	75 - 78	85.2% - 89.8%	99.7% - 99.8%	73.1 - 75.9	91.6 - 94.4	75.5 - 75.9	91.2 - 91.8	221	30	18	6	0	918	540
27-Jul-79	13:15 - 13:50	7 - 8	255 - 305	75 -81	88.3% - 89.8%	99.8% - 100%	75.9	94.3 - 94.4	74.1 - 75.6	90.7 - 91.3	8	21	27	0.8	0	886	173
28-Jul-79	09:10 - 11:00	9 - 13	240 - 270	69	91.7% - 92.1%	99.8% - 99.9%	77.6 - 77.9	96.9 - 97.1	73.9 - 74.7	89.8 - 90.5	389	171	89	1	0	2624	1494
28-Jul-79	11:19 - 13:29	7 - 9	250 - 360	69 - 74	91.7% - 92.1%	99.7% - 99.9%	77.6 - 78.1	96.8 - 97.1	74.6 - 75.4	90.2 - 90.8	709	342	27	12	0	2755	2412

Date	Ambient Temperature Range (°F) Surface	Surface min	Surface max	1m	1m min	1m max	2m	2m min	2m max	3m	3m min	3m max	4m	4m min	4m max	Surface Current (1640 ft offshore) Speed (fps)	Direction (°)^	Surface Current (3280 ft offshore) Speed (fps)	Direction (°)^
7-Sep-78	74.7	74.1	74.8	73.4	73.4	73.6	73.5	73.3	74.2	73.2	72.9	73.4	72.9	72.7	73.2	---	---	0.26	356
7-Sep-78	73.9	73.7	74.0	73.4	73.1	74.1	73.3	72.9	73.7	72.8	72.5	73.3	72.7	72.4	72.9	---	---	0.46	14
1-Nov-78	54.6	54.4	54.7	54.1	53.9	54.5	53.6	53.3	54.0	53.5	53.2	53.8	53.2	53.1	53.2	0.26	76	0.33	39
1-Nov-78	54.7	54.3	54.8	54.4	54.0	54.8	54.2	53.7	54.6	53.5	53.1	54.0	53.1	53.1	53.2	0.2	12	0.2	58
3-Nov-78	54.0	53.9	54.1	53.9	53.8	54.1	53.9	53.8	54.1	53.9	53.7	54.0	53.8	53.7	53.9	0.16	11	0.16	14
3-Nov-78	54.0	53.9	54.1	54.0	53.8	54.1	53.8	53.8	54.1	53.8	53.8	54.0	53.8	53.4	53.9	0.16	15	0.16	37
24-Jul-79	71.5	71.2	71.8	71.7	71.4	72.0	71.7	71.4	72.0	71.7	71.4	72.0	71.6	71.4	71.9	0.33	359	0.3	2
24-Jul-79	71.4	71.2	71.6	71.6	71.5	71.8	71.6	71.5	71.8	71.5	71.4	71.7	71.4	71.7	71.4	0.33	2	0.36	4
25-Jul-79	71.3	71.3	71.4	71.5	71.5	71.7	71.5	71.4	71.7	71.7	71.5	71.7	71.5	71.5	71.6	0.52	12	0.39	14
25-Jul-79	71.3	71.3	71.4	71.5	71.4	71.5	71.5	71.5	71.7	71.8	71.5	71.8	71.5	71.4	71.6	---	---	0.33	20
27-Jul-79	72.0	71.8	72.0	72.0	71.9	72.4	71.5	71.4	71.6	71.2	71.1	71.4	71.4	70.6	71.5	0.16	141	0.33	79
27-Jul-79	74.1	73.3	74.6	72.8	72.6	73.1	72.0	71.5	72.2	71.4	71.2	71.6	71.5	70.5	71.9	0.3	143	0.43	146
28-Jul-79	72.9	72.9	73.1	73.1	72.9	73.3	73.0	72.9	73.3	73.0	72.8	73.1	72.8	72.5	73.0	0.66	27	0.66	13
28-Jul-79	72.9	72.8	73.0	73.0	72.9	73.1	73.1	73.0	73.2	73.0	72.9	73.1	73.0	72.9	73.1	0.66	11	0.56	23

Plumes Mapped on Days When Swell/Waves Were Greater Than Two Feet.

Date	Time	Wind Speed (mph)	Wind Direction (°)	Air Temp. (°F)	Plant Reactor Power Unit 1	Plant Reactor Power Unit 2	Unit 1 Water Temp (°F) Intake	Unit 1 Water Temp (°F) Discharge	Unit 2 Water Temp (°F) Intake	Unit 2 Water Temp (°F) Discharge	Plume Area* (acres) Surface	Plume Area* (acres) 1 m	Plume Area* (acres) 2 m	Plume Area* (acres) 3 m	Plume Area* (acres) 4 m	Max Width @ 1 m (feet)	Plume Volume (acre-ft)
25-Aug-78	09:50 - 12:58	2 - 8	60 - 290	72 - 76	99.3% - 99.7%	100%	76.7 - 77.3	97.9 - 98.2	73.1 - 73.8	89.6 - 89.8	829+	193	47	28	27	2394	2327+
25-Aug-78	13:06 - 15:50	7 - 8	285 - 290	74 - 76	99.2% - 99.7%	99.6% - 100%	73.1 - 76.7	94.5 - 98.1	71.4 - 73.8	87.0 - 89.7	914	311	51	21	5	2362	2771
6-Sep-78	10:47 - 12:51	7 - 10	285 - 300	75 - 78	99.4% - 99.7%	97.3% - 97.4%	75.1 - 75.3	96.4 - 97.1	72.9 - 74.0	89.5 - 90.3	340	287	48	24	0	2165	1732
6-Sep-78	13:11 - 15:07	6 - 7	280 - 300	78 - 81	99.4% - 99.8%	97.2% - 97.4%	75.1 - 76.5	96.2 - 97.6	73.4 - 74.0	89.5 - 90.2	582+	117	36	23	0	1673	1537+
8-Sep-78	09:45 - 11:45	8 - 10	285	76 - 82	99.1% - 99.3%	97.0% - 97.2%	76.0 - 76.6	97.2 - 97.8	75.2 - 75.9	91.3 - 92.2	607+	549	225	44	0	5642	3678+
8-Sep-78	11:52 - 14:07	8 - 10	285 - 300	82 - 87	99.1% - 99.2%	97.2% - 97.4%	76.3 - 76.5	97.7 - 97.8	75.4 - 75.9	91.3 - 92.7	1087+	740	175	14	7	4264	4852+
2-Nov-78	10:10 - 12:11	12 - 16	250 - 260	50 - 54	99.3% - 99.4%	74.1% - 75.2%	57.1 - 58.1	78.1 - 79.4	58.6 - 59.3	69.9 - 71.0	208	142	71	20	0	2394	1105
2-Nov-78	12:29 - 13:24	13 - 16	255 - 260	54 - 57	99.2% - 99.3%	75.0% - 75.2%	57.1 - 58.1	78.3 - 79.3	58.6 - 59.9	69.9 - 71.3	333	200	60	37	0	1705	1520
26-Jul-79	07:05 - 08:45	10 - 12	15 - 30	61 - 69	78.0% - 81.2%	99.7% - 100%	74.2 - 75.5	91.6 - 91.8	75.5 - 75.9	91.2 - 91.4	365	149	29	2	0.3	1804	1190
26-Jul-79	09:20 - 10:28	10 - 12	20 - 45	69 - 75	81.2% - 85.2%	100%	74.2 - 75.3	91.6 - 91.8	75.4 - 75.9	91.2 - 91.8	325	269	53	11	0	2821	1625

Date	Ambient Temperature Range (°F) Surface	Surface min	Surface max	1m	1m min	1m max	2m	2m min	2m max	3m	3m min	3m max	4m	4m min	4m max	Surface Current (1640 ft offshore) Speed (fps)	Direction (°)^	Surface Current (3280 ft offshore) Speed (fps)	Direction (°)^
25-Aug-78	75.9	75.6	76.2	75.6	75.2	76.1	75.4	74.5	75.7	74.9	73.7	75.7	74.4	73.5	76.5	0.3	205	0.33	192
25-Aug-78	75.9	75.6	76.2	75.6	75.2	76.1	75.4	74.5	75.7	74.9	73.7	75.7	74.4	73.5	75.6	---	---	0.46	158
6-Sep-78	74.0	73.7	74.2	73.5	73.2	73.8	73.3	72.8	73.6	73.0	72.1	73.5	72.0	71.5	73.4	---	---	0.43	27
6-Sep-78	74.8	73.4	74.9	74.5	74.0	74.9	74.2	73.6	74.6	73.5	72.8	73.8	73.3	72.6	73.4	---	---	0.85	357
8-Sep-78	73.4	73.4	73.7	73.2	72.9	73.5	73.1	72.7	73.2	73.0	72.7	73.1	72.7	72.6	72.9	---	---	0.43	15
8-Sep-78	73.8	73.7	74.0	73.3	73.1	74.1	73.5	73.0	74.2	73.3	72.9	73.6	73.0	72.8	73.2	---	---	0.23	27
2-Nov-78	54.4	54.2	54.7	54.6	54.5	54.8	54.4	54.1	54.5	54.3	54.0	54.5	54.3	54.0	54.4	0.43	7	0.46	10
2-Nov-78	54.4	54.1	54.5	54.3	54.0	54.4	54.2	54.0	54.4	54.2	54.0	54.8	54.1	54.0	54.3	0.75	4	0.82	10
26-Jul-79	71.4	71.3	71.4	71.2	70.9	71.3	71.4	71.0	71.6	71.5	71.1	71.6	71.5	71.5	71.7	0.52	177	0.79	187
26-Jul-79	71.3	71.2	71.3	71.0	70.8	71.0	71.1	71.0	71.2	71.3	71.2	71.4	71.3	71.2	71.5	0.56	179	0.89	189

* Area measured within Δ3°F boundary

^ Rotated to conform to the convention that the D.C. Cook North-South Plant centerline is 0°
(Actual magnetic direction is 18°).

NDA: No Data Available

TABLE 2-2 SUMMARY OF AMBIENT LAKE TEMPERATURE DATA AVAILABLE ON PLUME MAPPING DAYS
COOK NUCLEAR PLANT, BRIDGMAN, MI

Plumes Mapped on Relatively Calm Lake Days

Date	Plume Mapping Time	Temperature Log Time	North Inshore Temperature*						South Inshore Temperature*						West Offshore Temperature*					
			19'	17'	14'	11'	8'	4'	19'	17'	14'	11'	8'	4'	29'	27'	24'	21'	17'	14'
23-Aug-78	15:53 - 16:42	15:30	73.24	73.96	74.81	75.38	76.66	77.93	57.18	67.02	72.83	73.21	73.80	75.03	46.09	46.12	46.74	51.74	68.33	71.87
		16:00	74.28	74.62	74.92	75.27	76.26	77.65	67.71	71.87	72.97	73.50	74.25	75.44	46.27	46.33	47.32	54.65	68.12	71.38
		16:30	74.23	74.68	74.87	75.35	76.15	77.34	71.60	72.78	73.10	73.55	74.48	75.47	46.51	46.80	48.43	61.74	69.68	72.11
		17:00	74.57	74.76	74.92	75.30	76.02	77.18	72.25	72.86	73.05	73.47	74.31	75.33	46.69	47.16	52.08	64.71	70.39	71.49
5-Sep-78	11:19 - 14:36	11:00	71.60	71.87	72.75	74.04	75.88	77.46	70.61	70.69	70.96	71.17	73.02	74.09	62.94	66.21	67.63	?	71.19	71.38
		11:30	71.71	71.90	72.62	73.29	75.83	77.87	70.29	70.61	71.00	71.38	73.10	74.23	60.35	65.54	67.39	?	71.14	71.46
		12:00	71.76	72.06	72.72	73.44	76.24	78.48	70.18	70.69	71.09	71.41	72.91	74.81	61.39	65.57	67.66	70.47	71.41	71.55
		12:30	71.87	72.11	71.81	73.69	76.32	78.70	70.02	70.85	71.22	71.52	73.38	75.00	60.62	63.96	67.14	70.47	71.14	71.57
		13:00	71.98	72.45	73.29	74.62	77.04	79.22	70.07	71.00	71.54	71.71	73.53	74.73	61.95	65.81	68.39	70.69	71.52	71.57
		13:30	73.02	73.53	73.93	74.87	76.93	78.75	70.39	71.30	71.55	71.90	73.36	74.89	61.07	65.76	69.35	71.02	71.63	71.73
		14:00	73.18	73.63	74.15	74.89	77.35	78.34	70.29	71.33	72.00	72.25	72.78	73.80	64.74	66.99	70.69	71.55	71.66	71.70
		14:30	73.24	73.82	74.20	75.56	77.51	78.57	71.38	71.79	72.09	72.56	73.69	75.22	64.74	68.92	71.28	71.52	71.66	71.73
5-Sep-78	14:51 - 17:42	15:00	73.13	73.85	74.37	76.15	77.46	78.37	71.49	72.00	72.35	72.83	73.80	75.33	65.68	69.13	70.93	71.52	71.50	71.73
		15:30	73.02	74.07	74.51	75.56	77.57	78.73	71.22	71.46	71.65	72.62	73.80	75.53	68.14	70.72	71.41	71.57	71.73	72.45
		16:00	73.29	74.07	74.40	75.24	76.50	78.97	71.38	71.65	72.22	72.99	74.25	75.85	68.25	70.74	71.38	71.71	71.79	72.14
		16:30	73.24	73.46	73.80	74.36	76.05	78.28	71.49	72.06	72.37	72.70	74.04	75.75	68.54	70.93	71.57	71.79	71.90	72.51
		17:00	72.37	72.75	73.36	73.80	75.22	77.02	71.55	72.06	72.45	72.97	74.15	75.06	67.39	70.74	71.60	71.79	72.00	72.45
		17:30	72.03	72.31	73.38	74.20	75.00	78.34	71.38	72.03	72.45	72.81	73.88	75.33	67.87	70.58	71.60	71.79	71.98	72.75
		18:00	71.87	72.26	73.24	73.85	74.51	78.50	71.71	71.95	72.22	72.64	75.06	75.96	65.97	68.70	71.46	71.68	71.95	72.70
7-Nov-78	12:30 - 14:30	12:30	54.19	54.28	54.35	54.82	55.13	56.19	54.09	54.11	54.22	54.35	54.71	55.16	53.74	53.77	53.77	53.80	53.82	53.92
		13:00	54.19	54.22	54.28	54.56	54.93	55.52	54.03	54.11	54.19	54.35	54.71	55.19	53.74	53.77	53.77	53.80	53.85	53.98
		13:30	54.19	54.28	54.37	54.68	54.99	56.26	53.98	54.06	54.17	54.28	43.20	55.19	53.74	53.77	53.77	53.80	53.89	53.98
		14:00	54.25	54.28	54.37	54.68	54.96	56.20	53.98	54.06	54.14	54.22	54.63	55.09	53.74	53.77	53.77	53.82	53.92	54.03
7-Nov-78	14:39 - 16:30	14:30	54.19	54.28	54.35	54.54	54.91	55.89	53.92	54.03	54.09	54.28	54.82	55.70	53.74	53.74	53.74	53.80	53.89	54.03
		15:00	54.03	54.06	54.37	54.59	54.80	55.52	53.92	54.01	54.06	54.11	54.43	55.19	53.74	53.74	53.74	53.80	53.82	53.98
		15:30	53.98	54.11	54.28	54.40	54.63	55.22	53.92	53.98	54.03	54.06	54.28	55.46	53.74	53.74	53.74	53.80	53.80	53.98
		16:00	54.14	54.22	54.28	54.37	54.48	54.93	53.92	53.95	54.01	54.06	54.72	56.02	53.69	53.74	53.72	53.77	53.85	54.01
		16:30	54.14	54.17	54.22	54.25	54.35	54.59	53.92	53.92	53.98	54.01	54.09	55.25	53.69	53.72	53.72	53.80	53.92	54.14

Plumes Mapped on Days When Swell/Waves Were Less than or Equal to Two Feet.

Date	Plume Mapping Time	Current Log Time	North Inshore Temperature						South Inshore Temperature						West Offshore Temperature*					
			19'	17'	14'	11'	8'	4'	19'	17'	14'	11'	8'	4'	29'	27'	24'	21'	17'	14'
7-Sep-78	09:34 - 11:06	9:30	72.59	73.26	76.27	76.55	76.77	77.21	72.86	73.05	73.24	73.35	73.71	73.95	72.03	72.17	72.22	72.45	72.64	72.81
		10:00	72.85	74.45	76.27	76.74	77.04	77.67	72.86	73.02	73.24	73.35	73.69	74.01	71.98	72.14	72.19	72.37	72.51	72.64
		10:30	74.57	75.64	76.32	76.68	77.04	77.70	72.91	73.02	73.18	73.26	73.63	73.90	71.87	72.11	72.17	72.28	72.45	72.62
7-Sep-78	11:12 - 12:54	11:00	76.15	76.52	76.87	77.32	77.81	78.70	73.13	73.18	73.41	73.47	73.90	74.40	72.03	72.17	72.19	72.35	72.45	72.59
		11:30	73.29	76.05	76.87	77.41	77.90	78.86	73.13	73.24	73.46	73.55	74.04	74.48	71.76	72.14	72.22	72.35	72.45	72.67
		12:00	74.07	75.67	76.66	77.27	78.03	79.01	73.24	73.32	73.55	73.63	74.15	74.48	72.03	72.17	72.28	72.48	72.99	73.05
		12:30	75.67	76.35	77.38	77.90	78.59	79.47	73.29	73.41	73.66	73.85	74.51	74.76	70.83	71.92	72.26	72.51	73.10	73.71
		13:00	74.89	76.27	77.32	77.90	78.67	79.67	73.35	73.50	73.77	73.93	74.48	74.92	61.72	67.23	72.03	72.51	73.08	73.61
1-Nov-78	12:34 - 14:22	12:30	52.74	52.79	53.16	54.11	56.23	58.49	53.19	53.21	53.24	53.49	53.82	54.45	52.61	52.66	52.66	52.79	52.84	52.95
		13:00	52.66	52.76	53.03	55.09	55.80	58.18	53.19	53.19	53.24	53.49	53.89	54.65	52.66	52.74	52.79	52.90	52.93	53.13
		13:30	52.45	52.50	53.32	54.32	55.46	59.01	53.19	53.21	53.24	53.49	53.86	54.56	52.66	52.76	52.82	52.90	52.95	53.01
		14:00	52.45	52.50	54.06	54.48	55.16	57.96	53.19	53.24	53.43	53.61	53.89	54.77	52.74	52.79	52.93	53.01	53.16	53.69
1-Nov-78	14:28 - 16:19	14:30	52.56	53.38	54.28	54.48	54.99	58.68	53.35	53.46	53.64	53.77	54.11	54.74	52.74	52.76	52.90	53.13	53.46	53.64
		15:00	53.85	54.22	54.40	55.04	57.21	59.13	53.40	53.55	53.74	54.17	54.40	55.13	52.79	52.84	53.01	53.19	53.24	53.35
		15:30	53.58	54.37	54.62	55.27	55.89	57.51	53.58	53.80	54.14	54.28	54.62	55.01	52.90	52.98	53.06	53.16	53.21	53.40
		16:00	53.69	54.56	54.96	55.09	55.41	56.42	53.85	54.06	54.45	54.56	54.74	54.93	53.01	53.03	53.06	53.21	53.29	53.58
		16:30	53.01	53.98	54.74	54.99	55.22	55.99	54.03	54.28	54.54	54.68	54.82	54.93	53.13	53.16	53.19	53.35	53.46	53.69
3-Nov-78	09.50 - 11:26	9:30	54.93	55.01	55.04	55.19	55.36	55.80	53.74	53.80	53.86	53.89	54.01	54.17	53.53	53.53	53.53	53.58	53.61	53.69
		10:00	54.93	55.01	55.09	55.41	55.62	56.16	53.80	53.82	53.89	53.98	54.11	54.35	53.53	53.55	53.55	53.61	53.66	53.72
		10:30	54.99	55.07	55.17	55.41	55.62	56.26	53.80	53.89	53.95	54.01	54.17	54.45	53.53	53.55	53.55	53.64	53.77	53.85
		11:00	55.17	55.25	55.41	55.75	55.97	56.70	53.80	53.89	53.98	54.09	54.31	54.68	53.53	53.58	53.58	53.69	54.01	54.32
		11:30	55.22	55.30	55.58	56.08	56.26	57.09	53.85	53.92	54.03	54.11	54.35	54.80	53.53	53.58	53.58	53.72	54.17	54.99
3-Nov-78	11:40 - 13:17	12:00	55.27	55.58	55.97	56.53	55.79	57.73	53.85	53.95	54.09	54.17	54.45	54.93	53.53	53.58	53.58	53.77	54.68	55.17
		12:30	55.27	56.02	56.56	56.95	57.18	58.29	53.92	53.98	54.09	54.19	54.54	55.08	53.53	53.55	53.58	53.77	54.74	55.22
		13:00	55.27	56.08	56.59	57.00	57.45	58.82	53.92	53.98	54.14	54.22	54.60	55.13	53.53	53.55	53.61	53.74	54.68	55.17
		13:30	55.38	56.17	56.65	57.09	57.98	59.34	53.92	54.01	54.14	54.28	54.68	55.22	53.53	53.53	53.55	53.72	53.85	55.01
24-Jul-79	11:46 - 13:08	11:30	72.25	72.75	72.91	73.02	73.24	73.29							70.88	71.06	71.17	71.30	71.36	72.03
		12:00	72.32	72.78	72.97	73.08	73.24	73.29							70.77	70.93	71.14	71.30	71.55	72.03
		12:30	72.43	72.81	72.97	73.02	73.13	73.18							70.12	70.47	70.99	71.30	71.73	72.43
		13:00	72.81	73.13	73.41	73.71	73.96	74.09							68.97	69.65	70.83	71.17	71.44	72.19
24-Jul-79	13:30 - 14:51	13:30	73.29	73.63	73.80	74.39	74.84	75.08							68.49	69.30	70.83	71.22	71.57	72.48
		14:00	73.63	73.85	74.15	74.76	75.22	75.53							69.03	70.02	70.88	71.36	72.09	72.37
		14:30	73.13	73.44	73.82	74.23	74.73	74.97							68.09	68.28	69.13	70.74	71.68	72.11
		15:00	73.53	73.74	74.34	75.03	75.53	75.96							70.18	70.85	71.19	71.84	72.26	72.32
25-Jul-79	11:37 - 12:38	11:30	72.64	79.89	72.81	72.94	73.08	73.10							71.55	71.60	71.60	71.68	71.92	72.03
		12:00	72.54	72.70	72.81	72.86	72.91	72.91							71.60	71.68	71.65	71.73	71.84	71.92
25-Jul-79	12:34 - 13:39	12:30	72.54	72.64	72.64	72.64	86.97	72.70							71.60	71.68	71.65	71.76	71.84	71.87
		13:00	72.75	80.02	72.99	73.16	73.29	73.47							71.60	71.63	71.71	71.90	72.03	72.19
		13:30	73.18	73.35	73.63	74.01	74.23	74.62							71.60	71.63	71.63	71.73	71.84	72.09
27-Jul-79	11:28 - 12:45	11:30	67.71	68.92	71.28	79.16	79.80	72.89							56.34	57.40	60.51	67.98	71.52	71.60
		12:00	69.13	69.83	71.00	79.29	79.92	80.19							56.68	57.69	60.51	64.12	71.52	71.76
		12:30	69.62	84.50	85.88	86.45	79.89	73.16							56.34	57.45	60.78	63.29	71.49	71.76
		13:00	69.51	84.78	85.71	79.27	72.67	73.35							57.45	58.54	61.97	65.58	71.52	72.64
27-Jul-79	13:15 - 13:50	13:30	68.65	69.59	78.30	79.29	87.03	73.77							57.69	58.54	61.74	65.62	71.52	72.64
		14:00	69.13	83.84	85.62	86.48	87.40	81.40							57.40	58.32	61.64	64.55	71.60	72.03
28-Jul-79	09:10 - 11:00	9:00	73.63	88.74	88.92	69.06	89.10	89.10							63.43	64.44	66.67	70.91	71.79	72.75
		9:30	74.12	88.89	89.09	89.26	89.38	89.38							61.72	63.80	68.42	71.22	72.06	72.91
		10:00	74.07	81.65	89.14	89.20	89.26	89.31							62.84	65.16	69.85	71.49	72.19	72.70
		10:30	73.69	88.86	89.09	89.09	89.12	89.15							64.36	66.94	69.80	71.46	72.64	73.35
		11:00	74.57	89.15	89.20	74.97	75.33	82.76							64.09	64.44	68.45	72.97	73.08	73.13
28-Jul-79	11:19 - 13:29	11:30	74.17	74.51	89.09	74.95	89.83	75.78							63.77	64.15	69.21	72.89	72.97	72.97
		12:00	72.86	87.42	88.22	88.86	89.55	89.83							67.55	69.48	72.14	72.72	72.89	72.86
		12:30	72.81	87.19	87.48	88.63	89.12	76.05							69.30	70.77	72.03	72.59	72.75	72.81
		13:00	72.70	87.13	87.83	81.80	75.83	76.74							67.87	70.31	72.43	72.72	73.26	73.35
		13:30	72.64	87.08	87.48	88.57	88.92	76.21							71.55	72.40	72.81	72.99	73.16	73.40

Plumes Mapped on Days When Swell/Waves Were Greater Than Two Feet.

Date	Plume Mapping Time	Temperature Log Time	North Inshore Temperature*						South Inshore Temperature*						West Offshore Temperature*					
			19'	17'	14'	11'	8'	4'	19'	17'	14'	11'	8'	4'	29'	27'	24'	21'	17'	14'
25-Aug-78	09:50 - 12:58	9:30	72.97	73.13	73.71	74.89	75.33	75.72	72.43	72.59	72.81	76.26	73.63	73.80	67.23	68.78	69.65	72.14	72.63	73.80
		10:00	72.86	72.99	73.80	74.95	75.33	75.99	72.19	72.40	72.54	72.78	73.29	73.77	66.56	68.36	70.07	72.28	72.67	73.44
		10:30	72.97	73.63	74.89	75.16	75.43	75.94	72.19	72.31	72.91	73.63	73.93	74.36	62.28	66.94	69.54	71.98	72.62	73.80
		11:00	72.91	73.13	73.41	74.95	75.33	75.72	72.14	72.37	73.26	73.90	74.28	75.14	59.85	64.61	69.35	71.41	72.62	73.47
		11:30	73.08	73.29	74.07	75.27	75.51	75.85	71.82	72.03	72.43	73.02	73.93	74.51	58.35	63.59	68.92	70.72	72.43	73.02
		12:00	73.08	73.35	73.56	74.25	75.56	76.21	71.49	71.73	72.46	73.18	73.90	75.16	57.74	63.43	68.65	71.36	72.51	73.02
		12:30	72.86	73.29	73.52	74.60	75.56	76.44	70.77	71.68	72.43	73.02	73.80	75.22	56.17	59.15	68.12	70.64	72.22	73.05
25-Aug-78	13:06 - 15:50	13:00	72.59	73.29	73.52	74.51	75.80	77.24	70.39	70.93	72.45	73.05	73.88	75.06	55.54	58.57	67.23	69.54	72.03	73.16
		13:30	72.75	73.24	73.58	74.36	75.88	77.32	70.56	71.55	72.59	73.18	73.85	75.00	53.24	55.38	64.23	67.77	71.73	73.16
		14:00	72.86	73.24	73.69	74.43	76.26	76.98	70.50	71.46	72.67	73.24	73.90	75.08	49.87	51.67	57.06	65.70	71.36	73.21
		14:30	72.86	73.18	73.63	74.81	75.33	76.10	70.07	70.85	72.64	73.13	73.80	74.20	48.54	49.46	53.61	63.59	69.74	73.21
		15:00	72.48	73.10	73.61	74.68	76.21	77.13	66.34	68.67	70.96	73.10	73.98	74.79	47.61	47.84	49.15	55.25	64.09	72.22
		15:30	68.49	71.82	73.85	75.83	76.32	76.82	62.22	66.01	70.83	73.08	73.90	74.81	47.26	47.26	48.20	52.32	62.41	71.85
		16:00	68.04	71.79	73.74	75.88	76.23	76.66	57.85	60.78	67.07	70.83	73.69	74.79	47.03	47.03	47.32	51.82	62.94	71.30
6-Sep-78	10:47 - 12:51	10:30	73.35	73.74	74.25	74.70	76.19	76.14	71.49	72.64	73.63	73.90	74.51	74.61	66.46	65.81	66.99	71.36	71.82	72.78
		11:00	74.01	74.17	74.45	74.95	75.91	76.82	72.59	73.16	73.93	74.23	74.65	74.81	65.52	66.32	67.32	69.27	71.76	72.28
		11:30	74.23	74.63	75.00	75.59	76.38	77.57	73.58	73.65	74.23	74.39	74.79	75.03	65.84	66.88	67.41	68.33	71.33	72.14
		12:00	74.84	75.19	75.67	76.50	77.73	79.39	72.14	74.15	74.42	74.60	75.06	75.33	65.03	66.42	67.87	69.16	71.71	72.25
		12:30	75.16	75.60	76.10	76.77	77.67	79.09	71.38	73.03	74.48	74.60	75.16	75.50	66.45	68.06	69.32	70.20	71.25	71.90
6-Sep-78	13:11 - 15:07	13:00	74.68	75.50	76.30	76.68	77.34	78.42	71.44	73.10	74.04	74.25	74.89	75.38	66.78	68.59	70.29	70.96	71.36	71.76
		13:30	74.44	75.75	76.41	76.98	77.95	79.09	71.38	71.98	73.98	74.25	75.11	75.56	65.89	67.85	69.93	71.02	71.52	71.95
		14:00	75.06	76.13	76.58	77.21	78.37	79.62	71.38	71.84	73.60	74.65	75.08	75.56	66.45	67.25	68.45	71.00	71.79	73.55
		14:30	74.89	75.94	76.60	77.01	77.82	79.29	71.33	71.71	73.98	74.54	75.06	75.61	66.94	69.16	70.77	71.02	72.11	73.61
		15:00	74.84	76.13	76.68	77.14	78.40	79.67	71.38	70.71	73.50	74.42	75.11	75.61	67.39	69.73	71.19	71.57	71.79	72.00
8-Sep-78	09:45 - 11:45	9:30	75.22	75.47	75.78	76.15	76.52	77.13	73.18	73.24	73.32	73.35	73.58	73.71	73.24	73.32	73.40	73.61	73.77	74.01
		10:00	75.11	75.42	75.83	76.38	76.93	77.79	73.24	73.29	73.41	73.47	73.80	73.98	73.24	73.29	73.32	73.53	73.80	74.12
		10:30	74.52	75.22	75.91	76.66	77.32	78.29	73.35	73.41	73.65	73.66	74.07	74.23	73.18	73.26	73.35	73.61	74.01	74.36
		11:00	74.73	75.53	76.18	76.71	77.62	78.73	73.35	73.46	73.69	73.74	74.17	74.40	73.18	73.26	73.44	73.80	74.07	74.23
		11:30	75.22	75.96	76.52	77.06	78.01	79.26	75.35	73.46	73.74	73.82	74.43	74.60	73.24	73.35	73.47	73.88	74.31	74.54
8-Sep-78	11:52 - 14:07	12:00	74.23	74.76	76.52	76.95	78.06	79.47	73.40	73.65	73.85	73.93	74.48	74.73	73.18	73.32	73.44	73.77	74.12	74.48
		12:30	74.12	74.43	76.02	77.27	78.26	79.67	73.47	73.63	73.93	744.07	74.68	74.95	73.13	73.26	73.35	73.55	73.77	74.07
		13:00	74.07	74.31	75.50	77.66	78.45	79.65	73.63	73.80	74.15	74.39	74.97	75.19	73.18	73.26	73.35	73.55	73.71	73.85
		13:30	74.12	74.43	?	77.78	78.62	79.67	73.80	73.98	74.34	74.57	75.14	75.43	73.24	73.32	73.44	73.55	73.71	73.80
		14:00	74.07	74.31	?	77.70	78.62	79.95	73.96	74.15	74.42	74.62	75.22	75.66	73.29	73.37	73.50	73.66	73.80	73.85
2-Nov-78	10:10 - 12:11	10:00	54.14	54.22	54.37	55.19	55.70	56.51	54.37	54.40	54.45	54.51	54.62	54.85	53.80	53.82	53.80	53.85	83.89	53.92
		10:30	54.54	54.74	55.25	55.89	56.31	57.20	54.37	54.37	54.43	54.51	54.62	54.93	53.80	53.82	53.82	53.85	53.89	53.92
		11:00	55.22	55.36	55.58	56.02	56.31	57.23	54.37	54.37	54.45	54.54	54.68	54.99	53.80	53.82	53.82	53.89	53.92	53.92
		11:30	55.04	55.13	55.30	55.78	56.06	56.98	54.32	54.37	54.43	54.51	54.68	55.04	53.85	53.85	53.85	53.92	53.92	54.01
		12:00	55.22	55.36	55.46	56.08	57.32	59.15	54.37	54.43	54.51	54.56	54.77	55.18	53.85	53.92	53.92	53.98	54.01	54.09
2-Nov-78	12:29 - 13:24	12:30	54.65	55.01	55.30	56.05	57.15	58.54	54.37	54.43	54.54	54.62	54.85	55.25	53.92	53.92	53.92	54.03	54.06	54.14
		13:00	54.54	54.80	55.07	56.08	57.07	58.71	54.37	54.43	54.54	54.62	54.88	55.27	53.92	53.98	53.98	54.03	54.06	54.14
		13:30	54.48	54.56	54.65	55.30	56.44	58.04	54.37	54.43	54.54	54.62	54.82	55.27	53.98	54.01	54.01	54.03	54.06	54.14
26-Jul-79	07:05 - 08:45	7:00	71.71	78.93	86.05	71.76	78.88	78.83							71.38	71.79	71.92	72.03	72.11	72.25
		7:30	71.60	78.76	78.80	71.65	71.65	71.65							71.87	71.95	71.95	72.00	72.03	72.03
		8:00	71.60	78.82	85.94	78.82	86.00	86.08							71.17	71.30	71.55	71.84	71.90	71.87
		8:30	71.71	86.05	71.87	71.87	72.03	72.19							71.33	71.57	71.71	71.82	71.84	71.82
		9:00	71.82	79.04	79.12	79.16	79.44	79.66							71.28	71.52	71.57	71.63	71.63	71.60
26-Jul-79	09:20 - 10:28	9:30	71.76	86.11	86.25	86.31	86.74	87.02							71.44	71.55	71.55	71.63	71.63	71.63
		10:00	71.76	86.16	79.19	86.40	79.74	72.91							71.22	71.44	71.52	71.60	71.63	71.63
		10:30	71.76	71.92	72.06	72.19	72.70	73.08							71.06	71.33	71.46	71.57	71.65	71.68

* °F by depth

TABLE 2-3 SUMMARY OF LAKE CURRENT DATA AVAILABLE ON PLUME MAPPING DAYS
COOK NUCLEAR PLANT, BRIDGMAN, MI

Plumes Mapped on Relatively Calm Lake Days

Date	Plume Mapping Time	Current Log Time	North Inshore Current		North Offshore Current		South Inshore Current		South Offshore Current	
			Speed (mph)	Direction (°)	Speed (mph)	Direction (°)	Speed (mph)	Direction (°)	Speed (mph)	Direction (°)
23-Aug-78	15:53 - 16:42	15:30	0.10	27	0.00	186	0.44	5	0.10	236
		16:00	0.08	37	0.00	224	0.33	7	0.12	236
		16:30	0.02	63	0.00	259	0.25	5	0.12	238
		17:00	0.05	60	0.00	262	0.35	9	0.13	238
5-Sep-78	11:19 - 14:36	11:00	0.27	44	0.00	180	0.25	315	0.05	197
		11:30	0.10	57	0.00	180	0.18	316	0.05	190
		12:00	0.28	52	0.00	180	0.25	311	0.03	197
		12:30	0.25	58	0.00	180	0.16	312	0.03	196
		13:00	0.28	56	0.00	180	0.14	299	0.00	196
		13:30	0.28	59	0.00	184	0.16	330	0.03	196
		14:00	0.33	60	0.00	185	0.11	1	0.07	195
		14:30	0.38	79	0.00	185	0.09	3	0.06	197
5-Sep-78	14:51 - 17:42	15:00	0.37	75	0.00	187	0.12	24	0.03	197
		15:30	0.42	66	0.00	195	0.09	83	0.00	194
		16:00	0.23	113	0.00	200	0.07	108	0.03	196
		16:30	0.22	202	0.00	194	0.23	155	0.08	194
		17:00	0.18	207	0.00	193	0.32	137	0.10	199
		17:30	0.10	194	0.00	191	0.11	155	0.08	199
		18:00	0.12	205	0.00	188	0.07	168	0.13	197
7-Nov-78	12:30 - 14:30	12:30	0.12	207	0.10	142	0.11	137	0.15	158
		13:00	0.16	215	0.16	145	0.09	136	0.10	158
		13:30	0.17	212	0.17	146	0.05	145	0.07	158
		14:00	0.17	205	0.17	151	0.09	145	0.03	158
7-Nov-78	14:39 - 16:30	14:30	0.17	203	0.14	152	0.05	161	0.08	158
		15:00	0.18	205	0.16	152	0.05	210	0.05	158
		15:30	0.13	193	0.16	152	0.02	241	0.00	159
		16:00	0.13	195	0.05	191	0.00	258	0.02	160
		16:30	0.15	187	0.17	217	0.02	244	0.07	162

Plumes Mapped on Days When Swell/Waves Were Less than or Equal to Two Feet.

Date	Plume Mapping Time	Current Log Time	North Inshore Current		North Offshore Current		South Inshore Current		South Offshore Current	
			Speed (mph)	Direction (°)	Speed (mph)	Direction (°)	Speed (mph)	Direction (°)	Speed (mph)	Direction (°)
7-Sep-78	09:34 - 11:06	9:30	0.20	19	0.00	182	0.33	359	0.13	200
		10:00	0.30	14	0.00	182	0.09	2	0.07	199
		10:30	0.35	16	0.00	182	0.25	359	0.07	200
7-Sep-78	11:12 - 12:54	11:00	0.32	21	0.00	192	0.26	351	0.07	202
		11:30	0.35	22	0.00	192	0.32	359	0.07	200
		12:00	0.37	10	0.00	192	0.37	3	0.05	200
		12:30	0.37	6	0.00	195	0.32	2	0.07	195
		13:00	0.32	5	0.00	203	0.25	3	0.03	197
1-Nov-78	12:34 - 14:22	12:30	0.30	6	0.03	302	0.02	357	0.02	304
		13:00	0.22	29	0.03	322	0.12	347	0.00	304
		13:30	0.20	37	0.12	336	0.14	332	0.05	303
		14:00	0.22	41	0.14	336	0.14	332	0.03	304
1-Nov-78	14:28 - 16:19	14:30	0.23	44	0.17	2	0.23	347	0.17	305
		15:00	0.25	37	0.12	339	0.23	347	0.15	304
		15:30	0.27	22	0.28	339	0.23	350	0.18	304
		16:00	0.27	14	0.05	337	0.25	351	0.17	304
		16:30	0.28	10	0.17	336	0.26	351	0.30	305
3-Nov-78	09:50 - 11:26	9:30	0.07	171	0.02	201	0.00	110	0.07	1
		10:00	0.07	192	0.23	200	0.00	94	0.12	0
		10:30	0.07	167	0.17	196	0.00	126	0.12	1
		11:00	0.12	167	0.19	196	0.00	141	0.12	1
		11:30	0.15	157	0.14	196	0.00	137	0.08	1
3-Nov-78	11:40 - 13:17	12:00	0.20	61	0.17	194	0.00	128	0.10	1
		12:30	0.02	85	0.21	185	0.00	137	0.12	2
		13:00	0.17	76	0.16	176	0.00	129	0.10	0
		13:30	0.20	58	0.89	175	0.00	144	0.10	0
24-Jul-79	11:46 - 13:08	11:30	0.13	162	0.41	198	0.05	141	0.28	178
		12:00	0.02	154	0.37	2.01	0.05	141	0.30	181
		12:30	0.03	130	0.25	199	0.12	141	0.28	189
		13:00	0.15	329	0.23	199	0.07	141	0.25	183
24-Jul-79	13:30 - 14:51	13:30	0.15	315	0.43	196	0.07	99	0.19	174
		14:00	0.10	322	0.17	196	0.14	62	0.19	174
		14:30	0.17	313	0.25	196	0.14	56	0.12	184
		15:00	0.32	313	0.26	195	0.14	52	0.25	188
25-Jul-79	11:37 - 12:38	11:30	0.25	10	0.10	177	0.21	7	0.18	3
		12:00	0.35	19	0.10	177	0.21	5	0.19	10
25-Jul-79	12:34 - 13:39	12:30	0.38	3	0.12	177	0.17	350	0.12	10
		13:00	0.08	6	0.12	177	0.21	350	0.21	3
		13:30	0.22	9	0.05	177	0.31	351	0.12	2
27-Jul-79	11:28 - 12:45	11:30	0.07	177	0.26	211	0.19	332	0.34	353
		12:00	0.05	306	0.25	211	0.05	332	0.35	352
		12:30	0.03	310	0.35	211	0.19	332	0.34	0
		13:00	?	18	0.25	212	0.21	331	0.35	1
27-Jul-79	13:15 - 13:50	13:30	0.09	21	0.21	211	0.09	331	0.37	352
		14:00	0.12	11	0.30	212	0.25	331	0.23	333
28-Jul-79	09:10 - 11:00	9:00	0.12	17	0.13	211	0.16	10	0.23	334
		9:30	0.42	29	0.17	211	0.16	15	0.34	326
		10:00	0.28	4	0.15	210	0.21	16	0.39	318
		10:30	0.23	6	0.31	208	0.24	21	0.40	319
		11:00	0.23	12	0.30	211	0.26	23	0.42	334
28-Jul-79	11:19 - 13:29	11:30	0.23	8	0.21	213	0.19	22	0.42	3
		12:00	0.42	27	0.26	212	0.21	24	0.41	14
		12:30	0.35	22	0.36	211	0.31	24	0.37	9
		13:00	0.32	29	0.40	212	0.37	22	0.42	7
		13:30	0.25	21	0.21	212	0.52	19	0.41	7

Plumes Mapped on Days When Swell/Waves Were Greater Than Two Feet.

Date	Plume Mapping Time	Current Log Time	North Inshore Current		North Offshore Current		South Inshore Current		South Offshore Current	
			Speed (mph)	Direction (°)	Speed (mph)	Direction (°)	Speed (mph)	Direction (°)	Speed (mph)	Direction (°)
25-Aug-78	09:50 - 12:58	9:30	0.30	197	0.00	179	0.21	121	0.18	186
		10:00	0.20	193	0.00	179	0.19	142	0.13	189
		10:30	0.33	193	0.00	184	0.12	139	0.18	186
		11:00	0.43	192	0.00	180	0.12	140	0.15	184
		11:30	0.22	189	0.00	188	0.09	142	0.18	178
		12:00	0.30	180	0.00	189	0.05	57	0.22	185
		12:30	0.30	193	0.00	189	0.09	292	0.15	183
25-Aug-78	13:06 - 15:50	13:00	0.27	190	0.00	192	0.00	306	0.13	186
		13:30	2.23	178	0.00	196	0.12	316	0.22	184
		14:00	0.25	187	0.00	198	0.12	9	0.10	182
		14:30	0.25	208	0.00	200	0.12	8	0.13	186
		15:00	0.28	215	0.00	198	0.18	10	0.17	183
		15:30	0.23	217	0.00	194	0.25	9	0.06	186
		16:00	0.30	215	0.00	55	0.26	11	0.07	185
6-Sep-78	10:47 - 12:51	10:30	0.30	15	0.00	37	0.25	21	0.15	205
		11:00	0.37	14	0.00	21	0.26	16	0.13	199
		11:30	0.45	7	0.00	244	0.21	9	0.02	199
		12:00	0.33	144	0.00	232	0.19	2	0.02	200
		12:30	0.25	32	0.00	221	0.32	4	0.10	200
6-Sep-78	13:11 - 15:07	13:00	0.35	25	0.00	202	0.35	3	0.15	201
		13:30	0.33	22	0.00	199	0.32	359	0.15	203
		14:00	0.25	30	0.00	197	0.28	256	0.12	203
		14:30	0.20	34	0.00	195	0.21	350	0.15	200
		15:00	0.32	29	0.00	191	0.09	319	0.17	201
8-Sep-78	09:45 - 11:45	9:30	0.33	5	0.00	3	0.32	13	0.27	344
		10:00	0.42	3	0.00	33	0.32	10	0.22	356
		10:30	0.40	2	0.00	3	0.32	7	0.22	358
		11:00	0.37	4	0.00	3	0.18	4	0.22	356
		11:30	0.37	2	0.00	3	0.32	3	0.25	356
8-Sep-78	11:52 - 14:07	12:00	0.38	6	0.00	4	0.35	0	0.25	355
		12:30	0.22	352	0.00	5	0.32	2	0.23	357
		13:00	0.33	5	0.00	6	0.39	0	0.23	357
		13:30	0.25	7	0.00	6	0.33	6	0.23	357
		14:00	0.30	6	0.00	1	0.26	356	0.22	335
2-Nov-78	10:10 - 12:11	10:00	0.48	10	0.42	23	0.23	359	0.30	13
		10:30	0.48	14	0.24	28	0.35	359	0.37	13
		11:00	0.53	14	0.31	16	0.26	2	0.28	10
		11:30	0.42	17	0.33	16	0.32	1	0.30	9
		12:00	0.58	11	0.26	12	0.32	1	0.18	6
2-Nov-78	12:29 - 13:24	12:30	0.53	8	0.33	11	0.28	2	0.25	3
		13:00	0.52	10	0.28	10	0.26	2	0.27	3
		13:30	0.40	14	0.38	5	0.25	0	0.28	2
26-Jul-79	07:05 - 08:45	7:00	0.37	190	0.33	186	0.04	167	0.16	172
		7:30	0.33	190	0.33	178	0.23	160	0.23	176
		8:00	0.35	191	0.35	178	0.24	162	0.18	162
		8:30	0.37	192	0.41	177	0.16	163	0.21	156
		9:00	0.32	186	0.40	176	0.21	161	0.25	164
26-Jul-79	09:20 - 10:28	9:30	0.33	193	0.36	179	0.28	160	0.28	166
		10:00	0.30	193	0.46	177	0.15	167	0.25	168
		10:30	0.33	187	0.43	172	0.35	165	0.19	144

?: can't read data

Table 3-1. Example Light Extinction Coefficients.

Water Body	Ke (m^{-1})	Light penetrating (m)
Lake Erie	For visible = 0.28 For infrared = 2.85	13
Lake Michigan	For visible = 0.21 For infrared = 2.85	17
Lake Tahoe	0.05	100
Turbid water	4.5	1

Table 3-2. Momentum Boundary Conditions for Performance Assessment.

Boundary	Prescribed Condition	Comments
A	$u(x_L,y,z,t) = 0.0$	No Flow on shore
B	$\frac{\partial \eta}{\partial t} - c\frac{\partial \eta}{\partial y} = 0$	Wave Radiation Condition $c \approx (gh)^{1/2}$
C	$\frac{\partial \eta}{\partial t} + c\frac{\partial \eta}{\partial x} = 0$	Wave Radiation Condition $c \approx (gh)^{1/2}$
D	$v(x,y_o,z,t) = 5$ cm/s	Alongshore Current

Table 3-3. Momentum Boundary Conditions for 1995 Simulation.

Boundary	Prescribed Condition	Comments
A	u= 0.0	No Flow on shore
B	$v = F(v_{LMMBS})$	LMMBS derived velocity
C	$\frac{\partial \eta}{\partial t} + c\frac{\partial \eta}{\partial x} = 0$	Wave Radiation Condition $c \approx (gh)^{1/2}$
D	$v = F(v_{LMMBS})$	LMMBS derived velocity

Table 3-4. Naming Convention for Turbulence Models.

Level	Variables	Implementation
0	$\bar{u}, \bar{v}, T$	Pacanowski and Philander (1981); Nunez-Vaz and Simpson (1994)
1	$\bar{u}, \bar{v}, T, \kappa$	Denbo and Skyllingstad (1996), Deardorff (1980)
2	$\bar{u}, \bar{v}, T, \kappa, \varepsilon$	Deardorff (1973)
2.5	$\bar{u}, \bar{v}, T, \kappa, \varepsilon, \overline{u_i' u_j'}$	Blumberg and Mellor (1987), Galperin et al. (1988),
3	$\bar{u}, \bar{v}, T, \overline{u_i' \phi'}, \overline{u_i' u_j'}$	no known geophysical implementations

Table 4-1. Surveyed Plumes by Month and Wind Speeds During the Measurement Period.

Month	Number of Plumes Measured	Maximum Wind Speed (m/s)	Minimum Wind Speed (m/s)
August 1978	3	3.6	0.9
September 1978	8	4.5	0.9
November 1978	8	7.2	0.9
July 1979	10	7.2	3.1

Table 4-2. Measured Plume Area and Computed Area for 2 °C, 1.67 °C, and 1.0 °C.

Survey #	Measured Plume Area (ha)	Computed Area 2 °C (ha)	Computed Area 1.67 °C (ha)	Computed Area 1 °C (ha)
1	62	110	154	309
2	157	137	179	365
3	57	45	64	164
4	81	45	61	228
5	265	65	132	360
6	257	90	140	415

Table 5-1. Operating Conditions for the Model Runs.

Plant Operation	Unit 1 ΔT °C (°F)	Unit 2 ΔT °C (°F)
15.8×10^9 BTU/hr (Low)	12.116 (21.809)	9.250 (16.650)
16.8×10^9 BTU/hr (Medium)	12.883 (23.189)	9.835 (17.703)
17.3×10^9 BTU/hr (High)	13.267 (23.881)	10.128 (18.230)

Table 5-2. Average Plume Area (hectares) at 1 meter Depth.

	High Plant Output	**Medium Plant Output**	**Low Plant Output**
April	293	238	198
May	394	348	249
June	92	82	55
July	43	37	29
August	177	157	123
September	161	157	137
October	131	121	119
November	162	112	91

Table 5-3. Representative Maximum Plume Area (hectares).

	High Plant Output	**Medium Plant Output**	**Low Plant Output**
April	1825	1804	1714
May	1766	1612	1289
June	1466	1436	1289
July	779	650	566
August	896	820	630
September	1141	1063	821
October	1034	997	929
November	1975	666	593

ATTACHMENT A

Attachment A.
CORMIX Application to the Cook Plant Discharge Structure

Technical Memorandum

TO: David Podber

DATE: May 15, 2000
PROJECT: Cook
COPIES: 1

FROM: Kristen Chaffin

SUBJECT: CORMIX Simulations for Model Calibration of Nearfield Behavior

Executive Summary

To verify the predictive capabilities of the nearshore model, mixing characteristics of the plume in close proximity to the effluent diffusers were evaluated using an independent computerized system able to predict nearfield mixing behavior. The nearfield system chosen for this purpose was the CORMIX System. The water surface plume temperatures predicted by CORMIX corresponded very well with the water surface plume temperatures predicted by the nearshore model with a plume surface temperature of 19 degrees C, at a distance of 16 feet from the diffuser. The hydrodynamic bulk dilution of 2.2 predicted by CORMIX was used to calibrate the vertical mixing of the nearshore model such that the model behavior near the diffusers reflected the CORMIX prediction.

Introduction

To verify the predictive capabilities of the nearshore model, mixing characteristics of the plume in close proximity to the effluent diffusers were evaluated using an independent computerized system able to predict nearfield mixing behavior. As explained earlier, the nearshore model consists of a one hundred by one hundred meter square grid and is intended to predict the macro transport, or farfield, plume phenomenon. This model is not designed to predict the micro transport phenomenon produced in the region influenced by the diffusers, the nearfield. It is therefore necessary to use a nearfield modeling program to understand these transport process in order to calibrate the behavior of the farfield, nearshore, model at the location of the diffusers. The system chosen for this nearfield prediction was the CORMIX System. By using the CORMIX system to evaluate the plume characteristics in the area close to the diffusers, the information gained from this fine scale, micro transport evaluation can be used the verify and calibrated the larger scale nearfield model.

Method Overview

Due to the simplicity in which the CORMIX System accepts data, the simulation of the Cook plant diffusers had to be performed in parts. After the individual features of the diffusers were modeled, an interaction analysis was performed to determine the extent and effects of plume interactions from the individual diffuser features. For this simulation, the two diffuser units were modeled separately. In addition to independent unit modeling, the individual flanges of the diffusers were modeled one at a time. The reason for this independent flange modeling was due to the effluent flow area

interpretation intrinsic to the CORMIX system. CORMIX interprets the flow area of each diffuser flange as a circular port. In the case of the Cook diffusers, if this flange were circular, the diameter of the port would be almost one half the depth of the water. When attempting to model a buoyant plume, and the travel time of the plume to the surface is a parameter of interest, this simplification is not acceptable. If the effluent flow areas are modeled as a horizontal series of smaller uniform circular ports with a diameter equal to the height of the flange opening and a total area of all of the ports equivalent to the actual flow area then the flange is more accurately portrayed. Figure A-1 illustrates this simulated diffuser layout. However, if this configuration is used for each of the flanges, CORMIX is not capable of conveying two rows of ports at an angle to each other, i.e., the row of ports must be on a linear axis. For this reason, each individual flange was modeled separately. Table A-1 contains the input parameters used for modeling the diffuser flanges. Figure A-2 depicts the layout of the two diffuser units.

Once all of the flanges of the two diffuser units were modeled, the output data from CORMIX was analyzed for interactions between the flanges. More specifically, the data was analyzed to determine if the effluent plume from each of the five diffuser flanges interact in the zone of interest, i.e., the nearfield mixing zone. This analysis was performed by plotting the plumes from each flange predicted by CORMIX and superimposing them to locate any points of interaction. Figure A-3 shows the superposition of the predicted plumes for diffuser unit one. This superposition analysis of the plumes revealed that the two diffuser units, located approximately ninety-one meters apart, do not interact with each other in the nearfield, the area of concern for the CORMIX simulation. Furthermore, the plumes from each of the flanges do not interact in the nearfield. This non-interaction allows for the use of the bulk dilution calculated by CORMIX for each flange as a comparative measure to assist in the calibration of the nearshore model.

The results of the CORMIX study were used to both verify and calibrate the nearshore model in the area of the diffusers. The water surface plume temperatures predicted by CORMIX corresponded very well with the water surface plume temperatures predicted by the nearshore model. This correlation served to verify the prediction of the nearshore model. In addition to surface plume temperature, the distance from the diffuser that the plume first reaches the surface and the location at which the plume was first fully vertically mixed were used as calibration parameters. Since the CORMIX System is more suitable to predict behavior in the area close to the diffusers, the nearfield, the vertical mixing parameter in the nearshore model grid cells containing the diffusers was adjusted to reflect the behavior of the nearfield, CORMIX System. This adjustment served to further calibrate the distance the plume needs to vertically mix and the distance the plume travel away from the diffuser before it reaches the water surface in the nearshore model. The memo attachment contains the output data from the CORMIX System for the two flanges of diffuser unit one, and Table A-2 contains selected numerical output from the CORMIX simulations for unit one.

Figure A-1 Simulated Diffuser Configuration for One Flange

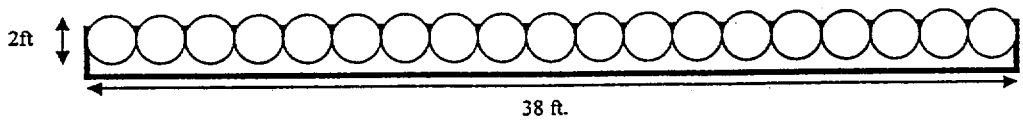

FIGURE A-2 DIFFUSER

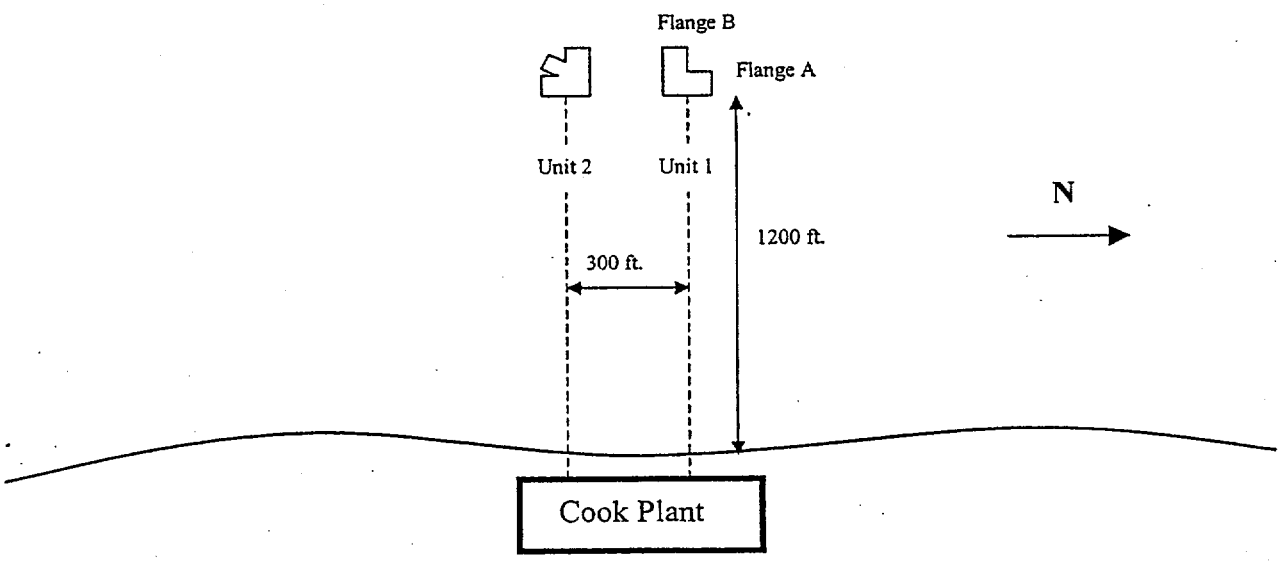

FIGURE A-3 SUPERPOSITION OF CORMIX FLANGE PLUMES PREDICTIED BY CORMIX FOR DIFFUSER UNIT 1

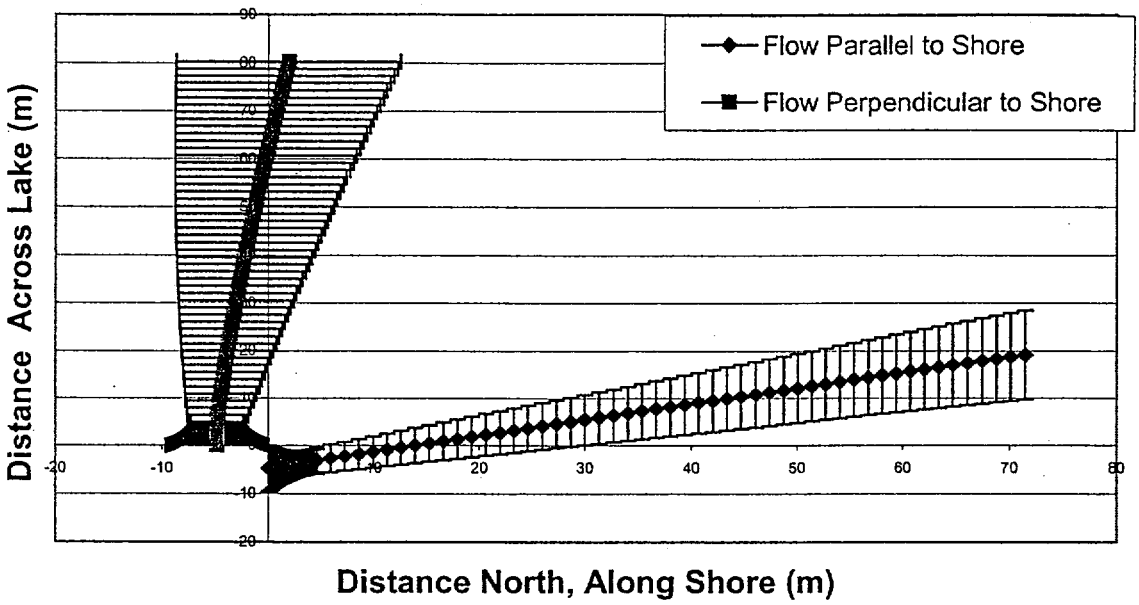

TABLE A-1. SUMMARY CORMIX INPUT PARAMETERS FOR MODELING ONE DIFFUSER FLANGE

Parameter Type	Parameter	Design Value/Description
Ambient	Average Nearshore Water Depth	7 m
	Water Depth at Discharge	5.6 m
	Ambient Lake Velocity	0.03 m/s
	Wind Speed	2 m/s
	Ambient Lake Temperature	12.17 °C
	Bounded verse Unbounded Water Body	Unbounded
	Water Density Profile	Uniform
	Fresh verse Salt Water	Fresh
	Tidal Flow	Non-Tidal
Discharge Structure	Submerged Single Port, Submerged Multiport, or Surface Discharge	Submerged Multiport
	Nearest Bank (Left/Right)	Right
	Distance to One End of Diffuser	Variable
	Distance to Other End of Diffuser	Variable
	Length of Diffuser	Variable
	Diffuser Height	0.762 m
	Port Diameter	0.6096 m
	Number of Ports	Variable

	Diffuser Arrangement (unidirectional/ staged / alternating or vertical)	Unidirectional
	Vertical Angle	0 °
	Horizontal Angle	Variable
	Alignment Angle	Variable
	Angle of Relative Orientation	90 °
Effluent	Flow Rate	Variable
	Effluent Temperature	Variable

TABLE A-2 CORMIX RESULTS

	Distance from Diffuser to Location where Plume just Reached Surface (m)	Plume Temperature at Surface (°C)	Hydrodynamic Bulk Dilution at Location where Plume Surfaces
Unit 1--Flange A	4.85	18.93	2.2
Unit 2--Flange B	4.85	19.04	2.2